Assessing the use of hydrogels to harvest atmospheric water for agriculture in arid and

semi - arid areas

A thesis presented in partial fulfilment of the requirements for the degree of

Master

of

Environmental Management

at Massey University, Manawatū campus, New Zealand.

Daniel Gyamfi Opoku

2021

ABSTRACT

Agricultural production in arid and semi-arid regions globally faces a growing challenge of water scarcity and initiatives to increase water-availability for crops are needed. The hygroscopicity of hydrogels underpins the real opportunity to desorb water that can be used to support agricultural production in water scarce areas. Research to date has predominantly focussed on direct contact absorption of water in a liquid phase. The opportunity for hydrogels to absorb water from the atmosphere is less studied. Specifically, the impact of relative humidity and temperature on hydrogel hygroscopicity and potential for desorption of this water under environmental pressures that might be expected in a plant root zone are poorly described in literature. Such information will underpin assessment of the extent to which atmospheric water absorption might serve as an alternative water source for plants use in the arid and semi-arid regions. This study was therefore undertaken to ascertain hydrogels hygroscopicity and desorption potential with specific consideration of agriculture in arid and semi-arid regions. The research aimed to provide information on the hygroscopicity potential of different hydrogels, and how different relative humidity percentages and temperature influence hydrogels hygroscopicity and different applied pressures impact water desorption from hydrogels. The effect of relative humidity, time and temperature on hygroscopicity was investigated using replicates of five hydrogels of different composition placed in five different relative humidity chambers (63 %, 76 %, 84 %, 95 % and 100 %) and under three different temperature levels (10 ℃, 20 ℃ and 30 ℃). The results showed that hydrogel type, relative humidity and time influences hygroscopicity significantly, and that the chemical composition of hydrogels can explain hygroscopicity. There was no influence of temperature on absorption. Hydrogels with no N content showed increased absorption of atmospheric water with time, and this is explained through the absence of an N-driven

crosslinking effect on water absorption. Absorption of atmospheric water by the best performing hydrogel (Yates Waterwise Water Storage Crystals; at 3.139 g/g at 100 % relative humidity and 30 ºC) in this study was explained by first order model behaviour at 20 ºC for all relative humidity levels except at 63 %. Further research was conducted on the hydrogels defined as the best and worst absorbing in the initial experiments. These hydrogels were placed in contact with liquid water to yield the freely swollen state, and then desorption potential for plant access was investigated using different pressure levels on suction plates. The results clearly showed that increasing pressure increases water desorption between 0.1 and 1 bar pressure. However, between 1 bar and 15 bar no further water is lost. The best absorbing hydrogels identified in this study desorbed more water than the worst. However, this work finds that for both tested hydrogels, pressure beyond 15 bar would be required to desorb hygroscopic water for plant access and use.

The study therefore infers that the hygroscopicity potential of hydrogels is optimum for hydrogels with no N content exposed to high relative humidity (above 84 %) over periods of daily cooling from late night and early morning where the dew point might be reached. Such conditions do overlap with some arid and semi-arid regions. However, even where these environmental conditions for optimal absorption are reached, plants are unlikely to be able to desorb the hydrogel water. Therefore, an engineering approach would be needed to physically or mechanical desorb water. In this scenario it is unlikely that hydrogels would be mixed into the soil. Instead, a system could be deployed where hydrogels are exposed to atmospheric water in 'banks' which can be closed periodically for desorption. Released water could then be channelled for irrigation. Solar power may be a viable energy source to drive this scenario, although further work is required to fully explore the opportunity.

ACKNOWLEDGEMENT

TABLE OF CONTENTS

LIST OF FIGURES

LIST OF TABLES

LIST OF ABBREVIATIONS

ºC	degree Celsius
RH	relative humidity
%	percentage
h	hour
$CaCO_3$	Calcium carbonate
mm	millimetre
SAP	Superabsorbent
g/kg	grams per kilogram
g/g	grams per grams
kg/ha	kilogram per hectare
g/plant hole	grams per plant hole
3D	3 dimensional
MBAm	N-methylene bis acrylamide
AAM	Acrylamide
mm^2/s	millimetre squared per second
mg/mm^3	milligram per millimetre cube
TGA	Thermogravimetry,
DSC	Differential Scanning Calorimetry,
DTA	Differential Thermal Analysis
NMR	Nuclear Magnetic Resonance
NH_4NO_3	Ammonium nitrate
NaCl	Sodium chloride
KCl	Potassium chloride
KNO_3	Potassium nitrate
AA-co-NNDMAAm	Acrylic acid with N, N-dimethylacrylamide
AAm–MSAS–AA	Acrylamide methallylsulfonate acrylate
N	Nitrogen
MPa	Megapascal Pressure Unit

<center>**CHAPTER ONE**</center>

1 RESEARCH OVERVIEW
1.1 Background to the study

Water scarcity is a global sustainability issue particularly in semi-arid and arid areas of the Earth. Semi-arid and arid regions dominate about one-third of the terrestrial surface, and these areas is increasing (Verheye, 2009). Globally, semi-arid and arid areas have similar abiotic and climatic features, including long drought, low humidity, and fewer rainfall periods. This creates less water supply, as well as high temperatures, increasing evaporation and loss of soil water. Consequently, soils in semi-arid and arid areas have nearly no available water to support both plant growth and soil development (Verheye, 2009). Such water-deprived lands are usually rendered unsuitable for agriculture but can support xerophytic plants with limited water requirements.

Water availability is a key requirement for agriculture (Chai et al., 2015; Shen & Pei, 2019). Plants depend on water for most of their growth process (Zlatev & Lidon, 2012). For example, during photosynthesis, plants require available water (Boyer, 1976). During photosynthesis, plants open their stomata to allow gas exchange with carbon dioxide being taken up and incorporated into carbohydrates and oxygen being released. Water is also lost to the atmosphere through the stomata (transpiration) (Boyer, 1976). Transpiration drives water from the soil through the roots and stems to the leaves due to the large potential energy difference between the atmosphere and soil (Campbell, 1986). Plants' water demand is high during the process and therefore, constant water availability in the soil is essential to prevent plant stress when transpiration occurs. In response to the water demands of agriculture, irrigation from freshwater sources to supplement rainfall water deficits has become common practice.

Freshwater is a limited resource, accounting for only about 30% of Earth's estimated surface water (Gleick & Palaniappan, 2010; Siddique & Bramley 2014). The agricultural

sector consumes approximately two-thirds of the world's freshwater (Chai et al., 2015) and the limited nature of global freshwater resources has led to socioeconomic competition throughout human history across (Chai et al., 2015). Irrigation for agriculture is generally an inefficient use of water and this has majorly contributed to high freshwater usage and loss through surface runoff, evaporation, leaching and underutilisation of irrigated water by plants (Koech & Langat, 2018). Irrigation technologies have improved in recent years but are socio-economically challenged, and hence are poorly adopted at global scale. Bazin et al. (2017) highlighted that economic challenges are very pronounced in arid regions and therefore farmers are unable to purchase improved irrigation technologies. Consequently, water is constantly wasted in areas that have limited water availability, driving a scenario of constant water demand for irrigation (Abedi-Koupai et al., 2008). This potentially creates an alarming water scarcity concern which is anticipated to increase due to future drought conditions from climate change at both regional (Fries et al., 2020; Mancosu et al., 2015) and global scale (Falkenmark, 2013).

Globally, climate change is projected to challenge agricultural productivity through increased drought and temperature which subsequently increases freshwater demand (Booker & Trees, 2020; Godfray et al., 2010; Hoegh-Guldberg et al., 2018) due to plant stress, high soil salinity and low infiltration rate (Paudel et al., 2020). Such a scenario is already acknowledged with substantial evidence of clean freshwater scarcity in arid regions (Pattanaaik et al., 2015).

High agricultural plant water demands induced by water scarcity in arid regions and the projected increasing water crisis due to increased temperature from climate change calls for new socio-enviro-economic initiatives which can support sustainable agriculture (Shen & Pei, 2019). One technology option is the application of hydrogels to water

storage. Hydrogels are a chemical compound with proven effectiveness and efficiency for absorbing and retaining water from irrigation to support soil moisture for agriculture. The primary aim of the research described in this thesis was to explore the potential of hydrogels to absorb atmospheric moisture and release it for plants use under plant water stress levels experienced under familiar to arid and semi-arid environmental conditions and projected environmental conditions that might be associated with climate change.

1.2   Overall structure of this thesis

The research chapters of this thesis explore the potential of hydrogels to absorb atmospheric moisture and release it as water for plant usage. Chapter 2 focuses on the literature review on characteristics of the arid and semi-arid areas regarding water scarcity and the properties of hydrogels' that offer out possibilities of absorbing and supplying water. Chapter 3 focuses on assessing the potential of different hydrogels to absorb atmospheric moisture under conditions of different relative humidity and temperature. Based on the best outcomes for atmospheric moisture absorption by hydrogels, Chapter 4 subsequently focused on release of absorbed water from selected hydrogels in form that can be used for plants growth. Chapter 5 discusses the outcomes of the thesis in the context of the research aims and draws conclusions on the potential usefulness of the findings of this research study for agriculture in arid regions.

CHAPTER TWO

2 LITERATURE REVIEW

2.1 Introduction

Enhancing the efficiency of soil water-retention has been identified among sustainable approaches to offset potential adverse climate change effects on soil water for agriculture (Bis et al., 2018; Brown et al., 2011; Hüttermann et al., 1999; Klein et al., 2014; Li et al., 2021; Zhao et al., 2020). Hydrogel application to soils, is considered one method for improving soil-water retention, that has proven effective in agriculture (Shahid et al., 2012). Adoption of the technology has increased significantly over the past 40 years (Zhang et al., 2016) for water-stressed soils (Ghobashy, 2020) especially in water-scarce regions (Kalhapure et al., 2016; Neethu et al., 2018; Pattanaaik et al., 2015).

Hydrogels can absorb water to over a hundred times their dry weight (Abedi-Koupai et al., 2008) and slowly release up to 95 percent of the absorbed water to soil (Kalhapure et al., 2016). Hydrogels are made of functional hydrophilic polymers in a three-dimensional crossed-linked network (Ahmed, 2015; Kalhapure et al., 2016; Zhang et al., 2016). Their associated physical and chemical properties characterise their water absorption, retention and release potential (Ahmed, 2015; Neethu et al., 2018; Zhu et al., 2015) even under water-scarcity enabling environmental conditions (Vundavalli et al., 2015). Hydrogels have potential to limit soil water and nutrient loss, lower irrigation frequency, improve soil biophysical properties, increase available soil water and nutrient availability to plants, and prevent the loss of nutrients to the surrounding environment (Abedi-Koupai et al., 2008; Gao et al., 2013; Ghobashy, 2020; Zohuriaan-Mehr & Kabiri, 2008).

The successful performance of hydrogels in agricultural fields (Farrell et al., 2013) has prompted scientists to undertake multiple research studies into their absorption (Zhang et al., 2017) and desorption (Kalhapure et al., 2016) properties in soil (Neethu et al., 2018).

Many of these studies have investigated absorption and desorption under contact with water for optimal soil moisture and plant production, and research has led to successful outcomes (Abedi-Koupai & Asadkazemi, 2006; Neethu et al., 2018; Pattanaaik et al., 2015). Studies such as Gomes (2015), Neethu et al. (2018) and Zohuriaan-Mehr and Kabiri (2008) have shown environmental factors such as atmospheric humidity and temperature can potentially influence the absorption and desorption capacity of hydrogels. However, comprehensive information relating to the interaction of hydrogels with such environmental parameters is limited. Such information is critical to the analysis of their potential role in agricultural scenarios that may be impacted by climate change. Del Genfo et al. (1991) projected that climate change is likely to increase atmospheric moisture and the abundance of clouds, due to increased evaporation associated with rising temperatures. Therefore, with respect to water scarcity in arid and semi-arid regions, atmospheric moisture could potentially become a major source of water for hydrogels. Research into the capacity of hydrogels to absorb atmospheric water as a function of different relative humidity and temperature levels and then release this for plant use is therefore a promising area. Such research could potentially quantify a new water source for hydrogels that could lead to improvements in soil-water stress conditions in locations that are projected to be at increasing risk of water scarcity.

2.1.1 Justification for the current study

The absorption, retention and desorption of water from hydrogels is influenced by multiple thermodynamic parameters (Ganji et al., 2010). These are dependent on the surrounding environment and determine hydrogel functionality. As such, the successful application of hydrogels in water-scarce areas with extreme atmospheric impacts, such as arid regions with high daytime temperatures and night-time atmospheric humidity, will

require comprehensive understanding of the thermodynamics of temperature, relative humidity and atmospheric pressure on the mechanisms of water absorption and desorption onto hydrogel surfaces. Research on the absorption capacity of hydrogels for atmospheric moisture could support increased application in agricultural production in parts of the world anticipated to experience temperature increases due to climate change. Hydrogels are composed of materials that are influenced by humidity (Wang et al., 2012), and it is important to understand how hydrogels could be used to extract water from the atmosphere for application to soils. Specifically, there is a need to prove whether hydrogels can absorb moisture from the atmosphere and release the adsorbed water for plant use.

2.2   Semi-arid and arid regions

Arid areas are characterised by very distinct dry climatic conditions. Depending on the amount of rainfall (Jafari et al., 2018), arid areas can be categorised as either hyper-arid, arid and semi-arid. High temperatures, coupled with low rainfall lead to low precipitation, increased evaporation, and wind action in arid regions (Verheye, 2009). Consequently, the climate, vegetation, and biological processes in these areas are often unique.

2.2.1   Soils in semi-arid and arid regions

Semi-arid and arid regions have unique soils characteristics. Associated soil types are spread across Africa in the Sahara, Namibian and Kalahari deserts; the Middle East in Afghanistan, Iran and the Arabian desert; in South and North America in the Mohave desert and Chile; and in the deserts of Australia (Verheye, 2009). Semi-arid and arid zones soil cover over a third of the world's total land surface globally (Khan & Duke, 2001),

and this is expanding further with time (Verheye, 2009). Semi-arid and arid regions have desert soils that possess little or no available water for soil formation and plant growth and are therefore often suited for xerophytic plants (Watson, 1992). The chemical fertility of soils in arid regions is compromised by a lack of soil moisture (Thomas et al., 2006). Such soils belong to the Aridisols in soil taxonomy and have characteristics of increased accumulation of $CaCO_3$ and other salt solutes in the soil profile, desert pavement, and patina. Although such soils could be free-draining (Thomas et al., 2006), the deficit due to low rainfall and high evaporation limits some soil processes such as dissolution and leaching. Furthermore, salts accumulated in the soil, such as calcium carbonate, draw and hold soil moisture by osmotic pressure to form salt solutions and consequently, limit free available water for plant use (Verheye, 2009).

2.2.2   Rainfall and moisture supply in the arid and semi-arid regions

Arid areas are characterised by mean annual rainfall of less than 100 mm for hyper-arid zones, between 100 mm to 250 mm for arid zones and between 250 mm to 500 mm for semi-arid zones (Verheye, 2009). Often, precipitation in these areas is limited to random short duration events associated with heavy rain downpour (Cheng et al., 2020). Subsequently, this limited soil moisture from rainfall evaporates due to characteristically low humidity and high solar radiation atmospheric conditions. In the African and the Australian deserts, studies have shown that the first 5-6 mm of rainfall to a heated soil surface is evaporated shortly after a downpour (Verheye, 2009). Hence, rainfall requires storage intervention in arid soils during the short but heavy rain downpour to realise availability for plant usage. Intervention is also required to capture soil moisture which returns as dew during relatively higher humidity at night.

2.2.3 Temperature and wind impacts in arid and semi-arid regions

Generally, temperatures observed in arid areas can be very high (Gaur & Squires, 2018). Temperatures vary significantly across the day and night periods and under certain circumstances (Ackerknecht & Gut, 1993). Soils in arid regions often lack vegetative cover and therefore have relatively higher air temperatures at the soil surface causing evaporation that decreases soil moisture (Ragab & Hamdy, 2008). This creates higher loss of the limited soil at soil surface. Temperature decreases with increasing soil depth thereby increasing soil moisture (Seneviratne et al., 2010). Therefore, mechanisms to conserve soil moisture at the soil surface are essential to manage soil moisture losses from evaporation due to high temperatures. Temperature affects the wind in the arid regions (Scholes, 2020). Increasing air temperature increases wind which consequently induces low humidity levels and high evaporation, thereby reducing soil moisture. Winds are often high in desert areas due to large variations in atmospheric conditions and their impacts can be significant on soils deprived of vegetation protection (Dwevedi et al., 2017). High-intensity wind impacts usually occur at fixed annual periods such as harmattan, sirocco or khamsin for the Sahara, North Africa and the Middle East, respectively. Aside from influencing soil moisture, wind affects a number of soil process, including accumulation, deflation, transport, abrasion and erosion.

2.2.4 Dew in the arid and semi-arid regions

Atmospheric moisture at the dew point is more important than rainfall for agriculture in arid regions but is often discounted due to the relatively low total amount of water involved (Agam & Berliner, 2006; Kalthoff et al., 2006). Dew encourages germination and initial plant development and enhances microbial activities and the volumetric spread of accumulated salts in arid soils (Baier, 1966). The dew concentration in arid areas results from high temperatures which enable high evaporation as well as other factors

including topography and surface roughness (Perry & Slatyer, 1969). Dew forms slowly over the soil surface during the night and early morning during periods of low evaporation rate (Hao et al., 2012). At such times, dew-point temperature is created when evaporation and temperature are reduced (Agam & Berliner, 2006). Below dew-point temperatures, adsorbed water vapour is usually the source of soil water addition in arid regions. Atmospheric moisture condenses and stays on the topsoil surface, usually up to 1 cm maximum soil depth. Dew measurements at night range from around 25-35 mm per year for the Negev desert in Israel, 12-15 mm per year for Amman in Jordan, 40 mm per year for Pretoria in South Africa (Verheye, 2009).

2.2.5 Water for agriculture in the arid and semi-arid environment

Water conservation aims to offset water deficits during low and no precipitation periods. Two approaches can be used to achieve water conservation in agriculture: ex situ and in situ (Kalhapure et al., 2016; Pathak & Wani, 2011). Ex-situ water conservation describes mechanical water harvesting approaches, including irrigation systems and reservoirs, to save rainwater for later usage (Kalhapure et al., 2016). In-situ water conservation uses techniques such as contouring, tillage, the adoption of good water conservation practices such as mulching, and the usage of chemical products such as hydrogels to conserve the water that falls on the soil (Hatibu & Mahoo, 1999). Most water conservation methods have been developed for landscapes that are suited to irrigation or that have rainfall suitable conditions. However, the arid and semi-arid environment is a very low rainfall environment and often lacks the necessary supply of irrigation water. The volume of water supplied by dew and water vapour in such areas often exceeds water supply from rainfall, making this the main source of soil moisture that supports the limited vegetation growth observed in deserts (Agam & Berliner, 2006). Soil water conservation methods

applicable to arid regions therefore require in-situ mechanisms to absorb and store water vapour from dew as soil moisture for subsequent plant usage.

2.2.6 Humidity in arid and semi-arid regions

Humidity is defined as the amount of water vapour present in the atmospheric. Generally, humidity in an area can be expressed as an absolute humidity, representing the water vapor present in a specific atmospheric gas volume at the area, and also as a relative humidity, representing the ratio of water vapor present in an atmospheric gas volume to the maximum capacity of water vapor that can be contained in that atmospheric gas volume at a particular temperature (Ingraham, 1998). Absolute humidity is measured in units of mg/ml or g/m^3 and relative humidity is measured in percentages (%), and both can be measured using a hygrometer.

Humidity or water vapor and other non-rainfall water sources in the atmosphere supply a significant amount of water in arid and semi-arid regions due to the scarcity of rainfall water (Zhang et al., 2016), and therefore largely depended on as the main water source for soil moisture and other biological processes (Huang et al., 2016; McHugh et al., 2015). Water vapour described by a relative humidity from 68 % up to nearly 100 % is apparent for some arid regions, including arid parts of Iran and is harvested for water (Davtalab et al., 2013). However, according to McHugh et al. (2015), relative humidity across arid and semi-arid regions generally ranges from 20 – 60 %. Relative humidity in arid and semi-arid regions varies in response to environmental conditions such as temperature which influences the water cycle (Agam & Berliner, 2006; Kosmas et al., 2001; McHugh et al., 2015). Changes in relative humidity in turn influences soil moisture, which consequently impacts the pattern and growth rates of vegetation (Kousari & Zarch, 2011; Ragab & Prudhomme, 2002). The potential for soil to adsorb moisture from water vapor at high relative humidity is greater on bare land than grassland or soil with vegetation cover

(McHugh et al., 2015). Water vapour is adsorbed into the soil by either natural or chemical processes, which may require either small or large energy input depending on the mechanical properties that describe the interaction of soil surface (adsorbent) and water vapor (Zhang et al., 2016).

2.2.7 Water availability fluctuations due to relative humidity and temperature interactions

The interaction between temperature and relative humidity determines the extent to which water vapour will generate non-rainfall water including fog and dew (Kousari & Zarch, 2011; McHugh et al., 2015). However, Luo and Lau (2019) and McHugh et al. (2015) reports that temperature has the overriding effect on relative humidity.

High air temperature causes evaporation which increases atmospheric water vapor content (Davtalab et al., 2013), and high temperatures constantly keep water vapor in the atmosphere if the water is unable to condense and fall back to Earth. If an excess supply of water is available for constant evaporation, the atmospheric water vapor concentration becomes saturated, and this phenomenon is referred to as fog (McHugh et al., 2015). Such a phenomenon is predicted to be associated with climate change temperature rises projections which may increase atmospheric water vapor (Eslamian et al., 2011; Held & Soden, 2006). In contrast, when surface water for evaporation is limited during such high temperatures, the relative humidity level and the atmospheric saturated water vapour concentration decreases (Luo & Lau, 2019). This is because the temperature increase over time for the same total content of water vapor becomes prevents increased atmospheric saturated water vapour concentration and hence relative humidity (the ratio of total water vapour to the saturated water vapour concentration) is reduced. A decrease in relative humidity is associated with an increase in atmosphere gas volume capacity to hold more

water vapour at the same water vapour concentration (Kousari & Zarch, 2011). The decrease in relative humidity with temperature rise can also be explained in terms of the relative atmospheric water vapor saturation degree which is defined as the ratio of actual water vapor pressure to saturation water vapor pressure in the atmosphere (Allen et al., 1998). However, Wei et al. (2021) reports that this mechanism of water vapor concentration is largely understudied especially with respect to wetting or drying potential on material surfaces. Wei et al. (2021) propose that absolute humidity should be used instead of relative humidity when describing atmospheric humidification or water vapour due to the impact of temperature on relative humidity, especially in arid and semi-arid areas. Kousari and Zarch (2011) reports that relative humidity has decreased over recent years.

Atmospheric temperature can decrease to, or beyond, a temperature level referred to as the 'dewpoint temperature' which results in a dew, another non-rainfall water event (McHugh et al., 2015). Dew is condensed water vapour that is formed when there is an air temperature drop or water vapour contacts a cold soil surface (Zhang et al., 2016). Any air temperature decrease at a specific relative humidity increases the actual water vapour saturation to a point that is either equal or exceeds the saturation vapour level at the same initial gas or air volume capacity. At this point there is less air or gas volume to hold onto water molecules and subsequently water vapour falls as condensed water. Generally, this phenomenon is observed during late nights and early mornings as temperature drops (Wei et al., 2021). Gaur and Squires (2018) reports midday temperature in arid areas range between 40-45 °C (but can occasionally drop to 15-25 °C on cloudy-low sun days) and night temperatures at 10 °C. McHugh et al. (2015) simulated a typical arid region daily temperatures fluctuation of 23 °C for 4h, 40°C for 8h, 23°C for 4h, and 10°C for 8h to assess the impact of variable temperature on relative humidity. On average

there was a 65.9 % increase in soil moisture relative to the initial soil of moisture 2.3 %

over the diurnal temperature simulation, with the 23°C treatment and the 40°C

temperature simulations increasing the soil moisture by 63.3% and 59.9% respectively.

Although this phenomenon contributes greatly to water availability in the drylands and

arid regions (Kidron et al., 2002; Malek et al., 1999; McHugh et al., 2015; Urbina et al.,

2021), it does not often occur (Agam & Berliner, 2004; Agam & Berliner, 2006) because

minimum temperatures in the early morning and late night often stay above dew point

temperatures (Kimball et al., 1997). McHugh et al. (2015) reports dew water cannot be

transferred to soil when the soil temperature is above dewpoint temperatures.

2.3 Hydrogels
2.3.1 History of hydrogels
The term 'hydrogel' was first published in an article in 1894, although the form of

hydrogel described in this initial article differs from the characteristics of hydrogel today

(Chirani et al., 2015). The production of water-absorbent polymers began in 1938

(Zohuriaan-Mehr & Kabiri, 2008) and the first 'modern' hydrogels were invented in the

late 1950s (Gómez, 2015). These first hydrogels were composed of hydroxyalkyl

methacrylate. Based on their ability to absorb water to 40-50% of their dry weight were

used to improve the performance of contact lenses (Zohuriaan-Mehr & Kabiri, 2008).

Later hydrogels were modified with polyhydroxyethylmethacrylate (pHEMA) to increase

their super-absorbing or high-water affinity capacities (Chirani et al., 2015) and were

produced using super-absorbent polymers (SAPs) in the 1960s by Union Carbide

(Mudiyanselage & Neckers, 2008). The Northern Regional Research Laboratory of the

United States Department of Agriculture (USDA) first developed commercial trials using

SAPs for agriculture in the 1970s using alkaline hydrolysis of starch-graft-

polyacrylonitrile (Gómez, 2015). This was a market failure due to structural shortcomings of weak gel strength and high product expense (Zohuriaan-Mehr & Kabiri, 2008). The commercialisation of SAP hydrogels began in 1978 in Japan with feminine sanitary pads. This led to the commercialisation of hydrogels in making other hygiene products, including baby diapers, in Germany and France around 1980.

Superabsorbent polymer (SAP) hydrogels are the most effective members of an extensive polymer group of hydrogels (Zohuriaan-Mehr et al., 2010). They can absorb about 1000 grams of water per hydrogel gram compared to 10 grams of water per gram of the standard hydrogel (Gómez, 2015; Kabiri et al., 2011). This property of SAPs has led to significant interest in product development over the past 30 years with near a million tons of SAPs produced since the 1990s (Zohuriaan-Mehr & Kabiri, 2008), about 80% used for infant diapers (Gómez, 2015). Despite the focus on sanitary products, ongoing development and application of SAP hydrogels has also occurred over the past 40 years to supply water for agricultural crops (Neethu et al., 2018).

2.3.2   Composition of hydrogels

Hydrogels are a uniquely soft or colloidal gel-like material composed of a three-dimensional network chain of macromolecular hydrophilic polymers crosslinked either physically or chemically to absorb and retain large water volumes (Chandrika et al., 2016; Ghobashy, 2020; Gómez, 2015; Neethu et al., 2018; Vermonden & Klumperman, 2015). Hydrogels can absorb water and swell to between 100 and 1000 times their weight (Abedi-Koupai et al., 2008; Mudiyanselage & Neckers, 2008). They do this by filling air spaces between polymers without dissolution (Kalhapure et al., 2016). Their composition characterises their absorption performance (Abedi-Koupai et al., 2008; Ganguly et al., 2020; Neethu et al., 2018), dissolution resistance (Ahmed, 2015) and structural integrity (Zhu et al., 2015).

2.3.3 Classification of hydrogels

Hydrogels are classified according to varying properties, including source, polymeric composition, configuration, cross-linking, physical appearance and network electrical charge (Ahmed, 2015). These properties influence single polymer molecules and determine their composition, structure, and behaviour in the large polymer molecule network chain that makes up a hydrogel.

Classification based on source. Hydrogels can be classified based on their production polymer source of origin (Ahmed, 2015). There are two main classes under this classification: natural and synthetic polymeric hydrogels (Abedi-Koupai et al., 2008). However, semi-synthetic hydrogels, a blend of the primary two classes, also exist. The differences in origin results in differences in characteristics and examples (Table 2.1).

Table 2.1 *Characteristics of source of origin-based hydrogel classes and their key example*

Class type	Characteristics	Key example
Natural polymer hydrogels	• Composed of forms like polypeptides (proteins) such as collagen and gelatine and polysaccharides such as starch, alginate and agarose (Bassas-Galia et al., 2017). • Also, fibrin, matrigel, hyaluronic acid, chitosan (Chirani et al., 2015), prokaryotic cells and eukaryotic cells (Ghobashy, 2020). • Often grafted to synthetic monomers for desirable properties (Ahmed, 2015; Ghobashy, 2020). Difficult to reproduce due to lack of understanding on characteristics (Chirani et al., 2015)	• Polysaccharides have a $(C_6H_{10}O_5)$n chemical formula and built-up of glycosidic (1-4)-linked glucose units bonded with sugar units (Ghobashy, 2020). • Based on properties, they are described as homopolysaccharides and heteropolysaccharides, charged neutrally, positively and negatively, and can be aqueous or non-aqueous soluble polysaccharides.
Synthetic polymer hydrogel	• Composed of polyacrylamides (PAM) and polyvinylalcohols as polymers (Abedi-Koupai et al., 2008) with base monomers such as lactic acid, acrylamide, vinyl acetate and ethylene glycol. • Source of polymers are petrochemical monomers like acrylic monomers and its salts (acrylates), and acrylic acid (Zohuriaan-Mehr & Kabiri, 2008), and plant-base monomers like lactic acid. • Modified to possess various desirable properties (Ghobashy, 2020).	• Polyacrylamide (PAM) is the most used polymer for synthetic hydrogels and can be either crosslinked or linearly linked to alter water dissolution characteristics (Kalhapure et al., 2016; Chalker-Scott, 2007). • Linear PAM can dissolve in water, whereas cross-linked PAM does not.

Classification based on polymer composition. The polymeric composition of hydrogels can differ from one to the other (Ahmed, 2015). Polymer composition influences the hydrophilic characteristics of the hydrogel's network matrix and biodegradability (Guilherme et al., 2015). Therefore, categorising the different polymer compositions in hydrogels into homopolymeric, copolymeric, multipolymer or interpenetrating polymeric (Ahmed, 2015) based on their individual monomers used in their production (Table 2.2) is essential for aligning hydrogels to target end uses. Individual monomers used for industrial hydrogels include acrylic acid, sodium or potassium salts of acrylic acid, and acrylamides whereas agricultural hydrogels include starch-grafted copolymers, cross-linked polyacrylates, cross-linked polyacrylamides and acrylamide-acrylate copolymers (Neethu et al., 2018). The main material composition is potassium polyacrylate polymerised with crosslinked acrylic to enhance high water retention efficiency and to mitigate concerns of ecotoxicity.

Table 2.2 *Description of polymer composition-based hydrogel classes*

Classification type	Description
Homopolymeric hydrogels	• Composed of a single type of monomer species which exists as the basic structural unit and forms the polymer network (Ahmed, 2015).
Copolymeric hydrogels	• Composed of two or more monomers, with at least one hydrophilic monomer (Ahmed, 2015) that are configured either on random, block or alternating arrangement on a polymer network chain. • Include cross-linked polyacrylates, polyacrylamides and maleic anhydride copolymers, hydrolysed cellulose-polyacrylonitrile, and starch-PAN graft copolymers (Zohuriaan-Mehr & Kabiri, 2008).
Multipolymeric hydrogels	• Composed of more than one polymer type in their composition which are synthesised together through crosslinking.
Interpenetrating (IPN) hydrogels	• Composed of a polymer network structure comprising of two independent crosslinked synthetic or natural polymer elements (Ahmed, 2015) with one of the polymers synthesised either within or around the other. • Usually, one of the polymers possess desirable characteristics required to improve hydrogel properties (Zohuriaan-Mehr & Kabiri, 2008). There are also semi IPN hydrogels that have a cross-linked polymer and non-cross-linked polymer in their composition (Ahmed, 2015).

Classification based on cross-linking types. Crosslinking of polymers is the fundamental factor that influences almost every characteristic of a hydrogel (Chirani et al., 2015). The type of crosslinking adopted in the production of a hydrogel can influence

its water absorption potential. Other properties that can be affected include porosity, mechanical and rheological characteristics, swelling kinetics, rate of degradation and toxicity (Guilherme et al., 2015). For example, Abdel-Halim & Al-Deyab (2014) reported that crosslinking during hydrogel preparation increases tensile strength as the polymer chains bind to each other more closely and firmly. Crosslinking polymers is achieved using a crosslinker, and the crosslinker concentration is positively correlated to its crosslinking density, which determines swelling and dissolution capabilities (Mudiyanselage & Neckers, 2008). Based on the nature of cross-link junctions which characterise the hydrogel network, hydrogels are classified either into chemical or physical cross-linked networks (Ahmed, 2015). Their crosslinking degree is regulated to alter hydrogel properties in targeting specific end use application characteristics (Chirani et al., 2015) (Table 2.3).

Table 2.3 *Description of differently crosslinked hydrogel types*

Cross-linking types	Description
Physical crosslinked hydrogels	• Possess reversible, weak and easily broken network junctions in hydrogels (Ahmed, 2015; Vermonden & Klumperman, 2015) due to polymers network entanglement and interaction with each other. • Weakly bonded over hydrogen bonding, hydrophobic chain interactions, and ionic interactions a polyanion and a polycation, or a polyanion and multivalent cations (Chen, 2019). Examples includes crosslinking interactions between polyelectrolytes and a multivalent ion (Chirani et al., 2015). • Polymer entanglement is the most widely used form of physical crosslinking.
Chemical crosslinking	• Possess permanently cross-linked bonded network junctions (Ahmed, 2015; Ganguly et al., 2020) from covalent or ionic crosslinking from either ultraviolet irradiation, heating or chemical reactions (Vermonden & Klumperman, 2015). These are produced during crosslinking of water-soluble polymers and such crosslinking can convert hydrophobic polymers into hydrophilic state (Chirani et al., 2015).

Classification based on hydrogels' physical appearance. Polymerisation techniques used during hydrogel preparation strongly influence the physical appearance of hydrogels (Ahmed, 2015). Physical appearance allows categorisation of hydrogels into matrix, film or microsphere hydrogel types.

Classification based on the network chain electrical charge. The presence or absence of electrical charge on crosslinked hydrogel networks differentiates hydrogels (Ahmed, 2015). As such, hydrogels can be grouped as non-ionic (neutral), ionic (anionic or cationic), amphoteric electrolyte (ampholytic – both acidic and basic), and zwitterionic

(polybetaines, composed of both anionic and cationic charge in every repeating structural unit) (Zohuriaan-Mehr & Kabiri, 2008). Most commercialised superabsorbent and conventional hydrogels are anionic.

Classification based on the starting point of production. Hydrogels, based on their starting point of production, can be classified into three groups. 1) Hydrogels produced by the preparation of monomers formed in a repeated copolymerisation style into a network of high-molecular-weight polymers. 2) Hydrogels from a network of low molecular weight polymers called prepolymers (oligomers), which are further polymerised. 3) Hydrogels produced from a network of existing polymers utilised in their production or synthesis.

Classification based on polymer configuration. Variations in chemical composition influence the physical structure of hydrogels. Maolin et al., (2000) and Ahmed, (2015) categorised the various physical forms of hydrogels as amorphous (non-crystalline), crystalline and semi-crystalline (a blend of amorphous and crystalline structure).

2.3.4 Properties of an ideal hydrogel

Hydrogels respond to external stimuli such as temperature, concentrated solvent and pH with a volume change (Bahram et al., 2016; Neethu et al., 2018). This expansion process influences the elasticity and viscosity properties and functions of a hydrogel (Ganguly et al., 2020). Zohuriaan-Mehr (2006) reports that an ideal hydrogel has high absorption capacity, retains maximum absorption even under load or pressure, high insolubility, maximum durability and stability during swelling and storage. The ideal hydrogel has a neutral pH after swelling in water, is non-toxic, has strong re-wetting capabilities, is

colourless and odourless, will eventually biodegrade, and is cheap. However, achieving all of these ideal features is likely to be impossible. Therefore, the most optimal properties required are identified for each field of hydrogel application (Ahmed, 2015). Improvements in the productivity and efficiency of hydrogels can be realised by modifying some of the properties of hydrogels (Ahmed, 2015). Neethu et al. (2018) proposed that swelling and reaction with the surrounding environment are the most important physicochemical properties of hydrogels.

In agriculture, an ideal hydrogel must ensure that nutrients absorbed in a water solvent are constantly available to plants to support plant growth and yield. Properties such as maximum absorption capacity (even under stress conditions), low price, insolubility, durability, soil stability, re-wetting, biodegradability and pH neutralisation are vital for agriculture hydrogels (Neethu et al., 2018). Hydrogels act as water reservoirs for soils and hold onto absorbed water, subsequently releasing this to plant roots when water demand creates a difference in osmotic pressure (Zohuriaan-Mehr & Kabiri, 2008). The impact of hydrogels on soil structure, texture, bulk density, evaporation and infiltration rate in agricultural soils must also be considered. Other properties such as the potential to enhance soil microbial activity, targeted reduction of soil compaction and mitigation of runoff, even in unfavourable climatic conditions, are desirable functions in agricultural application. Different hydrogels show variable performance under varied soil types. Stability in the soil, required rates for nursey and field soil application, compatibility with herbicides and fertilisers, and capacity to enhance plant endurance to water stress are all properties that can be targeted to specific soil types (Kołodyńska et al., 2016).

Hydrogels used for agriculture in semi-arid and arid areas possess high rates of water absorption even at temperatures between 40 to 50 ºC (Neethu et al., 2018). Even under such temperatures, hydrogels can absorb water to about 400 times their dry weight and

release it gradually into the soil pores for plant usage. The application of hydrogels to arid agricultural soils has been shown to enhance soil physical properties, encourage germination, promote root growth, improve water and nutrient utilisation, limit the need for irrigation, and delay plant wilting. Pattanaaik et al. (2015) and Taylor and Halfacre (1986) confirm hydrogels enhance plant water stress resistance in high temperature and dry climatic areas and thus improve food production. Callaghan et al. (1989) and Ekebafe et al. (2011) state that hydrogels encourage best crop yield performance in sandy soils (Johnson, 1984), which often predominate in semi-arid and arid areas.

2.3.5 Application rates of hydrogels in agricultural soils
The efficiency and effectiveness of hydrogels in conditioning soil and retaining moisture is often a function of the application rate. Applying the right amounts of hydrogels to soil can increase water retention to about 50-70 % and reduce about 8-10 % of soil bulk density (Neethu et al., 2018). Different soil types have different water retention needs and therefore have different hydrogel application dosages; rates need to be determined by soil analysis. However, generic hydrogel dosage application charts have been developed for some specific soil types and purposes to simplify hydrogel usage (Table 2.4).

Table 2.4 *Application rate of hydrogel in soils (Neethu et al., 2018)*

Type of soil	Suggested dosage of hydrogel
Arid and Semi-arid regions soils	4 – 6 g//kg soil
For all level of water stress treatment and improved irrigation period in soils in the arid and semi-arid area.	2.25 – 3 g/kg soil
To delay the permanent wilting point in sandy soils.	0.2- 0.4 g/kg or 0.8 % of soil, whichever is more
To reduce irrigation water by 50% in a loamy soil.	2 – 4 g/plant hole
To improve relative water content and leaf water use efficiency.	0.5 – 2.0 g/plant hole
To reduce drought stress	0.2 - 0.4 % of soil
To prohibit drought stress totally	225 – 300 kg/ha of cultivated area
To decrease water stress	3 % by weight

2.3.6 Applying hydrogels to support agriculture in arid/semi-arid regions

Generally, the application of hydrogels to agricultural soils improves the yield and growth of cultivated agricultural plants (Kazanskii & Dubrovskii, 1992; Pattanaaik et al., 2015). Callaghan et al. (1989), Save et al. (1995) and Specht and Harvey (2000) show a positive effect of hydrogel application on plant performance in tree seedling establishment in arid regions. For example, the tree species *Flindersia brayleana* (Queensland maple) and *Dysoxylum muelleri* (Red bean) which have poor drought-tolerance have been recorded to increase dry weight following hydrogel application in soils, indicating growth promotion. However, in this same study, the drought-tolerant tree species *Flindersia australis* (Australian teak) and *Grevillea robusta* (Silky oak) showed no significant

change in dry weight between the control and the hydrogel treated plants (Koupai et al., 2008).

2.4   Knowledge gap, opportunities, and the aims of the current research

Hydrogels have the technical potential to absorb atmospheric water and provide this water to plants in arid and semi-arid regions. If this potential is realised, hydrogels could be beneficial in mitigating water deficits in arid regions and could potentially alleviate water stress that might be anticipated from climate change. However, the potential of hydrogels to absorb atmospheric water under the particular relative humidity and temperature conditions of arid and semi-arid regions, and of those associated with projected climatic changes, has not been adequately assessed. Similarly, there has been limited study on the conditions needed to recover useful water from hydrogels where this water is absorbed from the atmosphere. Therefore, the current research was designed and conducted to assess the absorption atmospheric water by hydrogels under variable relative humidity and temperature condition, and the desorption of water from the hydrogels measured in relation to plants osmotic pressure. The conditions used in this research have been developed to model scenarios that might be expected in environments where hydrogels could be used to support agricultural production.

2.4.1   Specific objectives of the research

The specific objectives of the research are to

a. Assess the capacity of hydrogels to absorb moisture from the atmosphere under different humidity and temperature levels.

b. Assess the capacity of hydrogels to release the absorbed water under different suction pressures.

CHAPTER THREE

3 INVESTIGATING HYDROGEL HYGROSCOPICITY POTENTIAL

3.1 Introduction

The hygroscopicity of a substance is defined as its ability to absorb atmospheric water molecules (atmospheric humidity) and hold this water until an equilibrium moisture content is reached (Gómez, 2015). The hygroscopicity of a substance is determined through incremental changes in the gravimetric weight of the original substance after exposure to certain atmospheric temperature and humidity conditions. Increasing the amount of atmospheric water molecules increases the amount of water that can potentially be absorbed into a substance and polymeric materials have been recognised to have good atmospheric water absorption potential (Dubelley et al., 2017). As polymeric materials absorb water, their glassy state changes to a rubbery state. This change of state allows for large rates of absorption at temperatures above the glassy state temperatures.

Hydrogels, as super-absorbing polymers, have the potential to absorb water molecules from the atmosphere (Urbina et al., 2021). This property makes hydrogels an interesting target as a novel water reservoirs or source of freshwater for agriculture. However, to explore this potential, information on the rate and amount of water absorbed at specific air temperature and humidity levels is needed to optimise water absorption. Specifically, there is a need to investigate the temperature and relative humidity conditions that underpin the maximum hygroscopicity of hydrogels.

3.2 Water absorption in hydrogels

The process of water absorption in a hydrogel begins with hydration of the most polar hydrophilic groups on the hydrogel's gel surface by the first few water molecules that diffuses into the matrix of a dry hydrogel (Salleh et al., 2018). These water molecules that bind strongly to hydrogels as primary bound water (Mudiyanselage & Neckers, 2008).

Initial hydration enables swelling by unwinding the polymer network chain in an opposite direction to increase volume or size for increased absorption of subsequent water molecules (Ahmad et al., 2020; Zlatev & Lidon, 2012). This is attributed to electrostatic force repulsion created between negative charges left in the hydrogel after the bonding of functional groups with water molecules. Subsequently, hydrophobic groups are exposed to contact with water molecules (Zonatto et al., 2017), and this becomes weakly secondary bound water. Primary and secondary bound water are referred to as total-bound water (Chirani et al., 2015). An increased presence of hydrophobic groups lowers the degree of swelling when there is no negative charge repulsion created (Zonatto et al., 2017). After these processes, depending on pores and spaces available (Xie et al., 2009), unlimited water absorption is enabled into the polymer network through an osmotic force between the polymer network chains and water molecules until the osmotic force concentration difference is minimal at dilution. The large volume of absorbed water filling network gaps, pores and spaces is referred to as free water or bulk water (Chirani et al., 2015; Mudiyanselage & Neckers, 2008). Hydrogel crosslinking creates an elastic network 'elasticity force' that opposes absorption and prevents polymer network over-stretching and deformation (Ganji et al., 2010). When the absorbing osmotic force and the opposing absorption elasticity force equals each other, equilibrium swelling point is reached, and no further significant swelling occurs. Swelling in hydrogels is therefore not a continuous process, and definitively stops at a point. At water saturation or equilibrium point, the polymer network chains and crosslinks begin to degrade, dissolve or disintegrate at varying rates depending on the hydrogel's composition (Chirani et al., 2015).

3.2.1   Absorption and swelling capacity of hydrogels

Swelling and absorption potential is a hydrogels' primary desired characteristic and understanding the structure and properties of hydrogels is beneficial to determining the maximising swelling and absorption potential (Guilherme et al., 2015). Swelling and absorption in hydrogels depends not only on the hydrogel structure, but also on a hydrogel's porosity, as is common for most superabsorbent substances (Gómez, 2015). However, the internal and surrounding environment of a hydrogel also influences the absorption and swelling properties (Neethu et al., 2018). As such, realising the absorption potential of a hydrogel is dependent on several other factors and mechanisms besides the classical rules that 1) increasing number and size of porosity increases absorption, and 2) increasing bulk density decreases absorption. The chemical composition and crosslinking properties of a hydrogel, and its environmental factors, including pH, aqueous ionic strength concentration and temperature, determines a hydrogel's swelling potential (Chan & Neufeld, 2009; Flory, 1953; Guilherme et al., 2015; Khare & Peppas, 1995; Molloy et al., 2000; Moura et al., 2008; Paulino et al., 2011). Under hygroscopic absorption, air temperature and relative humidity are the fundamental environmental factors which determine a hydrogel's absorption and swelling potential (Urbina et al., 2021).

3.2.2   Factors influencing absorption and swelling in hydrogels

Absorption and swelling in hydrogels is influenced by multiple factors. Crosslinking concentration, degree and type present in a hydrogel influence the formation of the 3D polymer density and subsequently limits water absorption (Xie et al., 2009). Higher crosslinking concentration in hydrogel internal structure increases polymer entanglement leading to a denser and more compact hydrogel 3D polymer. This subsequently decreases water movement and also results in a reduced number of pores which limits absorption and swelling (Cheng et al., 2017). Hydrogels expand their 3D polymer network with an

elastic force to allow space for absorption within their structure. However, increasing the density of the 3D polymer network restrains hydrogel expansion capacity (Xie et al., 2009), and subsequently encourages low absorption and sort time absorption (Quintanilla de Stéfano et al., 2020). This is due to the osmotic force quickly pulling the water molecules into the hydrogel but or equally the constrained elastic force of 3D polymer expansion also increasing quickly. Ahmed et al. (2016) identified swelling differences in hydrogels by changing the crosslinking agent N, N-methylene bis acrylamide (MBAm) dose concentrations. N percentages in acrylamide AAM hydrogels have been associated with crosslinking components that reduce maximum absorption in hydrogels (Pooley et al., 2010; Zhou et al., 1997). Often, high N percentages leads to reduced swelling potential as it becomes a crosslinker after reaching maximum percentage to allow absorption and subsequently limit absorption. As such, N % in hydrogels based on the hydrogel composition, is require to be at the right composition percentage to enable absorption. Pooley et al. (2010) study shows AAm hydrogels with N % of 3.36 – 7.39 increased absorption but a further increment in N% to 7.68 – 9.84 reduced absorption. Furthermore, Ahmad et al. (2020) confirmed a decreasing effect on swelling ability after an early quick absorption rise when the borax cross-linker concentration was increased. All of these crosslinking attributes create potential self-entanglement that subsequently compacts the 3D polymer density structure and prevents swelling for absorption.

However, Mudiyanselage and Neckers (2008) describe a sufficient increase in crosslinking on hydrogel surfaces prevents surface collapse and the blocking of hydrogel particle surface pores. This leads to increased water uptake into the hydrogels as it enhances firmness for passage through pores that might otherwise have collapsed from load and pressure during a repetitive absorption and desorption process. This assumption on crosslinking is confirmed by Chavda and Patel (2011) who report that increasing

crosslinker concentration enhances the mechanical stability of hydrogels by decreasing swelling porosity. Applying the correct crosslinker concentration can therefore yield better swelling outcomes.

The presence or absence of hydrophilic and hydrophobic polar groups in the 3D polymer network stimulates absorption (Paulino et al., 2011; Zonatto et al., 2017). Hydrophilic functional group sites in a hydrogel polymer network initiate swelling by hydrating themselves with the first few water molecules (Chirani et al., 2015) to expand and open up the polymer network (Ahmad et al., 2020). Buchholz and Graham (1998) report the hydrophilic functional groups preferentially create strongly covalent bonds rather than hydrogen bonding with water hydrogen ions and dissociate as positive and negative ionic species on a polymer network chain when in contact with water molecules. The negative charges begin to repel each other by an electrostatic force to unwind the polymer chains and expand the swelling space for increased water absorption. However, such repulsion does not occur on the hydrophobic functional groups of a hydrogel when in contact with water, and this leads to less swelling space for water absorption. Therefore, increasing the abundance of hydrophilic functional groups increases water absorption and swelling in hydrogels whereas the reverse occurs with an increase in hydrophobic functional groups (Kalhapure et al., 2016). Guilherme et al. (2015) report an incremental change in equilibrium swelling when hydrophilic properties were enhanced by an increased concentration of carboxymethylcellulose (CMC). Ahmad et al. (2020) showed incremental changes in polyvinyl alcohol concentration in hydrogels can increase hydrophilicity and subsequently water absorption, but excessive addition may potentially block hydrophilic groups, and hence reduce swelling. Furthermore, the hydrophilicity capacity of hydrogels can be destroyed, effectively reducing swelling capacity under a

repetitive swelling-deswelling process (Montesano et al., 2015). Ahmad et al. (2020) explains the process potentially blocks and collapses the hydrophilic group sites.

Hydrogel particle size is also an important factor which controls the swelling ability of hydrogels (Gómez, 2015; Guilherme et al., 2015; Omidian et al., 2005). The smaller the hydrogel particle size, the greater the surface to volume ratio leading to increased binding potential. The opposite effect is apparent for large hydrogel particle size. The surface of a hydrogel is essential for absorption because the more hydrated the surface, the better the diffusion of water from the outside into the inside of the hydrogel (Mudiyanselage & Neckers, 2008). Hydrogel geometry also influences the water absorption mechanism. Neethu et al. (2018) reports that measurements of geometric dimension and shape changes could be used to assess hydrogel swelling progression. Hydrogels of fixed shape, such as water bead hydrogels, have high crosslinking properties whereas hydrogels of uneven and non-firm shapes have low crosslinking properties. Crosslinking increases mechanical strength but reduces absorption and swelling potential: hydrogels with a high swelling rate absorb water faster. The mechanical characteristics of a hydrogel can be weakened by swelling magnitude (Guilherme et al., 2015), ionic forces at active sites (Ahmed, 2015), and repetitive swelling and deswelling process. Mechanical strength collapse closes pores for absorption and subsequently limits the amount of water that can be absorbed or desorbed. Gómez (2015) and Zohourian-Mehr and Kabiri (2008) indicated that the swelling capacity of hydrogels is influenced by soil pressure and stress.

3.2.3   Diffusion and swelling mechanisms in hydrogels

The absorption mechanism in hydrogels is determined by the diffusion process (Ahmed et al., 2016; Buchholz & Graham, 1998). This is characterised by a haphazard, random and disarranged movement of molecular particles into the hydrogel. These diffused water molecules possess energy, creating an energy gain in the hydrogels due to external and

internal chemical reactions until an equilibrium absorption point is reached of equal exterior and interior water concentration (Ono et al., 2007). The movement of water molecules into hydrogels is observed is a slow process due to their small size relative to the hydrogel particle size and can be influenced by the hydrogels' crosslinking degree and polymer network density (Liu & Guo, 2001). Notably, water absorption and water release are the principal solvent transport mechanisms that are of scientific and technological interest in the application of hydrogels to soil. Water diffusion in hydrogels is characterised mainly by the Fickian diffusion model (Zonatto et al., 2017). Swelling kinetics have been characterised by Fick's model or a first order process, but during longer swelling periods swelling kinetics deviate to different swelling kinetics or mechanisms (Ahmed et al., 2016). Fickian diffusion assumes the constant flow of diffusant per unit area over time as a function of the concentration gradient (i.e. the concentration (φ), per unit length (x)) (Duncan & Broughton, 2007). Also, Bagley and Long (1955) and Bao et al. (2001) report the concentration gradient set up between polymers and the environment creates rapid diffusion at the initial stage. Gómez (2015) described the Fick's law with a diffusion flux proportional to the concentration gradient of water molecules (minus) from higher concentrations to low concentrations in a hydrogel. This can be mathematically represented by Equation 1 (Duncan & Broughton, 2007)

$$dJ / dt = -D \cdot (\partial c / \partial x) \text{ (Duncan \& Broughton, 2007)} \qquad \textit{Equation 1}$$

where J represents the diffusion flux (flux of diffusant per unit area), t represents time, D represents the diffusion coefficient and ($\partial c / \partial x$) represents the concentration gradient.

Equation 2 describes standard diffusion in polymers where the boundary surface layer of a particle is hydrated with contact of constant supply of water molecules which are drawn into the hydrogel by concentration gradient. The flow continues but at a decreasing rate with time as the concentration gradient decreases. From this point water molecules slowly and uniformly penetrate into the polymer sample (Jansen et al., 2020). Duncan and Broughton (2007) propose that Fick's second law equation can be used when the diffusion coefficient (D) does not depend on concentration but instead on time at the latter stages of the diffusion mechanism. The second slow diffusion stage can be explained by the slow relaxation process of polymer network chains as they expand, enabling more diffusant molecules to be absorbed in the process. Tanaka and Fillmore (1979) proved that the diffusion coefficient of a gel network for swelling dependent on time can be calculated. The coefficient of diffusion is dependent on temperature. Therefore, temperature increment increases the diffusion rate of water molecules and hastens system ageing (Duncan & Broughton, 2007). This is assumed as a one-dimensional approach which eliminates additional moisture from the edge effect when the ratio of face area to edge area is very large (Jansen et al., 2020). Mathematically, Fick's second law is represented by Equation 2

$$\partial C / \partial t = D \left(\partial^2 C / \partial x^2 \right) \qquad\qquad Equation\ 2$$

where diffusivity, D is in mm^2/s and concentration, C is in mg/mm^3.

The swelling kinetics of a hydrogel describes the velocity at which absorption occurs, and this gives in-depth knowledge on the behaviour and performance of hydrogels for absorbing surrounding water (e.g., water in the soil or in the atmosphere) (Gómez, 2015). Kinetic studies allow the hydrogel's swelling order to be determined by multiple diffusion

models (Bao et al., 2001). First order kinetics (Fick Model) can be observed for the early swelling times and second order kinetics (Schott Model) for swelling at longer absorption times when the hydrogel's density has increased leading to deviations from Fickian diffusion (Ahmed et al., 2016). Urbina et al. (2021) proved some of these absorption anomalies through the observation of irregular condensed water absorption on hydrogels relative to bare substrate due to processes including vapor adsorption. Their work found that hydrogels have high efficiency in capturing atmospheric water due to enhanced water capture by adsorbing vapor water and condensed water vapor. Jansen et al. (2020) observed diffusion absorption processes from a humidity chamber to be mildly non-linear with Fickian diffusion. Such diffusion dynamics have led to multiple swelling kinetic models derived from the second-order model equation that have been developed to analyse experimental data and model deviations in swelling process observed within hydrogels (Ahmed et al., 2016). Omidian et al. (1998) described the diffusion stages as a viscoelastic swelling behaviour which can be characterised with the Voigt-based viscoelastic model. Bao et al. (2001) explained recorded deviations as a factor of the plasticization behaviour of water absorbed molecules during moisture diffusion into hydrogels.

Bao et al. (2001) reports a range of dynamic models developed to describe non-Fickian diffusion including, stress-dependent diffusivity models, history-dependent diffusivity models and dual phase diffusion models. Diffusion in hydrogels can be described by concentration-gradient-driven Fickian diffusion and time-dependent relaxation non-Fickian diffusion. The standard diffusion mechanism assumes that a polymer sample during absorption first saturates its surface layer until constant or equilibrium water concentration is reached, after which time water slowly and uniformly penetrates into the polymer (Jansen et al., 2020). During absorption an incremental increase in surface

hydration is observed with time. Long and Richman (1960) describes diffusion variations with a model based on surface concentration and time. Bagley and Long (1955) in an investigation of acetone diffusion into cellulose acetate observed two-step swelling behaviour where the initial phase was associated with rapid diffusion and then a later slow diffusion stage until equilibrium was reached.

The two-stage swelling behaviour described here is often characterised by a rapid increase in absorbed water until a swelling equilibrium point is reached, then the absorption rate decreases, and swelling begins to level or decrease. Yin et al. (2007) attributed the rapid absorption to hydration and pore absorption due to the concentration gradient difference. Mudiyanselage and Neckers (2008) proposed that the high initial swelling rate is a factor of surface layer crosslinking creating stiffness and allowing super-absorption through high rates of water flow. These authors propose that incremental increases in surface crosslinking increase the swelling rate. The recorded decrease in swelling after maximum equilibrium absorption in their work was attributed to the function of internal crosslinking concentration. High crosslinking concentration makes the hydrogel polymer network denser, the network chains entangle and minimises pore space limiting flow for swelling and absorption (Ahmad et al., 2020). This highlights how porosity, elasticity network and the crosslinking extent of polymer hydrogels characterises hydrogels swelling and release properties (Chandrika et al., 2016; Kim & Park, 2004). Quintanilla de Stéfano et al. (2020) proposed that hydrogel swelling behaviour is dependent on boundary surface properties, solute movement, and the mechanical characteristics of the hydrogel. Hydrogel polymer composition, including crosslinking type, monomer functionality and structure, ensure an equilibrium point with the surrounding solvent concentration and temperature to maintain mechanical strength, stiffness and shape and avoid hydrogel dissolution which can create a scenario of limited and viscous flow (Chirani et al., 2015).

According to Ahmed et al. (2016), the second stage of absorption can be described by a second order swelling kinetic model, Equation 3

$$dS/dt = K_s \, (S_{eq} - S_t) \qquad\qquad \textit{Equation 3}$$

where dS/dt is swelling (as a function of time), K_s is the swelling rate constant, S_{eq} is the swelling degree at equilibrium and S_t is swelling at a particular time, t. The authors report the general diffusion can be modelled to explain hydrogel absorption of water in its three-dimensional network using Equation 4,

$$S \, (g/g) = w_t / \, w_{eq} = kt^n \qquad\qquad \textit{Equation 4}$$

when the weight of absorbed water mass at a specific time (w_t) is less or equal to 0.7 times the weight of absorbed water mass at equilibrium time (w_{eq}) [$w_t \leq 0.7 \; w_{eq}$]. k represents the swelling constant describing the polymer network of the hydrogel and n is the diffusion coefficient which is the parameter describing the mechanism by which water diffuses into hydrogels (Zonatto et al., 2017). Equation 4 can be transformed using natural logarithms (ln) into a linear equation, Equation 5 when,

$$\ln \, (w_t/w_{eq}) = \ln k + n\log \, (t), \; w_t < 0.7w_{eq} \qquad\qquad \textit{Equation 5}$$

With equation 5, a plot of $\ln(w_t/w_{eq})$ against $\ln(t)$ the slope gives n and the intercept $\ln(k)$. Diffusion in polymers is non-linear with transport processes of polymer relaxation and solvent diffusion driven by concentration through pores (Frisch, 1980). Swelling behaviour can be described by three transport categories based on rate: Fickian/case I

transport; case II transport; and anomalous transport where solvent the diffusion rate is slower than the relaxation rate of the polymer matrix, or rapid diffusion where the diffusion is faster than relaxation rate of the polymer matrix and where R_{diff} and R_{relax} are percentage-wise comparable respectively. Using the value of n from the linear equation from the plot of $\ln(w_t/w_{eq})$ against $\ln(t)$, diffusion transport can be identified. Aggor et al. (2010) and Ahmed et al. (2016) report that for cylindrical shaped hydrogels, a n value between 0.45 – 0.50 shows water movement into the hydrogel is by Fickian diffusion, and that water molecules move through the pores of the polymer chain. When n is between 0.50 – 1.0, the mechanism of water transport is non-Fickian, and the diffusion of water molecules is potentially through both absorption by swelling kinetics stages of pores and also by absorption by the macromolecular polymer network relaxation. Siepmann and Peppas (2012) reported use of a polymer geometric categorisation for n to determine the diffusion transport mode. For thin film polymers, Fickian diffusion is expected for an n value of 0.5, anomalous transport is expected for n in the range of 0.5 $< n < 1.0$, while case II transport is expected for n value of 1.0. For cylindrical shaped polymers, Fickian diffusion is expected for an n value of 0.45, anomalous transport is expected for n of range $0.45 < n < 0.89$ and case II transport is expected for n value of 0.89. For spherical shaped polymers, Fickian diffusion is expected for n value of 0.43, anomalous transport is expected for n of range $0.43 < n < 0.85$ and case II transport is expected for n value of 0.85.

3.2.4 Diffusion and swelling mechanism models

Moisture diffusion into hydrogels is not uniform and has been observed to deviate from Fickian diffusion (Chapter 3.2.3). A range of second-stage swelling behavior theories have therefore been proposed to describe the mechanistic process of polymer water absorption. Aside from the normal Fickian diffusion or first-order kinetics, the Korsmeyer

– Peppas and Collaghan-Garaghan diffusion models have been used to describe the swelling kinetics behaviour of hydrogels. The inverse of these models can also be used to describe the release or desorption kinetics or behaviour of water from polymers (Jansen et al., 2020; Paarakh et al., 2018).

3.2.4.1 First order kinetic model

The first order kinetic model is derived from a dual absorption process at the liquid/solid phase (Wu et al., 2021). The modelled water absorption rate into polymers is dependent on concentration (Paarakh et al., 2018). At high initial solute concentrations, the model is reported to be very accurate (Wu et al., 2021). First order kinetics can be mathematically described by Equation 6,

$$S = S_{max}\,[1 - exp\,(- k_f t)] \qquad\qquad Equation\ 6$$

where, K_f is the first order swelling constant rate factor (s^{-1}), t is time, S is the mass of water adsorbed per mass of adsorbent, S_{max} is the mass of water adsorbed per mass of adsorbent at maximum swelling.

3.2.4.2 Korsmeyer - Peppas Model

The Korsmeyer - Peppas model is a simple and often used non-linear diffusion transport model which is mathematically represented by an empirical equation of swelling exponent (n) and swelling rate constant (k). The Kosmeyer-Peppas model (described by Equation 7) is used to characterise non-linear Fickian diffusion swelling in a polymeric system (Paarakh et al., 2018; Wu et al., 2021).

$$M_t\,/\,M\alpha = K t^n \qquad\qquad Equation\ 7$$

where M_t is the mass of water absorbed or released at a time, t, M_α is the mass of water released or absorbed at equilibrium or maximum point or infinite time, M_t/M_α is the fraction of the absorbed or released water at a time, k is the rate constant with units of t^n which is dependent on structural and geometric characteristics of the polymeric system, and n is the absorption exponent used to describe the different water absorption transport mechanisms within the polymer (Paarakh et al., 2018; Wu et al., 2021). Application of the Korsmeyer - Peppas model is limited by inaccuracy above the first 60 percent of the swelling profile (Siepmann & Peppas, 2012).

3.2.4.3 Gallagher Corrigan model

The Gallagher Corrigan model is a modified Korsmeyer - Peppas model which is increasingly being used to describe absorption kinetics (Wu et al., 2021), especially in biodegradable polymers (Paarakh et al., 2018). The mathematical representation of the model (Equation 8) describes the fraction of absorbed water within a biodegradable polymeric system using a two-stage diffusion theory, first-order diffusion into the polymer matrix followed by slow-smooth diffusion causing polymer degradation as a consequence of matrix erosion (Gallagher & Corrigan, 2000; Paarakh et al., 2018; Wu et al., 2021)

$$S = S_1 \left[1 - \exp(-k_1 t) \right] + (S_{max} - S_1) \left[\frac{\exp\left(k_2 \{ t - t_{max} \} \right)}{1 + \exp\left(k_2 \{ t - t_{max} \} \right)} \right] \qquad \textit{Equation 8}$$

In Equation 8, S is the fraction of drug released in time, t; S_{max} is the mass of water adsorbed per mass of adsorbent at maximum swelling during process, S_1 is the mass of

water adsorbed per mass of adsorbent at stage 1 swelling, K_1 – the first order diffusion kinetic constant or swelling rate for the stage 1, K_2 – the kinetic constant for 2nd stage of smooth diffusion matrix degradation process; t_{max} – time to maximum diffusion rate. The calculated value of S is plotted against the time; and the corelation coefficient and coefficient of determination can be calculated to understand the suitability of the model.

3.2.5 Impacts of relative humidity and temperature on hygroscopicity

The relative humidity of an environment significantly influences the absorbed water content in hydrogels. Gómez (2015) and Jansen et al. (2020) showed that relative humidity increases moisture saturation levels and increases the probability of atmospheric water absorption into a hydrogel from its surroundings. Relative humidity is dependent of the partial pressure of water and the saturation vapor pressure of water (Dubelley et al., 2017). A high relative humidity at saturation point is the maximum amount of water molecules that atmospheric air can hold. As such, any further increase in relative humidity creates of 'free' water and can increase the water content in hydrogels especially at dew points and at low vapour pressure levels induced by low temperatures. This is because the partial pressure of water is often constant whereas the saturation vapor pressure of water is determined by a decrease or increase in temperature until saturation point.

Relative humidity can interact with many other factors before absorption by polymers (Dubelley et al., 2017). Gómez (2015) showed that increasing relative humidity increases the water content in hydrogels. This work proved a mild influence of particle geometry on differences in hydrogel water content indicating that relative humidity can affect the water content in hydrogels, but interaction with other factors may lead to further differences in potential absorbed water content. The influence of temperature on humidity saturation shows an increment in moisture content absorbed as a function of temperature

(Jansen et al., 2020). Increasing temperature can result in a rapid increase in relative humidity and this can lead to deviations from diffusion linearity. Increasing temperature at saturated relative humidity increases the energy associated with the motion of water molecules (Dubelley et al., 2017). This energy can drive absorption which subsequently increases the absorbed moisture content of hydrogels (Chen et al., 2011; Jansen et al., 2020). However, Jansen et al. (2020) reports that the impact of temperature on relative humidity as a driving factor on water absorption by polymeric materials is poorly described in literature.

Temperature also impacts swelling during absorption, and this has been reported in many studies. Increasing temperature creates thermal expansion of the polymer 3D network and destabilises jointed junctions to enhance opening and widening of the matrix after water has entered pores or voids (Guilherme et al., 2015). Furthermore, during viscoelastic processes or molecular relaxation due to water contact, temperature reduction is observed during the transition from the glassy polymer state to rubbery state (Dubelley et al., 2017). This creates an opportunity for pore space opening for free volume water absorption (De Vreugd, 2011). Increasing the temperature above the glassy polymer state temperature accelerates the viscoelastic or relaxation process creating soft and flexible polymers during absorption (De Vreugd, 2011). Chandrika et al. (2016) showed that an increase in temperature from 8 to 50 ºC increased the absorbed water content from 55 to 160 grams/grams, at which point the equilibrium swelling point was reached. Serrano-Aroca and Deb (2020) describe how multiple hydrogel research efforts are directed to target fast temperature sensitivity (thermosensitivity) to enhance hydrogel absorption capabilities. However, the impact of temperature on hydrogel swelling and absorption stops at critical points. Abdel-Halim and Al-Deyab (2014) reported a temperature increase from 120 to 150 ºC yielded enhanced swelling in hydrogels but a further temperature rise had no

subsequent effect on swelling and absorption. Analytical techniques such

Thermogravimetry – TGA, Differential Scanning Calorimetry – DSC, and Differential

Thermal Analysis – DTA have been used to determine the physical properties of

hydrogels such as melting and glass transition temperatures which describe hydrogel

thermal stability during swelling interactions with water (Guilherme et al., 2015).

3.2.6 Aims and objectives of research

The experiments conducted in this chapter aimed to assess the hygroscopicity potential

of different hydrogels under varied air temperature and relative humidity levels. This

aimed to assess the best-performed hydrogel under varied temperature and relative

humidity conditions, and to identify the associated diffusion and swelling profile that best

fits the recorded experimental data at particular temperature and relative humidity levels.

3.3 Methodology
3.3.1 Estimating hygroscopic water content in hydrogels

Hygroscopicity testing of the hydrogels used in this research was based on measuring the

gravimetric weight difference in the hydrogels as a result of absorbing hygroscopic water

from the atmospheric moisture at a particular time, t. This was recorded in grams of

absorbed water per grams of dry hydrogel weight.

To measure hygroscopic water content within the hydrogels, Equation 9 was used

$$HW_{t=i} = W_{t=i} - S - P_{t=0} \qquad\qquad Equation\ 9$$

where, $HW_{t=i}$ equals the hygroscopic water mass at time ($t = i$) in grams, $W_{t=i}$ equals the

combined mass of a plastic cap, the hydrogel sample and absorbed hygroscopic

water/moisture at a certain time ($t = i$) in grams, S equals the dried hydrogel mass in grams

at initial measurement at time ($t = 0$) and $P_{t=0}$ equals the mass of plastic cap initial

measurement at time ($t = 0$). The hygroscopic water content, $HW_{t=i}$, in grams was divided by the dried hydrogel mass in grams.

Hydrogel swelling simply implies the characteristic of absorbing and retaining water. The mass of absorbed atmospheric water was calculated using the swelling degree (SD) or swelling ratio (SR) of a hydrogel in Guilherme et al. (2015) by Equation 10,

SD = SR = (mass of swollen hydrogel - mass of dry hydrogel) / mass of dry hydrogel

Equation 10

These swelling parameters provide estimates of the amount of water that can be transferred from an environmental media (i.e., atmosphere or soil) in and out of a hydrogel. This is important as absorption or swelling of hydrogels is essential in characterising the performance of hydrogels under agricultural field applications conditions (Bao et al., 2001; Gómez, 2015; Wu et al., 2021; Zohourian-Mehr & Kabiri, 2008).

3.3.2 Hydrogel, temperature and humidity levels selection

Five different hydrogels, each characterised by different active ingredient in their chemical composition (Table 3.1), were assessed for their hygroscopicity characteristics under 5 different relative humidity levels (63% RH, 76% RH, 84% RH, 95% RH, and 100% RH) and 3 different temperature conditions (10 ℃, 20 ℃, and 30 ℃).

Table 3.1 *Hydrogels used, their active ingredient, physical description, experimental labels and sorption characteristics*

Label	Hydrogel name	Active ingredient	Geometric description	Sorption characteristics
A	Abzorber Root Dip	Starch grafted Propenoic Acid Potassium Propenamide	Thin film irregular shape	Retains water up to 125 – 250g of its weight
B	Root Soil Moist Water Crystals / Retention SAP Super Absorbent Polymer gel	Polyacrylamide	Thin film irregular shape	Retains water up to 400 times of its weight
C	Yates Waterwise Water Storage Crystals	Potassium base acrylic	Thin film irregular shape	Absorbs 400 times its weight
D	Daltons Water Storage Crystals	Acrylamide and Potassium Polyacrylate	Thin film irregular shape	Absorbs 500 times of its weight
E	Expanding water beads		Spherical shape	Expands to 400 times their original size

No information was sent on active ingredients for hydrogel E despite asking the manufacturer. Sorption characteristics are as stated by the manufacturer.

For hydrogel characterization, a C, N and H elemental analysis was carried out on a Vario MACRO cube CHNS Elemental analyser (Elementa Anlysensysteme Gmbh, Hanau, Germany) (Table 3.2).

Table 3.2 *Summary of C, H and N elemental analysis of the hydrogels used in the study*

Hydrogel sample label	N %	C %	H %
A	6.1	39.19	5.894
B	0.01	35.05	4.704
C	0	34.82	5.692
D	10.98	41.19	7.328
E	2.56	33.67	6.064

3.3.3 Experimental methodology on hygroscopicity test of the hydrogels

The five hydrogels used in this research were chosen based on their availability in New Zealand. Four were of synthetic origin and one of natural based. A total of 225 labelled plastic laboratory caps were weighed with an electronic mass balance of high precision to 4 decimal places in grams and allocated to treatments in humidity chambers. Labelling followed the hydrogel nomenclature described in Table 3.1 with three replicates for each gel for each temperature and humidity treatment R1, R2 and R3 in each humidity chamber. The humidity chambers were labelled as S1 for 63% relative humidity, S2 for 76% relative humidity, S3 for 84% relative humidity, S4 for 95% relative humidity and S5 for 100% relative humidity. The different temperature levels were labelled as T1 for 10 ℃, 20 ℃ labelled as T2 and 30 ℃ labelled as T3. The 10 and 30 ℃ temperatures were achieved by using 2 different ovens set at the described temperatures. The 20 ℃ temperature was achieved by setting up the relevant humidity chamber on a lab bench at controlled room temperature.

The humidity chambers were created in 316 mm x 224 mm x 94 mm 5 L snap lock plastic storer (Figure 3.1a) containing a 400 ml solution of dissolved salt at saturation concentration point to create the target relative humidity conditions. Salts of NH_4NO_3, NaCl, KCl and KNO_3 were dissolved in 400 ml deionised water to saturated levels to create 63 %, 76 %, 84 % and 95 % relative humidity levels (Albayrak et al., 2014). To create the 100 % relative humidity chamber, 400 ml of deionised water without salt was added to the humidity chamber. Three relative humidity chambers at each RH were made to allow for variable temperature of 10, 20 and 30 ℃. There were 15 humidity chambers in total. Each humidity chamber had a cut-to-fit metal mesh raised above the solution level on which the hydrogels in labelled plastic caps/containers were placed (Figure 3.1b).
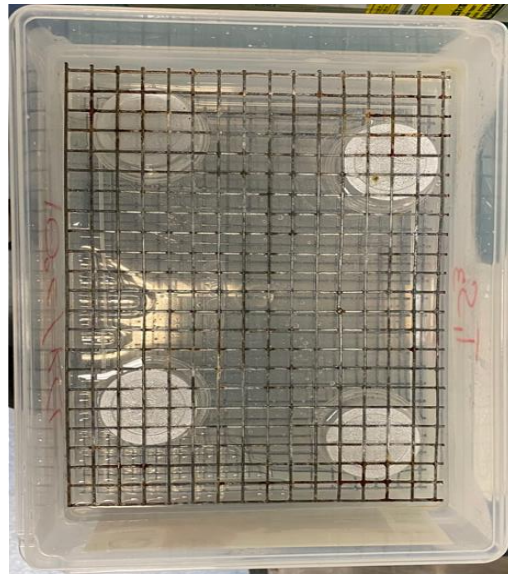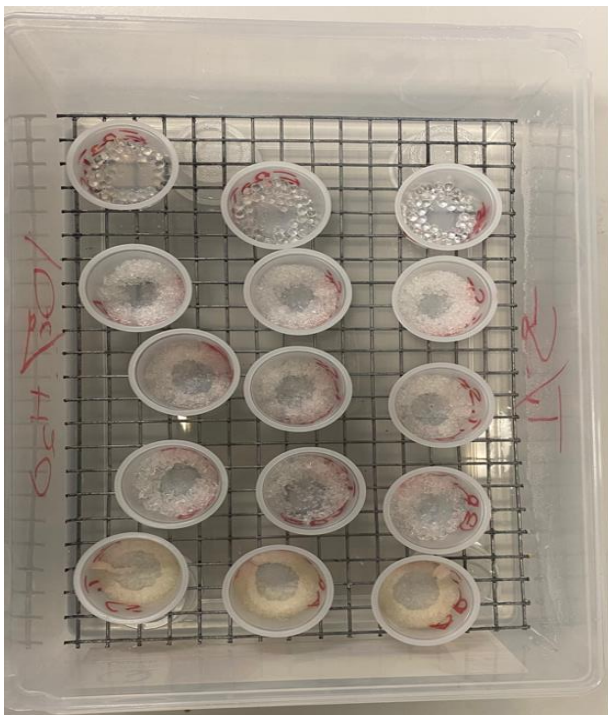
Figure 3.1 *Relative humidity chamber (a), relative humidity chamber with elevated metal mesh to hold hydrogel samples in plastic caps (b), replicates of different hydrogel samples in plastic caps in a humidity chamber (c) and establishment of relative humidity chambers in an incubator to control experiment temperature for humid moisture absorption (d)*

.

For every humidity chamber, triplicate samples of each hydrogel (0.5 grams) were weighed into 15 of the already weighed 225 plastic laboratory caps, and the cap was reweighed. Fifteen caps (triplicates of five hydrogel types) were placed in every humidity chamber in a completely randomised design. The hydrogel packs were sealed immediately after weighing as precaution to minimize the interaction of freshly opened hydrogel particles with the humid atmosphere. The humidity chambers were tightly closed immediately after the hydrogels in plastic caps were placed in the chamber to prevent any effect of the wider environment on the respective relative humidity levels (Castillo, 2011). The humidity chambers, each containing a total of 15 weighed hydrogels, were placed in accordance to their specific corresponding 10, 20 or 30 ºC temperature environment.

This experimental design aimed to expose the five hydrogel samples to the full range of relative humidity and temperatures used in this work, and to quantify atmospheric water absorption as a function of humidity and temperature. The experiment was run for 32 days (744 hours) and the mass of the hydrogels was measured at 24, 72, 168, 360 and 744 hours after initial establishment of the humidity chambers. The mass values gained were estimated in grams of absorbed water per grams of dry hydrogel weight (g/g) (Appendix 2) to investigate the performance of hydrogels in absorbing water.

3.4   Statistical data analysis

Microsoft Excel 16.50 software was used to calculate the weight of atmospheric water gained by the hydrogels in g/g using Equation 10 to organise experimental data for statistical analysis in R studio. The amount of atmospheric water gained was investigated as a function of hydrogel type, monitoring time, relative humidity percentages and temperature level using the linear model regression testing, and, when significant, Tukey

test was assessed for pairwise comparisons using R studio version 3.6.2 statistical software. The amount of atmospheric water gained by hydrogel CR was further compared for variations within monitoring time and relative humidity percentages, and monitoring time and temperature levels.

All data was tested for normality and long transformed. For all statistical analysis, a 95 % confidence level was used to determine significant variations between the means of the log-transformed ($\log_{10}(x+1)$) data for the mass of atmospheric water gained. All statistical analyses for pairwise comparisons were performed with R version 3.6.2. Results are presented graphically using log-transformed ($\log_{10}(x+1)$) data means and standard errors. Initial testing showed that hydrogel CR showed superior water absorption potential across most humidity and temperature conditions. To better understand the effect of relative humidity on water absorption by hydrogel CR at a fixed temperature, correlation analysis was conducted between the swelling ratios (Sgross) and the relative humidity ranges of 63 %, 76 %, 84 %, 95 % and 100 %. The analysis was conducted based on the Korsmeyer Peppas and First order kinetics absorption models to find the modelling coefficients such as diffusion rate constant, k and diffusion exponent, n. This correlation analysis was conducted using Microsoft Excel 16.50 software.

3.5   Results

3.5.1   Atmospheric water absorption by the hydrogels as a function of time

The data was investigated for the mass of water absorbed by the hydrogels, across all temperature and humidity levels, as a function of time. Linear regression testing showed significant differences between the mass of atmospheric water gained by the different hydrogels as a function of time ($P < 0.001$), with all hydrogels showing increased absorption of water with time (Fig. 3.2). Hydrogel CR was observed to gain the greatest mass of atmospheric water at all exposure time periods whereas ER hydrogel recorded the least amount of water at all time points. The mass of atmospheric water absorbed by BR hydrogel while low at 24 hours, increased rapidly between 24 and 72 hours to yield a final absorption mass similar to CR by the end of the monitoring period (744 hours). Overall, all hydrogels were observed to rapidly gain mass through the earlier periods, with the rate of mass increase tending to reduce at the end of the monitoring periods as indicated by the change in slope of the plot of water gain with time (Fig 3.2).
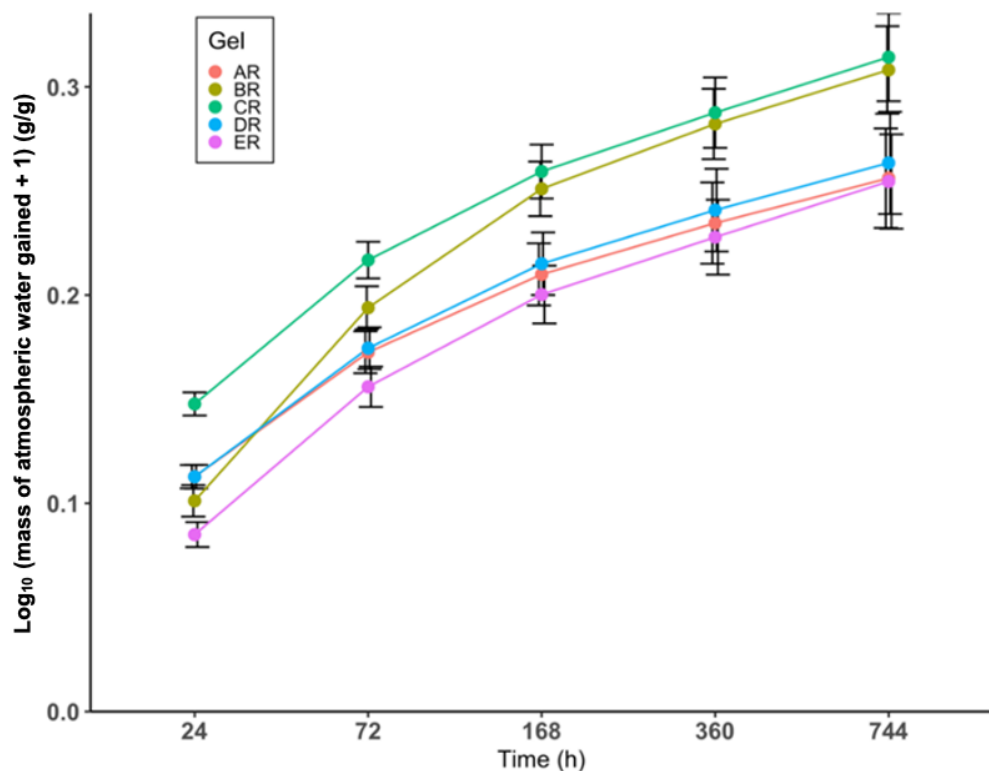
Figure 3.2 *Mass of water gained by the different hydrogels as a function of time (Bars show mean ± SE).*

The mass of water gained by each hydrogel at the end of the experiment under all the varied conditions measured is graphed in Figure 3.3. There were significant differences in the mass of water the different hydrogels adsorbed ($P < 0.001$). The mass of water gained by hydrogel CR was the highest, followed by the BR with the lowest mass of water gained by ER (Figure 3.3). The mean mass of absorbed water for these hydrogels was 0.824 g/g, 0.762 g/g and 0.594 g/g respectively. The mass of water gained by CR was significantly different to the other hydrogels except BR. In other words, although the results showed that CR has the highest water absorbing potential, absorbance by BR was statistically the same.
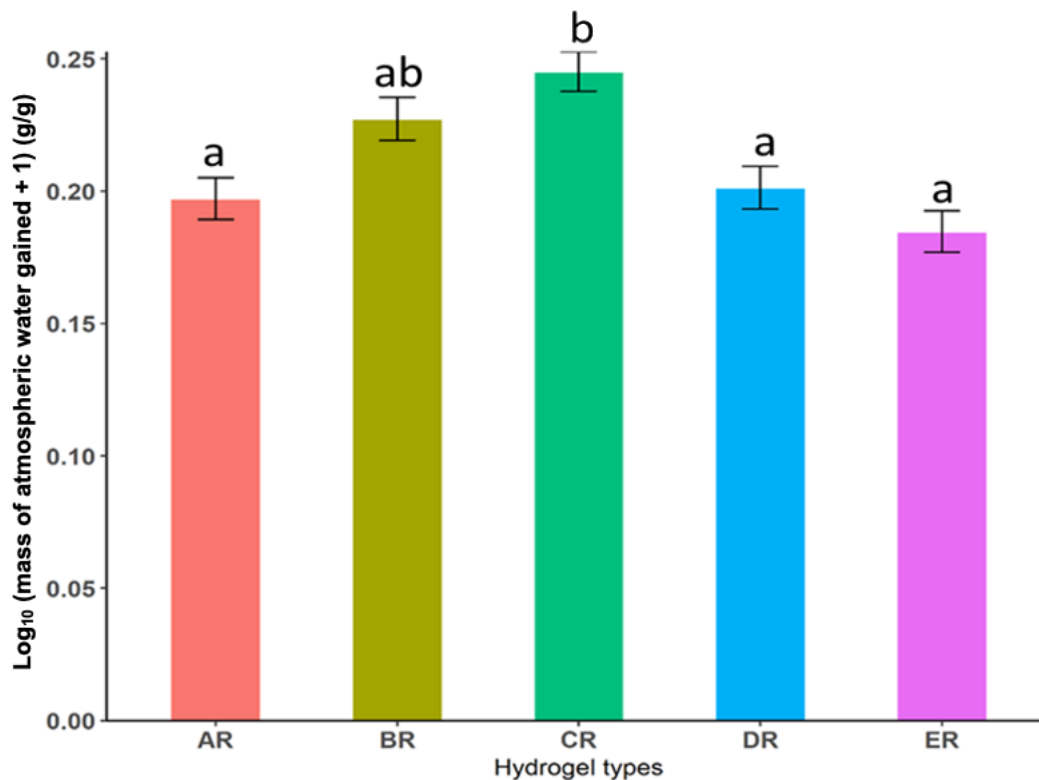
Figure 3.3 *Mass of water gained by the different hydrogels under all conditions at the end of the experiment (Bars show mean ± SE and different letters indicate significant difference between hydrogels).*

The mass of atmospheric water gained by hydrogels through adsorption is influenced by the time of hydrogel exposure to a humid environment, atmospheric temperature and the

relative humidity. As such, the effects of these factors on the mass of atmospheric water gained were assessed for their significance in the current research.

3.5.2 Atmospheric water absorption by different hydrogels as a function of temperature

Linear regression testing showed statistical differences between the masses of atmospheric water gained by the different hydrogels as a function of temperature ($P < 0.001$). However, analysis of these differences as the main effects showed that significant differences were due to the properties of the hydrogels, not the temperatures, with the mass of water absorbed by each hydrogel statistically the same at the three temperatures tested (Figure 3.4). There was a trend towards increasing mass of water absorbed by each hydrogel as a function of temperature, but the increases for each hydrogel were not statistically significant. This finding implies that temperature does not influence the mass of atmospheric water gained by the hydrogels tested for the experimental conditions used in this study. For all hydrogels there was generally a greater increase in the mass of water absorbed between 10 and 20 ⁰C, than between 20 ⁰C and 30 ⁰C, with all hydrogels except BR showing little increase between 20 and 30 °C. Hydrogel CR gained the highest mass of water across all three temperatures assessed in the study (10 ⁰C, 20 ⁰C and 30 ⁰C) with respective actual mean values of 0.784 g/g, 0.828 g/g and 0.859 g/g. In contrast, the lowest mass of atmospheric water was gained was by ER with actual mass of water values of 0.555 g/g, 0.600 g/g and 0.627 g/g at 10 ⁰C, 20 ⁰C and 30 ⁰C respectively.
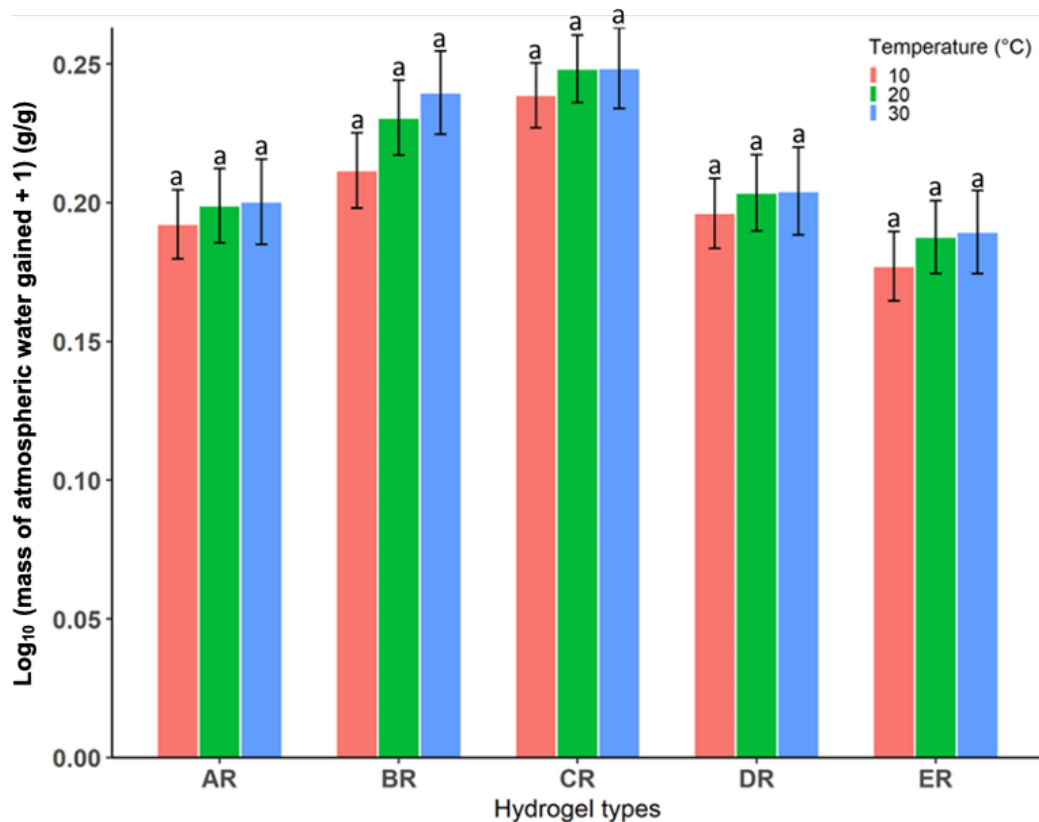
Figure 3.4 *Mass of water gained by the hydrogels at different temperatures (Bars show mean ± SE and different letters indicate significance differences between temperatures for each hydrogel).*

3.5.3 Atmospheric water absorption by different hydrogels as a function of relative humidity levels

Linear regression tests showed statistical differences between the masses of atmospheric water gained as a function of the percentage relative humidity ($P < 0.001$). Pairwise comparison showed differences were significant at all relative humidity percentages except between 63 % and 76 %. This implies that the amount of water vapour in the atmosphere influenced the mass of water absorbed by the hydrogels, with the increase of relative humidity from 76 to 100 % significantly increasing the mass of atmospheric water gained by all hydrogels (Fig. 3.5).

When considering the performance of the different hydrogels at the same relative humidity, at 63 % relative humidity the mass of water absorbed by BR and CR was greater than the other hydrogels, with differences between the five hydrogels becoming less obvious as relative humidity increased. The mass of atmospheric water gained by all hydrogels was substantially higher in 100 % relative humidity than the other relative humidity levels, with hydrogels absorbing about twice the mass of atmospheric water gained at 84 % relative humidity and four times the mass of atmospheric water gained at 63 % relative humidity particularly for hydrogels AR, DR and ER.
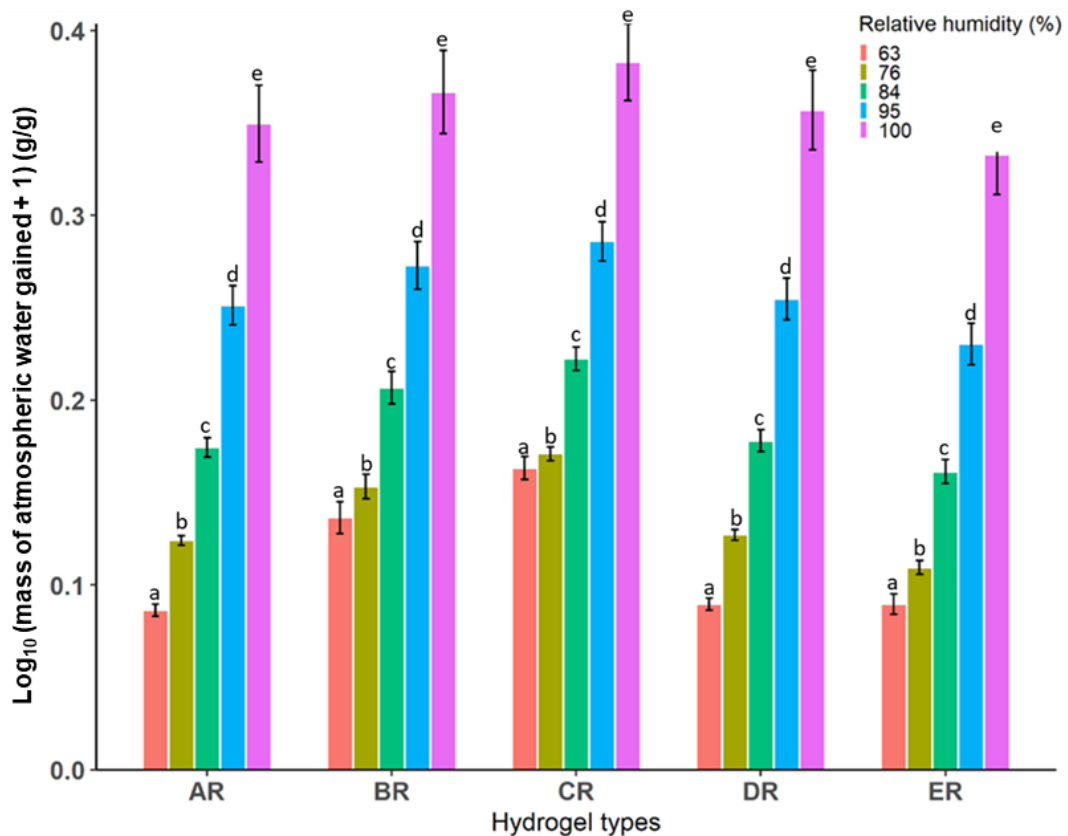
Figure 3.5 *Mass of water gained by different hydrogels at different relative humidity levels (Bars show mean ± SE and different letters indicate significant differences between relative humidity for each hydrogel).*

3.5.4 Using the results from this experiment to selecting the best hydrogel

To select the best performing hydrogel across the environmental conditions tested in this study, an analysis matrix plot of the relative humidity levels against the different temperature levels was constructed (Table 3.3).

Hydrogel CR was observed to gain the highest mass of atmospheric water across all relative humidity and temperature levels, except for humidity values of 76 % and 84 % at 30 ºC where hydrogel BR was observed to have superior water absorbance performance. Based on this analysis, hydrogel CR was selected for further absorption and desorption experimental work. The influence of the parameters time, temperature, and relative humidity on the performance of CR are analysed in the following sections of this chapter.

Table 3.3 *Summary of the best absorbing hydrogel and respective absorbed atmospheric water (g/g) at the temperature and relative humidity levels tested in this study.*

Relative Humidity/ Temperature	63 %	76 %	84 %	95 %	100 %
10 ºC	CR (0.732)	CR (0.579)	CR (0.889)	CR (1.469)	CR (2.269)
20 ºC	CR (0.633)	CR (0.540)	CR (0.829)	CR (1.326)	CR (2.561)
30 ºC	CR (0.465)	BR (0.504)	BR (0.728)	CR (1.083)	CR (3.139)

3.5.5 The impact of time exposure and relative humidity on the mass of water gained by CR hydrogel

The mass of water gained by CR at each relative humidity level, as a function of time, was compared using a linear regression test. There were significant differences in the mass of atmospheric water gained by CR at each relative humidity over time ($P < 0.001$). Increasing relative humidity significantly increased the mass of atmospheric water gained by CR and this increase become more apparent with time (Fig. 3.6). This implies that both the level of relative humidity in the air, and the length of exposure time to this atmospheric water vapour influences the mass of water absorbed by hydrogel CR. The highest mass of water gained by hydrogel CR was 2.656 g/g and this was observed under 100 % relative humidity after 744 hours exposure. The lowest recorded mass of water was 0.268 g/g observed under 63 % relative humidity after 24 hours of exposure (Fig. 3.6). The results show that CR was still gaining water at the 100 % relative humidity level after 744 hours suggesting that a point of equilibrium was not reached at the end of experiment. The gradual increment in mass of atmospheric water gained at the other relative humidity levels had reduced (to almost zero at a relative humidity of 76% after 360 hours of exposure) indicating the attainment of an equilibrium for mass of water gained. Statistically, there was no observed differences between the masses of atmospheric water gained by the CR hydrogel at 63 % and 76 % relative humidity percentages for all monitoring times. Also, the masses of water gained by CR at the 24th monitoring hour was insignificant between 76 % and 84 % relative humidity levels, 84 % and 95 % relative humidity levels, and 95 % and 100 % relative humidity levels.
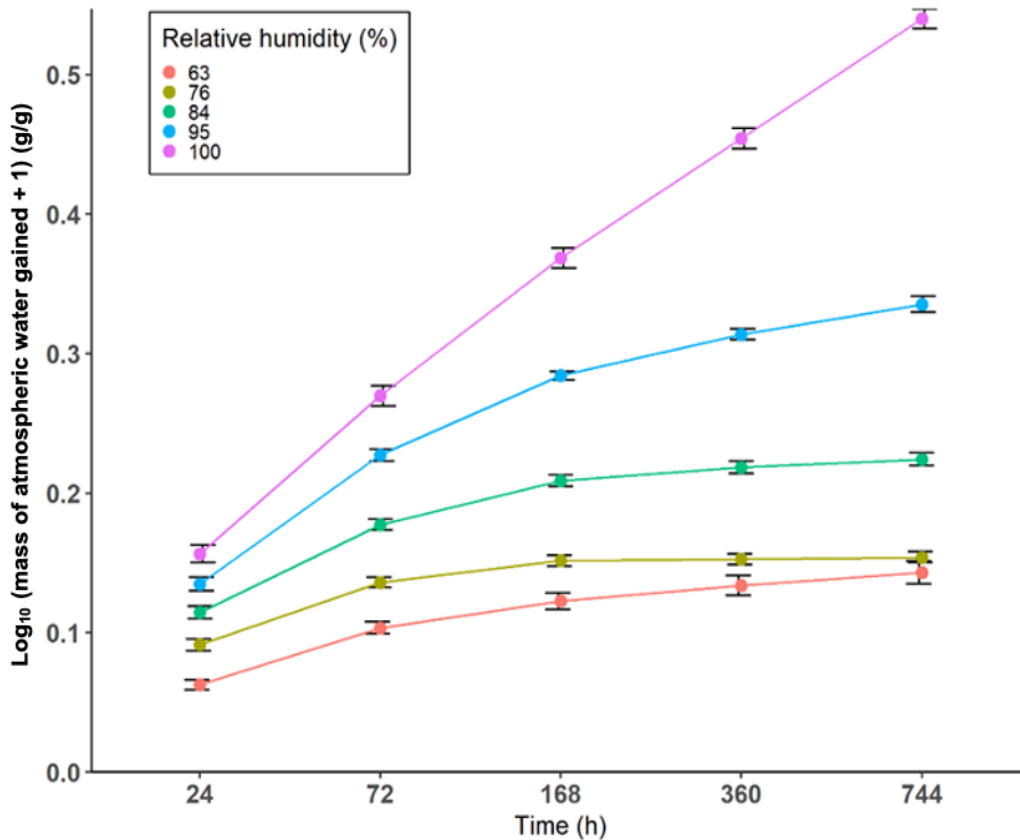
Figure 3.6 *Mass of water gained by the hydrogel CR hydrogel as a function of time at the different tested relative humidity levels across all temperature conditions (Bars show mean ± SE).*

3.5.6 The impact of time and temperature on the mass of water gained in CR hydrogel

Although temperature had no overall effect on the mass of atmospheric water gained by the different hydrogels investigated in this study, the linear regression testing for CR showed interaction temperature and exposed time periods to have significant differences between the masses of atmospheric water gained ($P < 0.001$). Generally, there was an increase in mass of atmospheric water gained as a function of temperature at all temperature levels for hydrogel CR (Fig. 3.7) although the change in mass trend between time points was not the same for all temperature after the first 168 hours of exposure period. Hydrogels incubated at 30 ºC gained relatively less water between 360 and 744 hours of exposure, than when incubated at 20 ºC and 10 ºC. After 744 hours of exposure the mass of water absorbed was greater for the lowest temperature. A pairwise

comparison using Tukey test showed that at all temperature levels, the mass of water gained at all monitoring times was statistically different compared to the 24th monitoring hour, except for the mass of water gained at the 72nd monitoring hour. However, after the 72nd monitoring hour, there were no significant differences in the mass of water gained at all temperature levels for all monitoring times except between the 72nd hour and 744th hour at both 10 ℃ and 20 ℃.
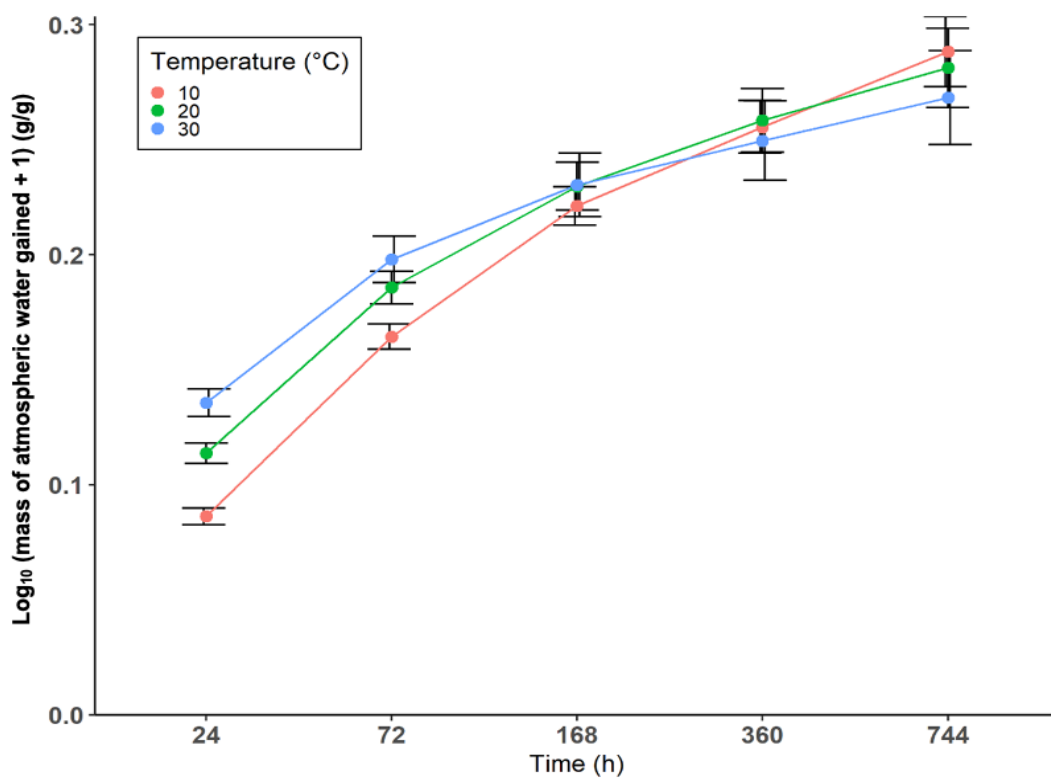
Figure 3.7 *Mass of water gained by hydrogel CR hydrogel as a function of time at the different tested temperatures levels (Bars show mean ± SE).*

3.5.7 Introduction to swelling kinetics results
The mechanisms describing atmospheric water absorption into the swelled hydrogel CR at 20 °C for the tested relative humidity levels of 63 %, 76 %, 84 %, 95 % and 100 % were investigated using the first order kinetic (3.2.4.1) and Korsmeyer Peppas models (3.2.4.2). This investigation, which was based on water content uptake as a function of

swelling time, showed the experimental data was in good agreement with both models. However, the first order kinetic model was observed to best explain the experimental data. Swelling or absorption of atmospheric water into hydrogel CR can therefore be explained as a first order kinetic model absorption process.

3.5.7.1 Fitting the experimental data to the swelling kinetics models

The R^2 values for model fitting (Table 3.3) showed no particular pattern of either increase or decrease in relative humidity in response for the first order kinetics model. However, from 76 % relative humidity, an increase in relative humidity increased the diffusion rate constant (k) and M_t/M_{max} ratio. The k_f values ranged from -0.0053 to -0.0435, with the highest k_f observed at 100% relative humidity. Also, M_t/M_{max} values ranged from 0.531 – 2.480 and the highest and lowest were observed under absorption at 76 % relative humidity and 100 % relative humidity respectively.

The mass of atmospheric water gained by CR for a relative humidity of 76 % had the highest R^2 value of 0.9818 and was therefore observed to have the best fit to the first order kinetics model. In contrast, data describing the mass of water absorbed at 63 % relative humidity was least well described by the first order kinetics model with an R^2 value of 0.9054.

For the Korsmeyer Peppas model, the R^2 values (Table 3.3) showed no particular pattern of an increase or decrease in relative humidity except from 76 % to 100 % relative humidity for which increasing humidity increased the parameters R^2, k, diffusion rate constant and n diffusion exponent as calculated from equation 7, $M_t/M_{max} = kt^n$. However, the diffusion exponent (n), which characterises swelling activity (Siepmann and Peppas 2012), and diffusion rate constant (k), increased with increasing relative humidity level from 76 % to 100 %. The k values ranged from 5.029 – 96.694, with the highest, observed

at 100% relative humidity. Also, n values ranged from 0.117 – 0.447, and the highest and lowest were observed under absorption at 76 % relative humidity and 100 % relative humidity respectively. The mass of water gained by hydrogel CR under 100 % relative humidity was observed to have the best fit to the Korsmeyer Peppas model with a R-square value of 0.9972 (Table 3.3). It is worth mentioning that the CR at 76 % relative humidity was observed to have the best fit to the first order kinetics model, but this condition was also characterised by the least best fit to the Korsmeyer Peppas model. The R^2, k_f and M_t/M_{max} values for the first order kinetics model and the R^2, k and n values for the Korsmeyer Peppas model were deduced from the swelling modelling graphs in Appendix Figure A1.2 and Appendix Figure A1.1 respectively.

Table 3.4 *Swelling parameters derived from fitting models applied to hydrogel CR at 20 ºC for different relative humidity levels*

Relative Humidity (%)	Korsmeyer Peppas model			First order kinetics model		
	R^2	k	n	R^2	k_f	M_t/M_{max}
63	0.9449	25.900	0.2260	0.9054	-0.0215	0.5908
76	0.7467	5.0292	0.1170	0.9818	-0.0435	0.5306
84	0.8506	14.494	0.1900	0.9654	-0.0282	0.7927
95	0.9266	63.139	0.2888	0.9567	-0.0159	1.2462
100	0.9972	96.694	0.4469	0.9656	-0.0053	2.4803

3.6 Discussion
3.6.1 Atmospheric water absorption by hydrogels as a function of time

The mass of atmospheric water gained by the hydrogels studied in the current research shows significant differences at the various monitoring periods (Chapter 3.5.1). This

follows the findings of Gómez (2015) who observed an increase in the mass of hygroscopic water absorbed by hydrogels exposed to four relative humidity levels for different periods of time.

The significant variations observed in water absorption with time between the hydrogels can be attributed to the swelling process and underpinning mechanisms (Ahmed, 2015) which describe variations in mass of water absorption with time by two-stage absorption processes (Chandrika et al., 2016; Kim & Park, 2004; Long & Richman, 1960). Such process is characterised by rapid initial surface hydration by randomly diffusing water molecules (Buchholz & Graham, 1998) interacting with hydrophilic functional groups of a hydrogel to initiate absorption (Chirani et al., 2015), and a later polymer network relaxation and expansion that drives water absorption and swelling through the secondary phase of absorption (Bao et al., 2001; Neethu et al., 2018). Such characteristics explain the quick mass of water gained early and slower later mass of water gained until equilibirum or maximum absorption for the hydrogels is reached at later monitoring hours. The different hydrophilic functional group characteristics of the hydrogels could explain observed differences in absorbed mass of water between the hydrogels at the monitoring times (Gun'ko et al., 2017).

The information gained in this work on differences in mass of water gained at different times by the different hydrogels provides an insight into how water absorption by hydrogels changes with time of exposure, with rapid and slow atmospheric water absorption at initial and late absorption times respectively. Such knowledge could inform the timing of field application for hydrogels including details on the time for maximum absorption at equilibrium, beyond which water absorption becomes insignificant. Subsequent desorption processes could be trigged at this point. Such knowledge also provides information on the dynamics required to enable the selection of hydrogels with

functional hydrophilic groups that enable high mass of water for specific field environmental conditions.

While all hydrogels continued to gain water with time, the mass of atmospheric water gained at each time point varied significantly across the different hydrogels with a trend in increasing mass of atmospheric water gained from ER (least), AR, DR, BR to CR (most). The observation of significant differences across the different hydrogels in the current study agrees with the findings of Pooley et al. (2010) who found differences in the mass of absorbed water in differently synthesized types of poly (AA-co-NNDMAAm) hydrogels and Zhou et al. (1997) who recorded differences in the mass of water absorbed across different synthesized types of copolymer (AAm–MSAS–AA) hydrogels.

The differences observed in mass of water gained among the hydrogels can be attributed to their chemical composition (Ahmed, 2015), particularly based on their N % (Table 3.2), which corresponds to their acrylamide compositions (Table 3.1). Nitrogen influences crosslinking density (Pooley et al., 2010; Zhou et al. 1997) and average molecular weight (Tomar et al. 2007), which subsequently determines a hydrogels' absorption capacity. High N % increases crosslinking and reduces average molecular weight which reduces hydrogel absorption potential. Hence, the differences in N % among the hydrogels (Table 3.2) could have led to their different water absorption capacities. Also, the differences could also be attributed to the physical characteristics of the hydrogel, particularly their geometry (Neethu et al., 2018), and size (Gómez, 2015; Guilherme et al., 2015; Omidian et al., 2005) which influences surface to volume area ratio (Mudiyanselage & Neckers, 2008), which determines absorption capacity. Small particle size hydrogels have high surface to volume ratio for high water absorption. Large sized particles induce the opposite effect. Additionally, fixed shaped hydrogels have high

crosslinking that limits absorption whereas uneven and amorphous shaped hydrogels have low crosslinking properties for high absorption.

For field application, especially under a scenario of changing climate and in arid areas, this information suggests that selection of the best absorbing hydrogel could be based on consideration of chemical composition characteristics including N % which can translate to relative abundance of acrylamide as crosslinking, and also the physical characteristics of irregular shaped and small particle hydrogels.

3.6.2 Atmospheric water absorption by different hydrogels as a function of environmental factors.

Absorption of water by hydrogels is also influenced by the surrounding environment with parameters such pH, aqueous ionic strength concentration and temperatures reported to affect swelling and absorption to some degree (Chan & Neufeld, 2009; Flory, 1953; Guilherme et al., 2015; Molloy et al., 2000; Moura et al., 2008; Paulino et al., 2011). While some of these parameters are not relevant to absorption of water from the atmosphere (many of these influences are more apparent in a soil environment) parameters such temperature and relative humidity levels are critical when assessing the hygroscopicity capacity of a hydrogel (Urbina et al., 2021).

3.6.2.1 Atmospheric water absorption by different hydrogels as a function of temperatures

The mass of atmospheric water gained at different temperatures did not vary for the same hydrogel but there was a general trend of increasing temperature effecting a relatively higher mass of water absorbed. This result contradicts literature which describes a change in absorbed water content by hydrogels in response to temperature (Neethu et al., 2018). Chandrika et al. (2016) reported an increase in water content from 55 to 160 grams/grams

for a 8 to 50 ℃ temperature increment. However, some studies, including Abdel-Halim and Al-Deyab (2014) reported significant mass of water gain with temperature increase from 120 – 150 ℃ after which no further significant increase in mass of water was observed.

Although no significant variations in mass of water gained were observed at the different temperatures for the hydrogels in the current work, the observed trend could be a function of thermal energy reducing crosslinking and destabilizing polymer joints for absorption (Abdel-Halim & Al-Deyab 2014). This would provide energy to effect a glassy-polymer state to rubbery-polymer state transition (De Vreugd, 2011; Dubelley et al., 2017), which then could have enabled higher swelling expansion to allow more water absorption as temperature increased (Guilherme et al., 2015). However, the 10 – 30 ℃ range used in this work might not have been sufficient to allow these processes to fully occur and therefore explain the observation of similar masses of water gained at all temperatures for all hydrogels. Tomar et al. (2007) and Begam et al. (2004) associated glassy-state temperatures with AAm and amide groups respectively, and both contain a high N %. The trend among the hydrogels at all temperatures could be aligned to the N % in the hydrogels. Such thermal enhancement potential has led to undergoing research aimed to develop and improve thermosensitive hydrogels which may enhance absorption capacities in the future (Serrano-Aroca & Deb, 2020).

When considering the field application of hydrogels, the information from this Chapter suggests that 10 – 30 ℃ temperature range will likely not yield different absorbed atmospheric water masses. However, arid region temperatures range from 10 – 40 ℃ (Gaur & Squires, 2018) and therefore further studies could be conducted at an increased temperature range to assess whether differences in mass of atmospheric water gained could be induced at a wider range of temperatures.

3.6.2.2 Atmospheric water absorption by different hydrogels as a function of relative humidity

Relative humidity had a strong influence on the mass of atmospheric water that each hydrogel absorbed (Figure 3.5.4), with all hydrogels showing a trend of increasing mass of water absorbed as a function of humidity. The results of this study agree with those of Gómez (2015) and Zhao et al. (2019) who observed a trend of increased mass of water absorbed with increased relative humidity.

The differences observed in the mass of water gained at different relative humidity levels for each hydrogel could be attributed to differences in atmospheric moisture saturation levels at the relative humidity percentages (Zhao et al., 2019). Moisture saturation determines the concentration gradient between the hydrogel and surrounding air (Ono et al., 2007) which creates diffusion strength for gaseous water molecules to undergo initial hydration at the surface of a hydrogel (Zonatto et al., 2017) and enable polymer network unwinding for water absorption (Ahmed et al., 2016). A high humidity environment with a high water molecule concentration gradient is required to maximise water absorption. For accurate atmospheric moisture estimations, Wei et al. (2021) argues that absolute humidity levels should be used rather than relative humidity.

The observation that a large mass of water gained was gained at relative humidity levels above 76 %, and the lack of difference between 63 % and 76% relative humidity, could indicate that the next relative humidity of 84 % is the critical point for substantial initial surface hydration. This critical point may be unique to the hydrogels of the current study as Jansen et al. (2020) and Gómez (2015) proposed 85 % and 65 % relative humidity levels respectively as critical levels for better absorption. McHugh et al. (2015) suggests that relative humidity at arid and semi-arid regions ranges from 20 – 60 % and requiring

relative humidity percentages above 76 % for better absorption could potentially limit field application of the tested hydrogels in most arid areas except in some parts of of Iran where Davtalab et al. (2013) reports relative humidity percentages from 68 % to near 100 %. Under all arid conditions, water absorption would be higher at night when relative humidity increases. Dubelley et al. (2017) and Gómez (2015) suggest that relative humidity interacts with many other factors during water absorption by polymers. Factors such as the chemical and physical properties of hydrogels explained in Chapter 3.6.2 could have contributed to performance differences between hydrogels at specific relative humidity levels.

3.6.3 The interaction of time and relative humidity on the mass of water gained by hydrogel CR

The observed trend that increasing relative humidity increased the mass of water gained by hydrogel CR hydrogel, at all monitoring times shows the interaction of time and relative humidity will change hydrogel structure over time enabling the hydrogel to absorb more atmospheric water. Better water absorption at high relative humidity and longer monitoring time indicates that high atmospheric moisture instigates rapid surface hydration, enabling structural change of the CR hydrogel creating a large absorption space through polymer relaxation and expansion which enables absorption of a high mass of water over the long monitoring time until equilibrium absorption. Equilibrium mass of water gained was reached at the 744th hour of monitoring for all relative humidity percentages below 100 % and the order of equilibrium point attainment with relative humidity provides evidence that CR hydrogels will reach maximum absorption potential at lower levels of relative humidity over time (Figure 3.6). This observation contradicts

Zhao et al.'s (2019) finding that early equilibrium time is reached at higher relative humidity percentages in the process of absorbing hygroscopic water.

However, the prolonged equilibrium time for CR hydrogel at 100 % relative humidity suggests increased hydrogel swelling and absorption space potentially due to the high atmospheric moisture level and dew formation on hydrogel surfaces yielding high initial rapid surface hydration. This suggests that field application of CR at 100 % relative humidity could yield more mass of water gained over longer time when applied on the field, although it must be noted that 100 % relative humidity is rarely recorded in most arid and semi-arid areas except (as already stated) for some parts of Iran. However, this understanding could guide the deployment of hydrogels in humid areas. The insignificant differences in water mass between the lowest relative humidity levels, 63 % and 76 %, at all monitoring times indicates that the hydration moisture or concentration water molecule gradient between these conditions was similar.

With this information, estimates of the absorption potential of atmospheric wate quantity into hydrogel CR can be made based on observed swelling kinetics for arid field conditions at specific monitoring time and relative humidity, to model the potential of this hydrogel to improve water absorption outcomes. Such information is essential in deploying hydrogels to obtain water from the atmosphere under different relative humidity levels and time that can be robust to future climatic conditions.

3.6.4 The interaction of time and temperature on the mass of water gained in CR hydrogel

As observed in section 3.5.6, an understanding of the interaction of time and temperature can be used to describe structural changes of the CR hydrogel over time. This is because different temperature levels provide different thermal energy to diffusing water molecules (as kinetic energy to enhance diffusion) (Dubelley et al., 2017). This is absorbed as energy

into the hydrogels upon contact with water molecules. This energy transfer enables structural expansion and swells the hydrogel allowing for more atmospheric water absorption. Thermal energy enables a rapid diffusion rate (Chen et al., 2011; Jansen et al., 2020) which enhances the diffusion coefficient and rate, and impacts on water absorption over time (Duncan & Broughton, 2007). Therefore, the allowed time of exposure interacts with temperature by enabling the process of expansion when temperature provides the thermal energy for this process. Kipcak et al. (2014) recorded increasing absorption in hydrogels with increasing temperature over time until equilibrium was reached between the 23rd and 28th hours.

However, the trend observed in the study suggests that the observed temperature impacts were not enough to create a constant increment of the mass of absorbed atmospheric water over time. This suggests that the mass of water absorbed in CR hydrogels would be similar under conditions of a 0 - 10 ℃ temperature range during field application. The reverse trend in mass of water gained observed at 10 ℃ and 30 ℃ in the CR hydrogel with increasing time could be attributed to partial pressure and air saturated vapour pressure variations with increasing or decreasing temperatures (Zhang et al., 2016). Such variations would result in either less (limited) or more (saturated) water vapour respectively in the atmosphere over the time period for absorption (Allen et al., 1998). This result implies that reduced temperatures at night would encourage water gain in hydrogels but about 360 hours would be necessary to achieve a saturated atmospheric water vapour condition over a stable continuous 10 ℃ temperature drop. This effectively limits the practicality of deployment under arid field conditions as such a timeframe is impossible. Jansen et al. (2020) reported that water absorption onto polymers under conditions of variable temperature and relative humidity needs further research.

The temperature-time interaction could have led to temperature impacts on absorption by hydrogel CR and this could explain the differences in mass of atmospheric water in the hydrogel at the earlier monitoring periods for all the temperature levels. The insignificant differences in mass of absorbed atmospheric water over the latter time periods could be associated with temperature impacts on the surrounding air which subsequently impacted the hydrogel. The effect of temperature on the surrounding environment was more pronounced at the latter absorption periods as can be deduced from the reverse absorption trend among the temperatures. The results from this study have revealed hydrogel CR at almost all tested temperatures was near maximum capacity at about hour 744. This suggests that 744 hours of exposure during any field application could have resulted in maximum atmospheric water absorption under the temperature conditions tested in the current work, but such temperature is unlikely to remain constant over that period.

3.6.5 Discussion on swelling kinetics of hydrogel CR absorption at 20 °C as a function of relative humidity levels.

Relative humidity levels affected the diffusion parameters dramatically in both swelling mechanism models. Observations from this study show that a higher relative humidity encourages a faster swelling and absorption process in hydrogel CR. Hence, the observation that increasing relative humidity level will lead to an increasing trend for parameters k and n in the Korsmeyer Peppas model, and an increasing trend of k and $M/Mmax$ for the first order kinetics model above 76% relative humidity. The 'off trend' k and n values for the Korsmyaer Peppas model and the k and M_t/M_{max} values for the First Order kinetics model at 63 % relative humidity could be explained according to the work of Gómez (2015) who suggested that atmospheric absorption of water below 65 % relative humidity was not significant. In other words, the mass of atmospheric water gained in by

hydrogel CR at 63 % relative humidity may not have been enough to conform to the trend in k and n for the Korsmeyer Peppas and k and M_t/M_{max} for the first order kinetics models.

The first order kinetics model best fitted the observed swelling behaviour of hydrogel CR at 20 ° C for all relative humidity levels based on the modelled R^2 values closeness to 1. According to Wu et al. (2021) first order kinetics is based on the biosorption process. Therefore, the biosorption activity of water molecules contacting the hydrogel surface boundary could have influenced the absorption process for the CR hydrogels. This biosorption process explains how an increase in relative humidity levels leads to an increased rate, k and equilibrium M_t/M_{max} due to the concentration gradient between the surrounding air and the boundary layer of the dry CR hydrogel. The concentration gradient is a driven by the difference between the water molecules in the atmosphere at a particular relative humidity and the water molecules present at the boundary layer surface of the dry CR hydrogels. Therefore, increasing relative humidity increases the relative concentration of atmospheric water molecule which in turn increases the concentration gradient and allows more atmospheric water molecules to be absorbed as observed in the reported results. Furthermore, the biosorption process at the surface layer occurs through a selective hydration process. As such, the increasing concentration of water molecules in the atmosphere allows highly selective surface hydration through the biosorption process increasing the diffusion rate for a larger internal polymer network opening in the hydrogels. This subsequently allows higher absorption and swelling and a relatively higher equilibrium mass due to faster transportation of diffused water molecules and the open network of pores or volume for absorption. Hence, the correlation of relative humidity with k and M_t/M_{max} yields faster k and M_t/M_{max} at 100 % relative humidity (the highest relative humidity in the study).

From this information, we can deduce that absorption kinetics by the CR hydrogel at 20° Celsius can be described by the first-order kinetics model and depending on the relative humidity variations, predictions on the diffusion rate constant, k can be made. The equilibrium mass of water gained at a specific relative humidity level between 76 % to 100 % can be made. Understanding this model can help predict or select the best field sites for application of CR hydrogels to absorb atmospheric water.

3.7 Conclusion

In conclusion, hydrogels are capable of absorbing atmospheric water. However, their absorption capacity is dependent on their chemical and physical properties, time and the surrounding relative humidity percentages of the hydrogel. Preferably, hydrogels of no N concentration and small size are best for atmospheric water absorption and should be considered when selecting hydrogels for atmospheric water absorption. Such hydrogels have large size to surface ratio and no crosslinking effects, even across different relative humidity levels at different times periods. The research concludes hydrogels absorb atmospheric water rapidly initially and slowly at latter stages until maximum absorption capacity of the hydrogels are reached under all relative humidity below 100 %. These hydrogels, particularly CR hydrogels, the best absorbing hydrogels behave in a first order kinetics model during the absorption of atmospheric water. Furthermore, it can be concluded from the study that hydrogels require relative humidity of 84 % and above to absorb substantial mass of atmospheric water over time irrespective of temperature fluctuations within 10-30 ℃ impacts on water molecule diffusion, hydrogel expansion and relative humidity percentage changes. As such, the high humidity periods over the night till early morning could be optimum for the atmospheric water absorption as they provide enough water molecules for the first absorption process in hydrogels, hydration. However, such observations could conclude for absorption time longer than actual 8 – 12

hours period observed for the night and early morning temperature drop and high relative humidity periods in the arid and semi-arid regions, and therefore further research could undertake observations on over shorter absorption time periods of about 8-12 hours range. Also, the research is limited with information on the impacts of increasing temperature and reducing relative humidity on absorbed water within hydrogels that occurs after the maximum absorption and therefore needs further research. Again, the study concludes temperature has no effect on atmospheric water absorption, however a further research with temperature range extended from $10 - 45$ ℃ to cover the true arid and semi-arid temperature range could be conducted to ascertain the true arid and semi-arid temperature impacts.

CHAPTER FOUR

4 INVESTIGATING HYDROGEL ABSORBED WATER RELEASE

4.1 Introduction

Many research studies have shown the capability of hydrogels to act as soil moisture conditioners retaining water to support agriculture (Abdallah, 2019; Cheng et al., 2018; Guilherme et al., 2015; Guilherme et al., 2010; Woodhouse & Johnson, 1991), particularly under conditions where irrigation is needed. Increasing drought intensity and frequency, especially in arid and semi-arid areas, has encouraged consideration for hydrogels (Bo et al., 2012; Kalhapure et al., 2016; Neethu et al., 2018) and even their potential to absorb water molecules from the atmosphere as a source of soil moisture for plant growth. Deployment of hydrogels in such a scenario for non-precipitation water sources could enhance agriculture production.

The release of absorbed water from hydrogels depends on multiple complex factors which are due to the structural complexity and dynamic absorption processes of hydrogels (Ako, 2017b). Therefore, understanding water release is critical to the deployment of hydrogels in such a scenario to achieve optimum field application outcomes. For example, absorbed water within hydrogels are categorised differently, and their desorption process occurs in the inverse of the absorption process (Ostrowska-Czubenko et al., 2011). Multiple research work has been carried out to study the impacts of potential water-release factors, syneresis (Ako, 2017b), temperature (Bellich et al., 2011) and pressure (Ako, 2017a; Guilherme et al., 2015) to understand hydrogel release behaviour, particularly under non-atmospheric water absorbing conditions. Important in this work is correlation of water release with consideration of plant-water stress levels especially where non-rainfall water sources are largely relied on for agriculture (Urbina et al., 2021; Zhang et al., 2016). Considering stress levels in the context of water release requires consideration of the

pressure on root and soil water concentration that is associated with the water content states of saturation, field capacity or wilting point (Lavergne et al., 2020).

The work described in this chapter seeks to assess the release of absorbed atmospheric water from hydrogels at osmotic pressure levels which characterises the various states of plant water stress levels to better inform the soil moisture conditioning and retention capacity and plant water access that might be enabled through capturing of atmospheric water by hydrogels. Most hydrogel studies conducted on osmotic pressures associated with states of plant water stress have considered the soil environment (Montesano et al., 2015; Narjary et al., 2012). The work presented in Chapter 3 showed the mass of water that could be absorbed by hydrogels from the atmosphere was relatively low when compared to the mass of water that can be absorbed from solution. Therefore, the work in Chapter 4 considers potential water release outside the soil environment. The work described here considers options for releasing the limited absorbed atmospheric water to plants in the context of some of the complexities associated with free and bound water types in absorbing hydrogels (Gun'ko et al., 2017).

4.2   Water retention and release in hydrogels
Release and retention characteristic of hydrogels provides key information on how much water can be retained by a hydrogel as a soil water conservation and conditioner (Cheng et al., 2018; Ghobashy, 2020). Also, a hydrogel water release model can guide water-nutrient mix solution release to plants and aid better agriculture.

The primary aim of soil water retention supplements such as superabsorbents (i.e., hydrogels) in agricultural soils is to hold soil water. This enhances soil water conservation, plant survival rate and growth, and the overall soil health (Cheng et al., 2018; Serrano-Aroca & Deb, 2020). However, processes that reduce soil moisture, such

as water respiration from the soil surface, are extremely high in arid regions that largely depend on non-rainfall sources (Zhang et al., 2015). Therefore, soil management with superabsorbent substances like hydrogels application has strong potential to enhance soil moisture retention where this water can be effectively delivered to where it is needed. The available water content for plant usage of soils treated with hydrogels has been shown to be readily increased relative to soils not treated with hydrogels (Narjary et al., 2012). The hydrogels prevent water loss through drainage by gravity and makes it available to plants. Koupai et al. (2008) showed that treating soil with hydrogel increases retention and water use efficiency.

4.2.1 Mechanism of hydrogel water release

Water is primarily released from hydrogels by diffusion through the polymer and polymer erosion (Kamaly et al., 2016), and release therefore depends on the hydrogel's polymer properties and concentration (Ghobashy, 2020; Paarakh et al., 2018). Hydrogel polymer concentration is positively correlated with the viscosity of the desorbing liquid which decreases the release diffusion coefficient. Due to the dependency of water release on the polymer concentration, swelling mechanism factors including polymer network chain relaxation, wetting, hydration and energy enthalpy change influences the process of water release from hydrogels (Skoug et al., 1993). The layer thickness of hydrogels also influences release mechanisms, with thick layered hydrogels releasing less water (Paarakh et al., 2018). Polymer network relaxation during water release can enhance subsequent absorption (Bagley & Long, 1955), however continuous desorption and absorption can lead to hydrogel structural collapse.

4.2.2   Factors that affect water release in hydrogels

A number of factors contribute to the release of absorbed water from hydrogels to plant and soil including pressure (Gómez, 2015; Guilherme et al., 2010; Lavergne et al., 2020), physical change strain and stress (Bagley & Long, 1955; Vundavalli et al., 2015), hydrogel syneresis (Ako, 2017b; Boral et al., 2010), temperature (Bellich et al., 2011) and hydrogel porosity (Chirani et al., 2015). Among these factors, pressure is most commonly used to describe water retention and release (Lavergne et al., 2020). Ionic concentration in the soil environment due to factors including soil salt and nutrients also compete with plant roots for soil water during water release and therefore influence water retention in soil (Łuczak et al., 2021). The concentration of salt crystals in arid soils (Chhabra, 2004) in particular can potentially influence the process of release or retention of absorbed water from hydrogels.

Plants use osmotic pressure between plant roots and soil moisture to draw water from soil to meet growth water demands (Abdi et al., 2017; Ako, 2017b; Guilherme et al., 2010; Urbina et al., 2021). An osmotic pressure range from 0.1 to 1.2 MPa (Urbina et al., 2021) characterises progress plant water stress levels of saturation point, field capacity and wilting point. The osmotic pressure represents the suction force that pulls water, and the force needed to suck water becomes higher as soil becomes drier and reduces as soils become wet (Lavergne et al., 2020). However, other external influences including soil texture, organic matter and structure also affect osmotic pressure.

At saturation, a high water concentration exists in plant roots and in the soil, and therefore a low osmotic pressure of about 0.1 MPa (Urbina et al., 2021) is required to pull water to meet plant needs. However, this water becomes progressively lost through draining until field capacity is reached where plants can readily access it (Lavergne et al., 2020). Further water loss to the moisture content characteristic of wilting point leads to soil moisture becoming progressively more readily unavailable (Abdi et al., 2017; Lavergne et al.,

2020). The osmotic pressure required for plants to suck water increases as soil dries from field capacity to wilting point, and the same pressure trend applies to water removal from hydrogels. Literature has reported 0.33 MPa and 1.2 to 1.5 MPa as a plant's osmotic pressure level at field capacity and wilting point respectively (Lavergne et al., 2020). Across this pressure range, the pressure level for releasing absorbed water for optimum plant growth is estimated to be around 0.8 MPa (Cheng et al., 2018) and 1 MPa (Narjary et al., 2012). Measuring water release from hydrogels at different pressures enables estimations and predictions on the potential for water held by hydrogels to be a direct source of soil moisture for plants (Cheng et al., 2018; Guilherme et al., 2010).

A unique characteristic of hydrogels is their potential to exhibit self-pressure due to the gelation processes that enables release of water (Ako, 2017a). The self-releasing pressure is dependent on the weight of the hydrogel (Ako, 2017b), the mechanical stress and strain from polymer network hydration, relaxation and expansion (Boral et al., 2010), and duration which the absorbed content has been stored (Mao et al., 2001). Also, capillary forces which influences water uptake contribute to the self-releasing pressure from hydrogels (Ako, 2017b). Largely, this release characteristic is seen among polysaccharides hydrogels as spontaneously. Such hydrogels quickly release their absorbed content after swelling or when swollen with absorbed content for a long period of time (Ako, 2017b). However, hydrogel self-releasing pressure varies between different hydrogel types as compositional differences determine absorbed content flow and viscosity of hydrogels. Generally, soft hydrogels can hold water for a longer period without exceeding a self-releasing pressure threshold than stiff hydrogels due to their elasticity characteristics (Ako, 2017b).

Varying temperature levels can potentially effect water release effect from swollen hydrogels as their matrices respond to heat energy (Ako, 2017b). Often, temperature

above a certain point (usually 37% although this is gel dependent), collapses the 3D network structure which triggers relaxation and expansion and the release of the absorbed water content (Kabir et al., 2018). Data from temperature effects on swollen hydrogels can aid understanding of the potential for hydrogels to both absorb and release water (from soil or atmosphere) when applied in arid and semi-arid locations that are characterised by high temperatures.

4.2.3 Pores in hydrogels for holding and releasing absorbed water

Generally, hydrogels use closed, open or interconnected void spaces within the bulk hydrogel material as pores to function as superabsorbents (Chirani et al., 2015). These pores include primary structural of original smaller pores within the 3D network as well as pores produced through phase separation during the production process. However, the techniques for finding and quantifying porosity have limitations due to complexities of molecular structure, and often disprove modelled equation assumptions (Chirani et al., 2015). Hydrogel pores are assessed with molecular probes and are quantified using labelled compounds of varied molecular weights or sizes. Generally, dry hydrogels have high porosity distribution relative to wet hydrogels where gelation fills pores with absorbed content (Chandrika et al., 2016). Damages to a hydrogel network structure reduces its pores space and absorption capacity.

4.2.4 Absorbed water types and measurement in hydrogels

Two main water types exist in a swollen hydrogel: free water and bound water (Gun'ko et al., 2017). Free water is stored in the hydrogel structure and can easily be released whereas bound water can be further divided into weakly and strongly bound water that is bound to the hydrogel surface or polymer network. Bound water cannot easily be released and defines the first water to be absorbed but the last to be released. Free water occupies

expanded space in the hydrogel after hydration and is desorbed first during desorption (Ostrowska-Czubenko et al., 2011).

Methods for estimating free and bound water volumes from total absorbed water in a hydrogel includes the use of small molecular probes, Differential Scanning Calorimetry (DSC) and Nuclear Magnetic Resonance (NMR) (Gun'ko et al., 2017). However, these methods have shortcomings that affect their accuracy. For instance, Proton Nuclear Magnetic Resonance which have proved that water exchanges between free and bound water are rapid at a rate of 1 water molecule in a every 10^{-9} seconds in hydrogels, and thus accurately measuring these water types using the small molecular probe and DSC methods can be challenging (Alam et al., 2014).

4.2.5   Aims and specific objectives
The experimental work described in this chapter aims to assess the desorption potential of hydrogels under varied suction pressure levels that mimic water stress levels in plants. The general aim of this work is to assess water release from hydrogels as a function of osmotic pressure, and to relate this back to potential application of hydrogels to support agricultural production in arid and semi-arid regions hydrogels under different pressure levels that could be used to assess plant growth stress.

4.3   Methods and methodology
4.3.1   Absorbed water release from hydrogels under varied pressure levels
The processes controlling the release of absorbed water from hydrogels is a function of multiple factors and high absorption potential does not necessarily equate to high desorption potential.

To explore variations in water release from hydrogels, the best and worst absorbing hydrogels, from Chapter 3 (CR and ER) were used for the absorbed water release experiments described in this Chapter. The primary aim of this experiment was to assess if water absorbed by hydrogels from the atmosphere could be released and the pressure level at which this release occurred. The two hydrogels used in this experiment had distinct features. Hydrogel CR is a non-uniformly shaped semi-solid material, while ER is a uniquely uniform shaped rounded hydrogel. The experiment was carried out using the pressure plate experiment for determining water retention or hydrostatic equilibrium (van Lier et al., 2019; Wang et al., 2015).

4.3.2 Procedure

Three grams of each of CR and ER hydrogels were weighed separately into 2 separate 100 ml urine cups and transferred into separate 1 litre bottles. The two 1 litre bottles containing 3 grams of ER or CR were filled with 900 litres of deionised water to allow free swelling to the point of maximum or equilibrium absorption over a 24-hour period. The CR hydrogels swelled faster compared with the ER hydrogels during this period of free swelling absorption. The excess unabsorbed water from both 1 litre bottles was drained through a 250-micron mesh sieve. The weight of the swollen hydrogels was measured to check the volume of water that was absorbed by each hydrogel. Using the density of water, 1 gram = 1 ml, the weight to litres conversion was made based on the volume of water absorbed by both hydrogels in grams/grams.

Nine replicates of 10 grams of the swollen CR hydrogels were accurately weighed into 9 labelled urine containers with caps of known mass and sealed immediately to prevent water loss from evaporation. The same procedure was repeated for the swollen ER hydrogels. The hygroscopic swollen ER and CR hydrogels under 100% relative humidity

at 20 and 30 ℃ from the hygroscopicity experiment in chapter 3.1 were also weighed to provide data for this experiment. Pressure levels of 0.1 bar, 1 bar and 15 bar were subsequently used to represent saturation point, field capacity point and wilting point plant water stress levels respectively as identified in Lavergne et al. (2020).

Pressure plates at 0.1 bar, 1 bar and 15 bar pressures were soaked in water overnight for the air pores to be filled with water for the pressure experiment. Three of the nine replicate ER hydrogels were placed on 3 different wetted 0.45-micron filter papers surrounded with cylindrical rings of volume range from 13.6 cm^3 to 15 cm^3 on each of the three pressure plates. The same procedure was repeated for the 9 weighed freely swollen CR hydrogels. Three replicates of each of the weighted hygroscopic swollen ER and CR hydrogels at relative humidity of 100 % and temperature of 20 ℃ from Chapter 3 were placed on 6 different wetted 0.45-micron filter papers surrounding by the same volume cylindrical rings as the freely swollen hydrogels on the 15-bar pressure plate. This same procedure was repeated for the weighed hygroscopic swollen ER and CR hydrogels at relative humidity 100 % and 30 ℃ which were placed on the 1 bar pressure plates.

A total of 12 sample rings were subject to each of 1 bar and 15 bar pressure plates. Six of these rings contained 10 grams of freely swollen ER and CR hydrogels (3 each) and 6 contained 10 g of hygroscopic swollen ER and CR hydrogels (3 each) (Figure 4.1). However, only a total of six rings containing 10 grams of freely swollen ER and CR hydrogels (3 each) were subject to 0.1 bar pressure. All pressure plates with swollen hydrogels were tightly sealed to ensure a 100 % relative humidity condition before pressurisation set to match their respectively pressure plates for the experiment to begin. The room temperature for this experiment was 20 ℃.

Water release at 0.1 bar pressure was visibly recorded to stop after 4 days and the weight of hydrogels after desorption was measured. The water release at 1-bar and the 15-bar

pressure plate stopped after 12 days, and the weight of each ER and CR hydrogel for (both freely swollen and hygroscopic swollen) was measured at this time.

To investigate desorption, CR and ER hydrogels were transferred to an individual 50 ml beaker and then oven dried at 105 ºC overnight for all the absorbed water remaining in the swollen hydrogels to desorb. After drying the hydrogels were weighed again to calculate their final dry weight. Data was therefore collected on how much water was released at each pressure level, how much water was left after the pressure plating experiment, but before drying; and the weight of the hydrogel crystals swollen to an absorbed mass of 10 grams. These parameters were needed to determine the desorbed water in gram/grams of dry hydrogel. To calculate the desorption water, the final weight of the hydrogel after desorption was subtracted from the initial weight of each swollen hydrogel before desorption and divided by their respective dry hydrogel weight. The values were presented in grams/grams for all data analysis.

During the experiment it was noted that the hydrogels which had absorbed hygroscopic water (Chapter 3) absorbed extra water from the pressure plate rather than desorbing water, and hence results from these experimental units is not further discussed in this study. The results presented and discussed in the following section is therefore limited to the hydrogels that absorbed water through free swelling.

Figure 4.1 *CR and ER hydrogels on pressure plate after applied pressure desorption*

4.4   Statistical data analysis

Microsoft Excel 16.50 software was used calculate the freely swollen hydrogel water weight gained, desorbed water weight and retained water in g/g and organized for R studio analysis. Statistical comparisons were made for variations between before and after pressure effects on water weight for all hydrogels, variations in desorbed water among pressures for both hydrogels, and variations in retained water at different pressures for both hydrogels using the linear model regression testing. Where differences were significant, a Tukey test was assessed for pairwise comparisons. For all statistical analysis, a 95 % confidence level was used to determine significant variations between the means of the log-transformed ($\log_{10}x$) data of the water weight in or desorbed from hydrogels. All statistical analyses for the comparison were performed with R version 3.6.2. Results were presented in graphs with raw data means and standard errors.

4.5   Results

4.5.1   Effect of applied pressure on the desorption or water from hydrogels CR and ER

Linear regression tests showed statistical differences between the mass of water contained within the studied hydrogels before and after the application of different pressure levels for both CR ($P < 0.001$) and ER ($P < 0.001$). A general trend of high mass of absorbed water before pressure application and low mass of absorbed water after pressure application was observed at all pressure levels indicating that water was released from the hydrogels through the application of pressure (Figure 4.2. and Figure 4.3). The effect of pressure on water release increased with the pressure level applied. Desorption values show that a pressure of 15 bar removed the highest mass of water from the hydrogels with a pressure of 0.1 bar removing the least amount of water for both studied hydrogels.
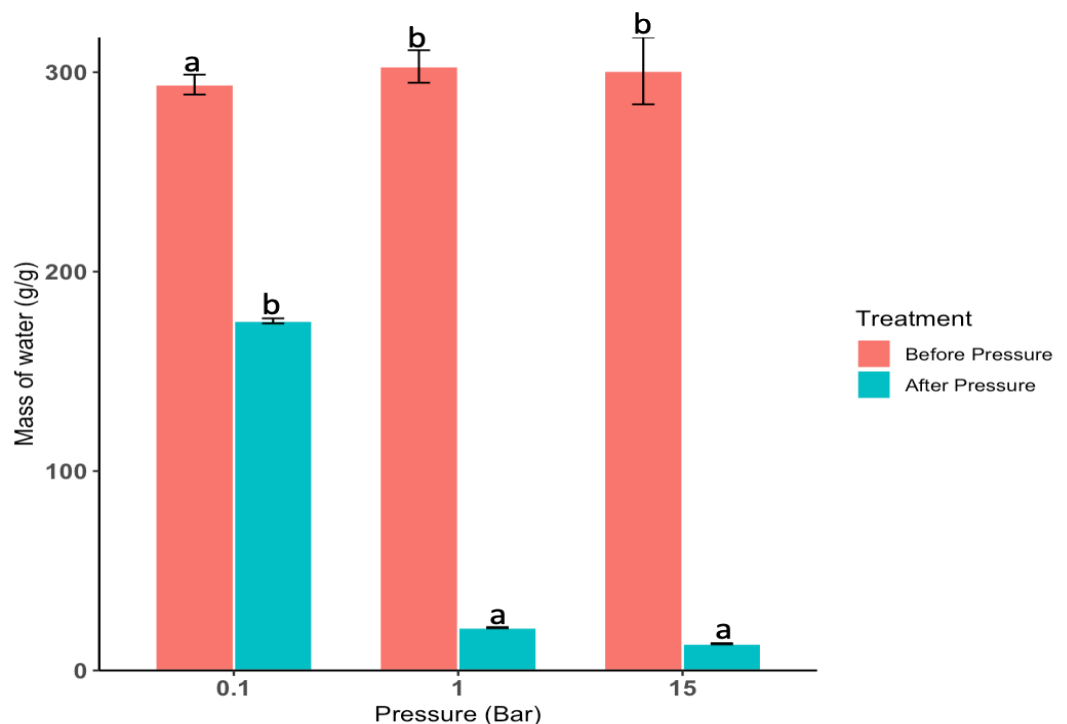
Figure 4.2 *Effect of pressure on the mass of water absorbed by hydrogel CR (Bars show mean ± SE and different letters indicate significant differences between before and after pressures for the different applied pressures).*
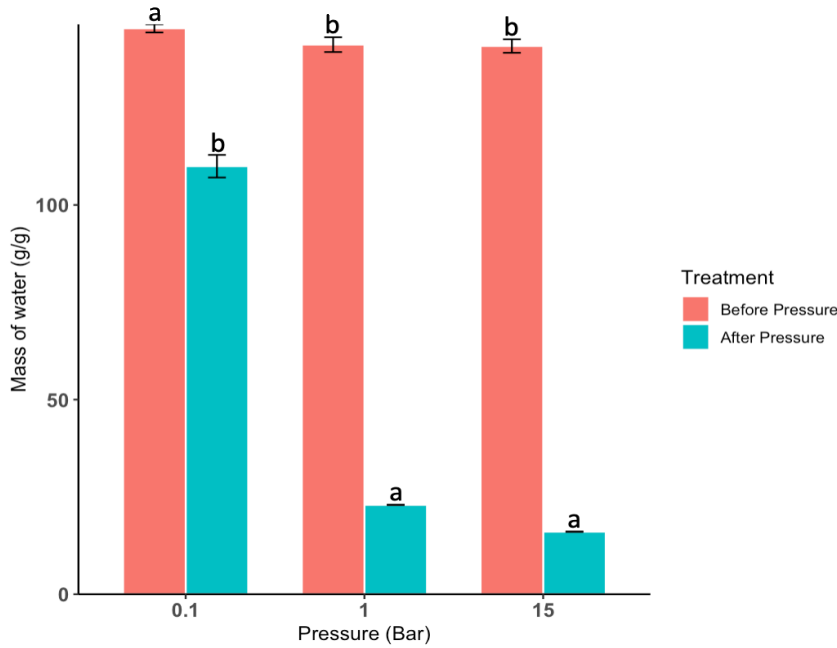
Figure 4.3 *Effect of pressure on the mass of water absorbed by hydrogel ER (Bars show mean ± SE and different letters indicate significant differences between before and after pressures for the different applied pressures).*

4.5.2   Mass of water released from hydrogels at different pressure levels

Linear regression testing showed statistically significant differences between the mass of water released at different pressure levels by both hydrogels (P < 0.001). Pairwise comparison showed statistical differences among all pressure levels except between 1 and 15 bar pressure levels for both hydrogels. Also, significant differences were observed among the hydrogels at each pressure level. Greater water release occurred from hydrogel CR compared to ER at each of 0.1, 1 and 15 bar pressure levels (Fig. 4.4). The greatest mass of water release was from hydrogel CR at the 15-bar pressure level (287.278 g/g) whereas hydrogel ER at 0.1 bar pressure released the least water (mean value of 118.50 g/g). Analysis of main effects showed significant differences were observed between ER and CR at all pressure levels studied. There was a significant increase in mass of water lost from both hydrogels as the pressure increased from 0.1 to 1 bar, but no statistically significant differences were observed between 1 bar and 15 bar for either ER or CR. This

shows that the 15 times pressure level increase from 1 bar to 15 bar removed no additional water mass from the hydrogels.
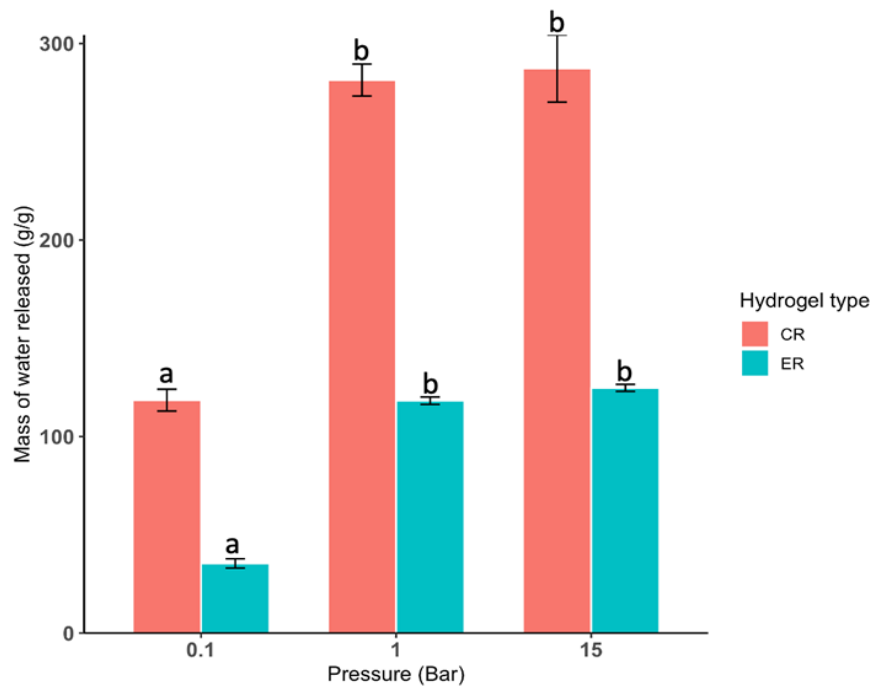
Figure 4.4 *Mass of water released from hydrogels CR and ER as a function of applied pressure (Bars show mean ± SE and different letters indicate significant differences between hydrogels for each pressure level).*

Linear regression analysis showed differences in water retention by both CR and ER at the different pressure levels (P < 0.001). A pairwise comparison showed differences in the water retained among the hydrogels at the same pressure and also among different pressure levels for each hydrogel. The residual mass of water retained by the hydrogels decreased as a function of pressure (Figure 4.5). The mass of water retained by CR was higher than that retained by ER at 0.1 pressure bar but dropped below the mass of water retained in ER at both 1 bar and 15 bar pressure levels. The greatest mass of water retained in the study was observed at 0.1 bar by hydrogel CR (mean value of 175.308 g/g) whereas

the lowest mass of water retained was observed at 15 pressure bar for hydrogel CR with

a mean actual water content of 13.389 g/g.
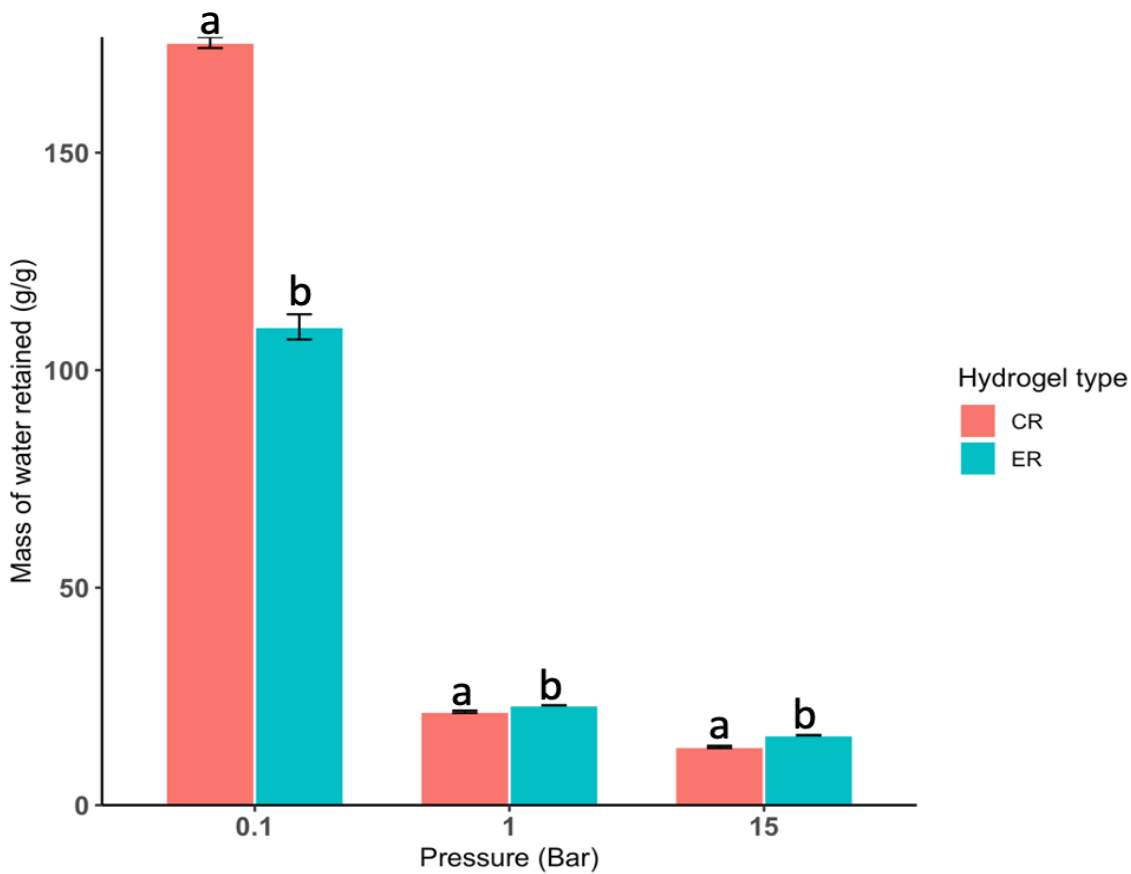
Figure 4.5 *Mass of water retained by hydrogels CR and ER as a function of applied pressure (Bars show mean ± SE and different letters indicate significant differences between hydrogels for each pressure leves).*

4.6   Discussion
4.6.1   Effect of applied pressure on desorption of the mass of water from CR and ER hydrogels

The mass of water contained by hydrogels ER and CR was significantly different both

before and after application of pressure at all the pressure levels applied, and the

difference increased with increasing pressure level. Water release from hydrogels for

plant utilisation is often described according to pressure levels which define plant-

available water in soils (Lavergne et al., 2020). Such pressures characterise concentration differences between plant roots and the surrounding soil in the context of pressure strength, force, or energy for drawing water (Ako, 2017; Guilherme et al., 2010; Urbina et al., 2021). The significant variations observed in the current study for the mass of retained water after and before pressure application for both hydrogels could be attributed to differences in energy or force associated with the osmotic pressure in drawing the water. An equilibrium point occurs at a specific pressure level which models the concentration gradient between plant roots and soil for drawing water. The increase in difference for water retained before and after applied pressure with increasing pressure level for both hydrogels' models the increased energy or force associated with drawing water from the hydrogel structure of CR and ER to the point where bonds in the polymer network may begin to break. Lavergne et al. (2020) reports that optimum readily-available water to plants occurs at field capacity (1 bar) with water to wilting point (15 bar pressure) being plant-available but progressively more difficult to access. Water requiring a pressure greater than 15 bar is considered non-accessible water to plants. Between 0.1 and 1 bar pressure, soil water readily drains through gravitational force and its availability is transient.

The data from this experiment suggests that any water released at a pressure of 0.1 bar could therefore be readily lost and hence action would be required to capture this water for subsequent use. The difference in water content before and after application of 1 bar pressure for both ER and CR hydrogels indicates the mass of optimum readily-available water for plants absorbed by the hydrogels. Plants under their highest water stress level after utilising the readily-available water at field capacity can use extra pressure up to 15 bar to draw additional absorbed water. This extra mass of water released up to 15 bar pressure is associated with plant-available water, and the corresponding mass of plant-

available water can be calculated as the difference in absorbed water mass before and after the application of 15 bar pressure for both ER and CR hydrogels.

Assumptions on free, weakly and strongly bound water in hydrogels, based on the work of Cursaru et al. (2010) and Gun'ko et al. (2017) can be used to explain the observed differences in water content at each of the pressure levels in the context of energy or force for drawing water. Free water type could have been recorded as the mass of water difference between before and after applied pressure at the 0.1 bar pressure level and the additional mass of water difference in the hydrogels between the before and after application could characterise weakly bound water at 1 bar due to the water storage mechanism in hydrogels. However, the energy or force at 15 bar pressure could be sufficient to characterise this strongly-bound water as inaccessible to plants and characteristic of plant wilting point. The weakly bound and strongly bound could be categorised as freezing and non-freezing bound water in the hydrogels.

A summary of these water types and their relationship to osmotic pressure and plant availability is presented in Table 4.1.

Table 4.1 *Summary of water types and their relationship to osmotic pressure and plant availability*

Osmotic pressure (bar)	Plant water status	Potential water type limit to be accessed based (binding strength)
0.1	Plant available (free draining)	Up to free water
1	Plant available (readily available)	Up to weakly bound water
15	Plant available	
>15	Not plant available	Up to strongly bound water

4.6.2 Mass of water released from CR and ER hydrogels at applied pressure levels

Comparison of the mass of water released per gram of hydrogel and the mass of water retained per gram of hydrogel, at the different pressure suction levels for both ER and CR showed statistical differences. Increasing the pressure level increased the mass of water released from hydrogels and decreased the mass of water retained. Significant water was released from hydrogels from 0.1 bar with increasing bar pressure level until 1 bar to 15 bar where water released was statistically insignificant for both hydrogels. These results agree with the work of Guilherme et al. (2010) and Cheng et al. (2018) who reported an increasing mass of water release from hydrogels to pressures of 3.5 and 7 bar respectively, after which there was no further decrease in the mass of water retained. Pressure is associated with energy or force that increases and that can draw either the free or bound absorbed (Gun'ko et al. 2017). The mechanism of pressure to desorb water from hydrogels occurs as the inverse of how it is absorbed (Ostrowska-Czubenko et al., 2011). Basing on Lavergne et al. (2020) classification of water types, and the correlation of osmotic pressure and plant availability (Table 4.1) the type of water released at 1 bar and 15 bar in both hydrogels was structurally the same as bound water (though freezing (weakly) bound is released before non-freezing (strongly) bound). This can explain the lack of significance in the mass of water released from both hydrogels at these pressures. This implies that pressure levels should be set above 15 bar for significant water release after 1 bar pressure, but if no further significant water is released with pressures beyond 15 bar, then the mass of atmospheric water absorbed as discussed in Chapter 3 may not be useful to plants. The reactivity of water molecules makes it challenging to categorise water as either bound or free water (Alam et al., 2014), however identifying the water type released at the different pressures in future studies could further improve understanding of hydrogel desorption.

Although significant differences were observed for the mass of water released at all pressure levels between the hydrogels, the pattern of incremental water release was similar, and this indicates that differences in absorbed water mass within hydrogels also influenced water release at the pressure levels. Hydrogels with high absorbing potential are recognised to desorb more absorbed water (Gun'ko et al., 2017). Skoug et al. (1993) in Paarakh et al. (2018) reported that differences in polymer concentration enable viscosity to limit the hydrogel's release coefficient, and therefore variations in N % concentration between the two hydrogels could be responsible for release differences. Ako (2017) and Paarakh et al. (2018) highlighted that flexible hydrogel structure and thin surface layer enables water release and therefore the flexible structure and thin surface layer in CR as opposed to the rigid structure and thick surface layer of ER could explain observed differences. Flexible hydrogel structure encourages absorbed water release whereas a rigid structure limits water release.

It is worth mentioning that the mass of retained water under all three tested pressure levels was higher than the greatest mass of water absorbed from the atmosphere for both hydrogels, and therefore desorption of atmospheric water could require higher pressure energy than 15 bar or even heat energy for evaporation and later condensation. Hydrogel CR, the hydrogel with the greatest absorption potential, showed a strong correlation with biosorption absorption from a first order kinetic model indicating that higher energy could desorb the majority of water molecules that may have strongly bound to the hydrogel surface or polymer network during absorption. Urbina et al. (2021) report that transportation of swollen hydrogels in arid areas leads to water loss and therefore movement of the swollen hydrogel to sites with high energy for desorption could lead to loss of the already small mass of water absorbed. Assessing water release characteristic of these hydrogels provides information on how absorbed water can be utilised for soil

water conservation and conditioning (Cheng et al., 2018). This information on water release at different pressures can inform how fully hydrated ER and CR hydrogels might release water at soil and plant water stress point levels of saturation, field capacity and wilting point.

4.6.3 Mass of water retained in CR and ER hydrogels at applied pressure levels

In the context of water retention, Figure 4.5 shows significant differences in the mass of water retained by both ER and CR hydrogels at all pressure levels. Figure 4.5 shows that the highest mass of retained water was apparent for hydrogel CR at 0.1 bar, although CR also showed the lowest mass of retained water at 1 bar and 15 bars. These observations could be attributed to water type (Gun'ko et al. 2017) and the processes for water absorption and release described in Chapter 4.6.2 (Ostrowska-Czubenko et al., 2011). The trend for the change in mass of water retained, especially at 1 and 15 bar, could be due to the bound water which depends on the hydrogel surface chemistry and crosslinking degree during hydration (Gun'ko et al. 2017). The chemical composition of both hydrogels could have influenced the mass of bound water gained at the 1 bar and 15 bar. Furthermore, Gun'ko et al. (2017) reported decreasing hydration increases the strongly bound water fraction in hydrogels, with high crosslinking indicative of less hydration but more water molecules clinging to the polymer network as bound water. Therefore, the higher bound water content (potentially strongly bound water) in hydrogel ER relative to CR at 1 and 15 bar pressure could be due to differences in crosslinking composition. However, the slight increase in mass of water in hydrogel CR relative to ER at 0.1 bar could be a function of differences in swelling capacity which is responsible for absorbing freezing free water absorption into the hydrogel structure. Again, the assumption could be made that 0.1 bar pressure was not sufficient to draw all free water from CR; a further increase to 1 bar and 15 bar suction pressure level was needed to release all usable and

readily available water. Based on this observation, it can be inferred that CR hydrogel is better at water absorption and desorption as a function of its chemical composition. Hydrogel CR could release more water at pressures below 15 bar.

4.7   Conclusion
The experimental work in this chapter has shown that hydrogels can release absorbed water under applied pressure. However, the highest modelled plant water stress pressure applied in this research (wilting point) was not sufficient to release the highest mass of atmospheric water absorbed form Chapter 3. This research shows that hydrogels release a statistically similar mass of absorbed water at field capacity as at wilting point. Further studies could be undertaken to assess if hydrogels can release more water at pressures beyond the plant wilting point pressure level of 15 bar, and to ascertain the pressure required to release the absorbed atmospheric water. The work in this chapter concludes that best performing hydrogels release more and retain less water, and this is a function of the hydrogel's chemical and physical composition.

CHAPTER FIVE

5   GENERAL DISCUSSION AND CONCLUSION

5.1   Hydrogels and the arid environment

Global water scarcity is increasing, and it impacts have largely been seen in arid and semi-arid regions (Xu et al., 2020). The severity of water scarcity has led to agricultural production decline and threatened lives throughout these arid and semi-arid regions. Increasing water scarcity is accepted to be coupled with climate change (Falkenmark, 2013; Kalhapure et al., 2016; Neethu et al., 2018).

As a potential mechanism to hold water after irrigation and to release this more slowly to plants, reducing water loss and plant water stress in arid areas, hydrogels, among other absorbents, have been used as soil conditioners because of their water absorption potential. However, water sources for irrigation are increasingly becoming limited due to evaporation under the high temperature and low relative humidity that is characteristic of arid and semi-arid areas (Dehghanisanij et al., 2006). As a consequence, attention has shifted to the earth's atmosphere as a source of freshwater using water harvesting methods that rely on sorbents to absorb atmospheric water vapour and subsequently release this for productive use (Li et al., 2018). However, application of this ideas is challenging because of the low relative humidity and high temperature environmental conditions characteristic of target regions. The potential of many sorbents including zeolites, metal-organic framework (MOF) and hygroscopic salts in atmospheric water harvesting sorption have been widely studied (Kallenberger and Fröba, 2018; Li et al, 2017). Hydrogels are one class of sorbents that have shown specific promise to absorb irrigation water and to slowly release this to plants even under temperature conditions of 40 - 50 ºC. However, the hygroscopicity of hydrogels under high temperatures and low humidity conditions has been poorly studied. Therefore, the potential application of hydrogels to absorb water from the atmosphere, and to release this for plant use in arid and semi-arid

regions is poorly explored. The research described in this thesis was therefore conducted to assess the hygroscopic behaviour of hydrogels in terms of the amount and rate of atmospheric water absorbed under different relative humidity percentage and temperatures levels, and to investigate the pressure level required to desorb the absorbed atmospheric water. Understanding of this absorption and desorption potential will underpin application of hydrogels to capturing atmospheric water and to mechanisms for delivering this to plants to sustain agriculture in arid and semi-arid environments.

5.2   Summary of key findings

The experiments conducted in this study quantified atmospheric water absorption by hydrogels and their desorption potential to model the interaction of hydrogels with this potential water source in arid and semi-arid regions. Results found that the chemical and physical properties of hydrogels largely influence the mass of atmospheric water a hydrogel can absorb. This was evident with the presence of N % in all hydrogels except hydrogel CR, which significantly restrained the atmospheric water absorption capacity of all hydrogels except CR due to the contribution of N % to crosslinking effects. The lack of crosslinking factor in hydrogel CR significantly increased atmospheric water absorption mass to about 8 - 39 % over the other hydrogels. Hydrogel size and geometry was shown to impact on atmospheric water absorption and could explain differences in absorption potential between the least and best absorbing synthetic polymer hydrogels. However, these factors did not apply to the natural polymer hydrogel AR. It may be that chemical composition differences owing to synthetic pathway (natural vs industrial) may further explain the differences described here.

The experimental results described in Chapter 3 showed that external factors, including time and relative humidity, significantly influence the potential of hydrogels to absorb atmospheric water. Relative humidity at 84 % and above was observed as the optimum

condition for maximum atmospheric water absorption. This environmental condition constrains field application and practicality of using hydrogels to absorb atmospheric water under arid conditions, although predictions for climate change suggests more atmospheric water and increased relative humidity in some semi-arid/arid regions.

Although the current study indicates that temperature changes between 10 and 30 °C cannot influence absorption, the absorption trend observed in this work changed over 168 hours as a function of temperature presumably due to changes in saturated vapor pressure and partial vapor pressure fluctuations caused by temperature on the atmospheric water content in the humidity chamber. The findings of the current work suggest that future research should avoid using salt solutions for relative humidity percentages especially for studies where the impact of wide temperature ranges that may occur in the future due to climate change is a design aim.

Results from the current study allow the inference that the response of the tested hydrogels to high relative humidity, even over the daily period of 8-12 hours that occurs from night to early morning, may not allow hydrogels sufficient time to reach their full absorption capacity due to the low absorption rates observed. Furthermore, observations made on the absorption curves (for absorption below 100 % relative humidity) indicate that hydrogels may take longer than 72 hours to attain maximum equilibrium absorption of very low hygroscopic water under environmental conditions. For the tested hydrogels (particularly CR) absorbing at 100 % relative humidity, increased absorption can continue but such environmental conditions may only exist for 8-12 hours in a day, after which time desorption may occur. As such, desorption of the water may be appropriate immediately after the absorption period.

For the desorption of absorbed atmospheric water from hydrogels, the results from Chapter 4 showed that absorbed water cannot be desorbed under the natural pressure

levels exerted by plants at different water stress levels tested in this research. The results from Chapter 4 infer that the plant water sucking power (pressure potential) at saturation point, field capacity and wilting capacity is too low to desorb absorbed atmospheric water in the hydrogels for plant use even at the highest absorbed water mass. Therefore, research into further pressure levels beyond the 15-bar wilting point pressure (for example, 30, 60 and 90 bar) is needed to ascertain the optimum desorption pressure level for absorbed atmospheric water. It is worth noting that 0.35 g/g of atmospheric water is the mass of atmospheric water absorbed under 100 % relative humidity. This level of relative humidity is rarely seen in water scarce regions, and this suggests that the optimum pressure required to desorb absorbed water under low relative humidity percentages possibly might be higher than the maximum pressure plants can exert. Hence, this thesis finds that water is unlikely to be released from hydrogels to encourage plant germination and growth, enhance nutrient utilization, reduce irrigation periods and limit plant wilting unless other desorption measures are employed. Increasing the pressure level to facilitate desorption will therefore require an engineering solution and the associated energy requirements will lead to higher financial cost. Such options could allow water release from hydrogels that could then be piped and supplied for irrigation. Considerations of less costly energy and more environmentally friendly options like low grade thermal energy from solar radiation could be explored to facilitate the use of hydrogels in the atmospheric water harvesting scenario for arid and semi-arid regions described here (Li et al., 2018). The research in this thesis finds that irregular shaped hydrogel particles containing no N%, deployed at a relatively humidity level of 84 % and beyond over an extended time, leads to the best atmospheric water absorption even though the amount of water absorbed is substantially lower that MOFs, GO membrane and zeolites which will absorb water at equivalent relative humidity levels (Wang et al., 2019). However, hydrogel CR absorbed

a higher atmospheric water content than Manganese Dioxide and Silica Gel in the same study by Wang et al. (2019). The current research has found that the best absorbing hydrogels also desorb the most water due to their high absorption capacity. However, this study shows that plants are unlikely to access such absorbed atmospheric water even at critical water stress levels associated with the osmotic pressure required for desorption. Further investigation of economical viable and eco-friendly means of desorption should be explored for releasing atmospheric water that is absorbed by hydrogels.

5.3   Opportunities for application to water harvesting

Although this work has shown that high relative humidity percentages are required for optimum hydrogel hygroscopicity, and that this may limit the potential for water absorption due to the length of time during a day when humidity levels are above the minimum required value, the modelled effect of climate change on atmospheric water content predicts an increase in vapor due to increased evaporation (Del Genfo et al., 1991). This could enhance scenarios for the field application of hydrogels to atmospheric water collection over a future-looking time frame. Due to the observation that a plants' highest osmotic pressure was not enough to desorb the water from the hydrogels, it may not be viable to incorporate hydrogels in soil. Instead, hydrogels but could be separated from the soil and raised up as "banks" to allow absorption through direct atmospheric humidity contact. Application of hydrogels in this way could more effectively capture available moisture that existing approaches, although simple engineering techniques would be needed to facilitate desorption. The application of hydrogels could be costly where there was regular replacement of sorbent as it degrades. However, understanding hydrogel behavior could lead to utilization of gels for multiple absorption and desorption cycles where hydrogel structure collapse is minimized due to absorption below maximum

absorption capacity (Guilherme et al., 2015). This could effectively increase hydrogel cycling stability and durability for absorption and desorption, reducing operating costs. In other word, the relatively small amount of water that this research has shown can be absorbed from the atmosphere compared to its full absorption capacity will lead to less expansion stress and reduced structural collapse compared with hydrogels that absorb water by liquid contact, facilitating effective utilisation for longer periods of time.

Basing on the absorption trend with temperature for hydrogel CR, best absorbing and desorbing hydrogel, the low temperatures at early morning and late night could provide opportunity for the absorption from the high humid atmosphere over the same period. This will enhance optimal absorption which is expected over low temperature periods in water scarce areas due to relative humidity percentages often below 100 %. Such absorption characteristics make hydrogels more applicable than MOFs, as while MOFs have high absorption capacity for a range of dew temperature and relative humidity environments, they are not effective at relative humidity below 50 % (Kim et al., 2017). Decreased temperature during nighttime could lead to dew point if the temperatures go beyond the dew point temperature, giving hydrogels directly exposed to the atmosphere higher surface affinity for absorbing water than a bare surface. However, limitations of this scenario should be noted. The instances of dew occurrence are limited in water-scarce areas due to relative humidity levels commonly in the order of 40% (Kim et al, 2018). At this humidity level, the water content in hydrogels absorbed from atmospheric water vapor may be higher than the water content absorbed from dew point alone because a dew condition is not often present. With hydrogels directly exposed to the atmosphere, rather than being incorporated into the soil, the need for high energy thermal or mechanical desorption of the low amount of water vapor absorbed could be managed through integrating a readily-available solar energy to drive desorption (Kim et al., 2017; Li et al.,

2018); the arid and semi-arid areas of the world where this scenario is envisaged are abundant in solar energy. With this potential for using solar energy to drive desorption, absorption could occur over the cooler night and early morning periods, with desorption carried out over the warmer daytime conditions (Kallenberger & Fröba, 2018). The absorbed water can be heated with solar energy, condensed, and then channeled for irrigation.

5.4 Challenges to practical application in water harvesting

The application of this research to arid and semi-arid field areas may be hindered by the need for relative humidity at or above 84 % for optimum atmospheric water absorption, a condition is not common in these water scarce areas. Furthermore, the absorption time of about 72 hours to 168 hours to reach hydrogel maximum absorption may not be met because relative humidity at or above 84 % may only be realised during the 8 - 12 hours period during night and early mornings as the air temperature drops towards dew point. Under such conditions, absorption of a relatively low amount of water by hydrogels might be expected. There is a risk that this low amount of water may be subsequently desorbed naturally through evaporation during the day (low relative humidity and high temperature) if no measures are taken to isolate, protect or otherwise desorb and capture this water. Future research could be undertaken to improve understanding of hydrogel behaviour especially under conditions of continuous absorption across alternating cycles of high/low temperatures and low/high relative humidity.

Most sorbents, including hydrogels, are considered to be good candidates for water absorption from air because of their capacity to absorb water even under low relative humidity without using energy (Li et al., 2018). Although this would allow field application of sorbents such as hydrogels for water harvesting in arid and semi-arid

regions, the application is challenged by the high energy required to desorb the low amount of absorbed water. Hydrogels could be modified to enhance their absorption properties so that they may be desorbed using less energy. However, field application may still be challenging for people without the economic resources to purchase the optimum engineering technologies for desorption. Furthermore, other water harvesting techniques such as refrigeration and fog harvesting which have seen success across a wide range of relative humidity levels (Li et al., 2018) and could have been made alongside sorption using the hydrogels to deploy the best system to support agricultural production in arid and semi-arid areas is limited due to the arid and semi-arid environmental conditions.

5.5   Recommendations for ongoing work

The synthesis of deliquescent or hygroscopic salts including $CaCl_2$ into hydrogels has yielded positive outcomes on atmospheric water absorption volume, rate and their desorption (Li et al; 2018). As such, future research could explore the opportunity to modify hydrogels (such as CR) with these salts to increase the absorption of atmospheric water over a wider relative humidity percentage range. Such studies should consider relative humidity percentages as low as 20 % to allow for further consideration of application to arid and semi-arid zones. There is also an opportunity to explore chemical structures that are characterised by steeper or faster absorption rates in the water sorption curve over shorter periods even under conditions of low relative humidity. Such work has been advanced for zeolite and metal-organic frameworks that underpin existing water harvesting mechanisms (Kim et al, 2017; Wang et al., 2019).

With the increasing adoption of solar energy usage, the potential of adopting solar-driven heat as the energy for desorption could be studied on the original CR and CR - $CaCl_2$ modified hydrogels. Such work would allow comparison on how these hydrogels perform

in terms of their solar thermo-sensitivity and energy requirements for desorption that is specifically targeted to semi-arid and arid regions (Matsumoto et al., 2018). Such information will advance understanding of the low critical solution temperature threshold beyond which water may be released and below which water might be absorbed. Information will also allow understanding of the themo-responsive behaviour of absorbed water in the hydrogels before they are heated to drive out and condense desorbed atmospheric water for irrigation.

Further research could explore the size and geometry dependency of hydrogels on atmospheric absorption potential, and how such effects vary across natural and synthetic hydrogels to better understand the anomalous behaviour of the natural hydrogel AR observed in the current study. This information will increase understanding of literature reports on the impact of hydrogels size and geometry on the absorption of atmospheric water.

The literature indicates that hydrogels absorb better under conditions of re-absorption compared with immersion due to expansion created within the hydrogel structure during the absorption-desorption cycle. Collapse effected during absorption will inhibit further absorption. Further research could therefore explore structural changes during hygroscopic absorption, providing estimations on possible absorption-desorption process cycle counts that will quantify the useful lifetime of hydrogels for atmospheric water absorption.

CHAPTER SIX

6 REFERENCES

Abdallah, A. M. (2019). The effect of hydrogel particle size on water retention properties and availability under water stress. *International Soil and Water Conservation Research, 7*(3), 275-285.

Abdel-Halim, E., & Al-Deyab, S. S. (2014). Preparation of poly (acrylic acid)/starch hydrogel and its application for cadmium ion removal from aqueous solutions. *Reactive and Functional Polymers*, *75,* 1-8.

Abdi, A. M., Boke-Olén, N., Tenenbaum, D. E., Tagesson, T., Cappelaere, B., & Ardö, J. (2017). Evaluating water controls on vegetation growth in the semi-arid Sahel using field and Earth observation data. *Remote Sensing, 9*(3), 294.

Abedi-Koupai, J., & Asadkazemi, J. (2006). Effects of a hydrophilic polymer on the field performance of an ornamental plant (Cupressus arizonica) under reduced irrigation regimes. *Iranian Polymer Journal, 15*(9), 715.

Abedi-Koupai, J., Eslamian, S. S., & Kazemi, J. A. (2008). Enhancing the available water content in unsaturated soil zone using hydrogel, to improve plant growth indices. *Ecohydrology & Hydrobiology, 8*(1), 67-75.

Abedi-Koupai, J., Sohrab, F., & Swarbrick, G. (2008). Evaluation of hydrogel application on soil water retention characteristics. *Journal of plant nutrition, 31*(2), 317-331.

Ackerknecht, D., & Gut, P. (1993). Climate Responsive Building: Appropriate Building Construction in Tropical and Subtropical Regions.

Agam, N., & Berliner, P. (2004). Diurnal water content changes in the bare soil of a coastal desert. *Journal of Hydrometeorology, 5*(5), 922-933.

Agam, N., & Berliner, P. R. (2006). Dew formation and water vapor adsorption in semi-arid environments—A review. *Journal of Arid Environments, 65*(4), 572-590.

Aggor, F. S., Ahmed, E. M., El-Aref, A., & Asem, M. (2010). Synthesis and characterization of poly (acrylamide-co-acrylic acid) hydrogel containing silver nanoparticles for antimicrobial applications. *Journal of American Science, 6*(12), 648-656.

Ahmad, S., Manzoor, K., Purwar, R., & Ikram, S. (2020). Morphological and Swelling Potential Evaluation of Moringa oleifera Gum/Poly (vinyl alcohol) Hydrogels as a Superabsorbent. *ACS omega, 5(*29), 17955-17961.

Ahmed, E. M. (2015). Hydrogel: Preparation, characterization, and applications: A review. *Journal of Advanced Research, 6*(2), 105-121.

Ahmed, E. M., Zahran, M. A., Aggor, F. S., Elhady, S., & Nada, S. S. (2016). Synthesis and swelling characterization of carboxymethyl cellulose-g-Poly (Acrylic acid-co–Acrylamide) hydrogel and their application in agricultural field. *International Journal of ChemTech Research, 9*(8), 270-281.

Ako, K. (2017). Yield study with the release property of polysaccharide-based physical hydrogels. *International Journal of Biological Macromolecules, 101*, 660-667.

Alam, T. M., Childress, K. K., Pastoor, K., & Rice, C. (2014). Characterization of Free Surface-Bound and Entrapped Water Environments in Poly (N-Isopropyl Acrylamide) Hydrogels via 1H HRMAS PFG NMR Spectroscopy. *Journal of Polymer Science. Part B, Polymer Physics, 52*(SAND-2014-15247J).

Albayrak, C., Barım, G., & Dag, Ö. (2014). Effect of hygroscopicity of the metal salt on the formation and air stability of lyotropic liquid crystalline mesophases in hydrated salt–surfactant systems. *Journal of Colloid and Interface Science, 433,* 26-33.

Allen, R. G., Pereira, L. S., Raes, D., & Smith, M. (1998). Crop evapotranspiration-Guidelines for computing crop water requirements-*FAO Irrigation and Drainage paper 56*. Fao, Rome, 300(9), D05109.

Bagley, E., & Long, F. (1955). Two-stage sorption and desorption of organic vapors in cellulose acetate1, 2. *Journal of the American Chemical Society, 77*(8), 2172-2178.

Bahram, M., Mohseni, N., & Moghtader, M. (2016). *An introduction to hydrogels and some recent applications. In Emerging concepts in analysis and applications of hydrogels*. IntechOpen.

Baier, W. (1966). Studies on dew formation under semi-arid conditions. *Agricultural Meteorology, 3*(1-2), 103-112.

Bao, L.-R., Yee, A. F., & Lee, C. Y.-C. (2001). Moisture absorption and hygrothermal aging in a bismaleimide resin. *Polymer, 42*(17), 7327-7333.

Bassas-Galia, M., Follonier, S., Pusnik, M., & Zinn, M. (2017). Natural polymers: a source of inspiration. In Bioresorbable polymers for biomedical applications (pp. 31-64): *Elsevier.*

Bazin, F., Hathie, I., Skinner, J., & Koundouno, J. (2017). Irrigation, food security and poverty–Lessons from three large dams in West Africa. *International Institute for Environment and Development, London.*

Begam, T., Nagpal, A. K., & Singhal, R. (2004). A study on copolymeric hydrogels based on acrylamide-methacrylate and its modified vinyl-amine-containing derivative. *Designed Monomers and Polymers, 7(*4), 311-330.

Bellich, B., Borgogna, M., Cok, M., & Cesàro, A. (2011). Release properties of hydrogels: water evaporation from alginate gel beads. *Food biophysics, 6*(2), 259-266.

Bis, Z., Kobyłecki, R., Ścisłowska, M., & Zarzycki, R. (2018). Biochar–Potential tool to

    combat climate change and drought. *Ecohydrology & Hydrobiology, 18*(4), 441-

    453.

Bo, Z., Renkuan, L., Yunkai, L., Tao, G., Peiling, Y., Ji, F., Weimin, X. & Zhichao, Z.

    (2012). Water-absorption characteristics of organic–inorganic composite

    superabsorbent polymers and its effect on summer maize root growth. *Journal of*

    *Applied Polymer Science, 126(*2), 423-435.

Booker, J. F., & Trees, W. S. (2020). Implications of Water Scarcity for Water

    Productivity and Farm Labor. *Water, 12*(1), 308.

Boral, S., et al. (2010). Syneresis in agar hydrogels. *International journal of biological*

    macromolecules, 46(2), 232-236.

Boyer, J. (1976). Water deficits and photosynthesis. *Water deficits and plant growth, 4*,

    153-190.

Brown, I., Poggio, L., Gimona, A., & Castellazzi, M. (2011). Climate change, drought

    risk and land capability for agriculture: implications for land use in Scotland.

    Regional Environmental Change, 11(3), 503-518.

Buchholz, F. L., & Graham, A. T. (1998). Modern superabsorbent polymer technology.

    John! Wiley & Sons, Inc, 605 Third Ave, New York, NY 10016, USA, 1998.

    279.

Callaghan, T., Lindley, D., Ali, O., El Nour, H. A., & Bacon, P. (1989). The effect of

    water-absorbing synthetic polymers on the stomatal conductance, growth and

    survival of transplanted Eucalyptus microtheca seedlings in the Sudan. *Journal*

    *of Applied Ecology, 6*63-672.

Castillo, J. M. (2011). *Relative humidity: sensors, management, and environmental*

    effects. Nova Science Publishers.

Chai, Q., Gan, Y., Zhao, C., Xu, H. L., Waskom, R. M., Niu, Y., & Siddique, K. H. (2015). Regulated deficit irrigation for crop production under drought stress. A review.

Chan, A. W., & Neufeld, R. J. (2009). Modeling the controllable pH-responsive swelling and pore size of networked alginate based biomaterials. *Biomaterials, 30*(30), 6119-6129.

Chandrika, K. P., Singh, A., Rathore, A., & Kumar, A. (2016). Novel cross linked guar gum-g-poly (acrylate) porous superabsorbent hydrogels: characterization and swelling behaviour in different environments. *Carbohydrate polymers, 149*, 175-185.

Chavda, H., & Patel, C. (2011). Effect of crosslinker concentration on characteristics of superporous hydrogel. *International journal of pharmaceutical investigation, 1(*1), 17.

Chen, S., Hu, J., & Zhuo, H. (2011). Study on the moisture absorption of pyridine containing polyurethane for moisture-responsive shape memory effects. *Journal of materials science, 46(*20), 6581-6588.

Chen, Y. (Ed.). (2019). Hydrogels Based on Natural Polymers. Elsevier.

Cheng, D., Liu, Y., Yang, G., & Zhang, A. (2018). Water-and fertilizer-integrated hydrogel derived from the polymerization of acrylic acid and urea as a slow-release N fertilizer and water retention in agriculture. *Journal of agricultural and food chemistry, 66*(23), 5762-5769.

Cheng, W.-M., Hu, X.-M., Zhao, Y.-Y., Wu, M.-Y., Hu, Z.-X., & Yu, X.-T. (2017). Preparation and swelling properties of poly (acrylic acid-co-acrylamide) composite hydrogels. *e-Polymers, 17(*1), 95-106.

Cheng, Y., Yang, W., Zhan, H., Jiang, Q., Shi, M., & Wang, Y. (2020). On the Origin of Deep Soil Water Infiltration in the Arid Sandy Region of China. *Water, 12*(9), 2409.

Chhabra, R. (2004). Classification of salt-affected soils. *Arid Land Research and Management, 19*(1), 61-79.

Chirani, N., Gritsch, L., Motta, F. L., & Fare, S. (2015). History and applications of hydrogels. *Journal of biomedical sciences, 4*(2).

Cursaru, B., Stanescu, P. O., & Teodorescu, M. (2010). The states of water in hydrogels synthesized from diepoxy-terminated poly (ethylene glycol)s and aliphatic polyamines. *UPB Scientific Bulletin, Series B: Chemistry and Materials Science, 72*(4), 99-15.

Davtalab, R., Salamat, A., & Oji, R. (2013). Water harvesting from fog and air humidity in the warm and coastal regions in the south of Iran. *Irrigation and Drainage, 62*(3), 281-288.

De Vreugd, J. (2011). The effect of aging on molding compound properties-aging characterization of molding compounds and its modeling. *TU Delft.*

De Wit, M., & Stankiewicz, J. (2006). Changes in surface water supply across Africa with predicted climate change. *Science, 311*(5769), 1917-1921.

Dehghanisanij, H., Oweis, T., & Qureshi, A. S. (2006). Agricultural water use and management in arid and semi-arid areas: current situation and measures for improvement. *Annals of Arid Zone*, *45*(3/4), 355.

Del Genfo, A. D., Lacis, A. A., & Ruedy, R. A. (1991). Simulations of the effect of a warmer climate on atmospheric humidity. *Nature, 351*(6325), 382-385.

Dubelley, F., et al. (2017). Water vapor sorption properties of polyethylene terephthalate over a wide range of humidity and temperature. *The Journal of Physical Chemistry B, 121*(8), 1953-1962.

Duncan, B. C., & Broughton, W. R. (2007). *Measurement good practice guide No. 102 absorption and diffusion of moisture in polymeric materials.* Tech. Rep. 102, National Physics Laboratory, Teddington, Middlesex, United Kingdom.

Dwevedi, A., Kumar, P., Kumar, P., Kumar, Y., Sharma, Y. K., & Kayastha, A. M. (2017). Soil sensors: detailed insight into research updates, significance, and future prospects. In New pesticides and soil sensors (pp. 561-594): *Elsevier.*

Ekebafe, L., Ogbeifun, D., & Okieimen, F. (2011). Effect of native cassava starch-poly (sodium acrylate-co-acrylamide) hydrogel on the growth performance of maize (Zea may) seedlings. *American Journal of Polymer Science, 1*(1), 6-11.

Eslamian, S., Khordadi, M. J., & Abedi-Koupai, J. (2011). Effects of variations in climatic parameters on evapotranspiration in the arid and semi-arid regions. *Global and Planetary Change, 78*(3-4), 188-194.

Falkenmark, M. (2013). Growing water scarcity in agriculture: future challenge to global water security. Philosophical Transactions of the Royal Society A: *Mathematical, Physical and Engineering Sciences, 371*(2002), 20120410.

Farrell, C., Ang, X. Q., & Rayner, J. P. (2013). Water-retention additives increase plant available water in green roof substrates. *Ecological Engineering, 52,* 112-118.

Flory, P. J. (1953). Principles of polymer chemistry. Cornell University Press.

Fries, A., Silva, K., Pucha-Cofrep, F., Oñate-Valdivieso, F., & Ochoa-Cueva, P. (2020). Water balance and soil moisture deficit of different vegetation units under semiarid conditions in the andes of southern Ecuador. *Climate, 8*(2), 30.

Frisch, H. (1980). Sorption and transport in glassy polymers–a review. *Polymer Engineering & Science, 20(*1), 2-13.

Gallagher, K., & Corrigan, O. (2000). Mechanistic aspects of the release of levamisole hydrochloride from biodegradable polymers. *Journal of controlled release, 69*(2), 261-272.

Ganguly, S., Das, P., & Das, N. C. (2020). Characterization tools and techniques of hydrogels. In Hydrogels Based on Natural Polymers (pp. 481-517): *Elsevier.*

Ganji, F., Vasheghani, F. S., & Vasheghani, F. E. (2010). Theoretical description of hydrogel swelling: a review.

Gao, L., Wang, S., & Zhao, X. (2013). Synthesis and characterization of agricultural controllable humic acid superabsorbent. *Journal of Environmental Sciences, 25*, S69-S76.

Gaur, M. K., & Squires, V. R. (2018). Geographic extent and characteristics of the world's arid zones and their peoples. In *Climate variability impacts on land use and livelihoods in drylands* (pp. 3-20). Springer, Cham.

Ghobashy, M. M. (2020). The application of natural polymer-based hydrogels for agriculture. In *Hydrogels Based on Natural Polymers* (pp. 329-356). Elsevier.

Gleick, P. H., & Palaniappan, M. (2010). Peak water limits to freshwater withdrawal and use. *Proceedings of the National Academy of Sciences, 107*(25), 11155-11162.

Godfray, H., Beddington, J., Crute, I., Haddad, L., Lawrence, D., Muir, J., Pretty, J., Robinson, S., Thomas S.M. & Toulmin, C. (2010). Food security: the challenge of feeding 9 billion people. *Science, 327*(5967), 812-818.

Gómez, J. S. (2015). Characterization and effects of cross-linked potassium polyacrylate as soil amendment. *University of Seville, Seville, Spain.*

Guilherme, M. R., Aouada, F. A., Fajardo, A. R., Martins, A. F., Paulino, A. T., Davi,
M. F., Rubira, A. F., & Muniz, E. C. (2015). Superabsorbent hydrogels based on
polysaccharides for application in agriculture as soil conditioner and nutrient
carrier: A review. *European Polymer Journal, 72,* 365-385.

Guilherme, M. R., Reis, A. V., Paulino, A. T., Moia, T. A., Mattoso, L. H., &
Tambourgi, E. B. (2010). Pectin-based polymer hydrogel as a carrier for release
of agricultural nutrients and removal of heavy metals from wastewater. *Journal
of Applied Polymer Science, 117*(6), 3146-3154.

Gun'ko, V. M., Savina, I. N., & Mikhalovsky, S. V. (2017). Properties of water bound
in hydrogels. *Gels, 3*(4), 37.

Hao, X.-m., Li, C., Guo, B., Ma, J.-x., Ayup, M., & Chen, Z.-s. (2012). Dew formation
and its long-term trend in a desert riparian forest ecosystem on the eastern edge
of the Taklimakan Desert in China. *Journal of Hydrology, 472*, 90-98.

Hatibu, N., & Mahoo, H. (1999). Rainwater harvesting technologies for agricultural
production: A case for Dodoma, Tanzania. Conservation tillage with animal
traction, 161.

Held, I. M., & Soden, B. J. (2006). Robust responses of the hydrological cycle to global
warming. *Journal of Climate, 19(*21), 5686-5699.

Hoegh-Guldberg, O., Jacob, D., Bindi, M., Brown, S., Camilloni, I., Diedhiou, A.,
Djalante, R., Ebi, K., Engelbrecht, F., Guiot, J., Hijioka, Y., Mehrotra, S., Payne,
A., Seneviratne, S. I., Thomas, A., Warren, R., Zhou, G., Halim, S. A., Achlatis,
M., & Zougmoré, R. B. (2018). *Impacts of 1.5 C global warming on natural and
human systems. Global warming of 1.5 C*. An IPCC Special Report.

Huang, J., Yu, H., Guan, X., Wang, G., & Guo, R. (2016). Accelerated dryland
expansion under climate change. *Nature Climate Change, 6*(2), 166-171.

Hüttermann, A., Zommorodi, M., & Reise, K. (1999). Addition of hydrogels to soil for prolonging the survival of Pinus halepensis seedlings subjected to drought. *Soil and Tillage Research, 50*(3-4), 295-304.

Ingraham, N. L. (1998). Isotopic variations in precipitation. In *Isotope tracers in catchment hydrology* (pp. 87-118). Elsevier.

Jafari, M., Tavili, A., Panahi, F., Esfahan, E. Z., & Ghorbani, M. (2018). Reclamation of Arid lands: *Springer.*

Jansen, K. M. B., Zhang, M. F., Ernst, L. J., Vu, D. K., & Weiss, L. (2020). Effect of temperature and humidity on moisture diffusion in an epoxy moulding compound material. *Microelectronics Reliability, 107*, 113596.

Johnson, M. S. (1984). Effect of soluble salts on water absorption by gel-forming soil conditioners. *Journal of the Science of Food and Agriculture, 35*(10), 1063-1066.

Kabir, A., Dunlop, M. J., Acharya, B., Bissessur, R., & Ahmed, M. (2018). Water recycling efficacies of extremely hygroscopic, antifouling hydrogels. *RSC Advances, 8*(66), 38100-38107.

Kabiri, K., Omidian, H., Zohuriaan-Mehr, M., & Doroudiani, S. (2011). Superabsorbent hydrogel composites and nanocomposites: a review. *Polymer composites, 32*(2), 277-289.

Kalhapure, A., Kumar, R., Singh, V. P., & Pandey, D. (2016). Hydrogels: a boon for increasing agricultural productivity in water-stressed environment. *Current science*, 1773-1779.

Kallenberger, P. A., & Fröba, M. (2018). Water harvesting from air with a hygroscopic salt in a hydrogel–derived matrix. *Communications Chemistry*, *1*(1), 1-6.

Kalthoff, N., Fiebig-Wittmaack, M., Meißner, C., Kohler, M., Uriarte, M., Bischoff-
Gauß, I., & Gonzales, E. (2006). The energy balance, evapo-transpiration and
nocturnal dew deposition of an arid valley in the Andes. *Journal of Arid
Environments, 65(*3), 420-443.

Kamaly, N., Yameen, B., Wu, J., & Farokhzad, O. C. (2016). Degradable controlled-
release polymers and polymeric nanoparticles: mechanisms of controlling drug
release. *Chemical Reviews, 116*(4), 2602-2663.

Kazanskii, K., & Dubrovskii, S. (1992). Chemistry and physics of "agricultural"
hydrogels. Polyelectrolytes hydrogels chromatographic materials, 97-133.

Khan, M., & Duke, N. (2001). Halophytes-A resource for the future. *Wetlands Ecology
and Management, 9*(6), 455.

Khare, A. R., & Peppas, N. A. (1995). Swelling/deswelling of anionic copolymer gels.
Biomaterials, 16(7), 559-567.

Kidron, G. J., Herrnstadt, I., & Barzilay, E. (2002). The role of dew as a moisture
source for sand microbiotic crusts in the Negev Desert, Israel. *Journal of Arid
Environments, 52*(4), 517-533.

Kim, D., & Park, K. (2004). Swelling and mechanical properties of superporous
hydrogels of poly (acrylamide-co-acrylic acid)/polyethylenimine
interpenetrating polymer networks. *Polymer, 45*(1), 189-196.

Kim, H., Rao, S. R., Kapustin, E. A., Zhao, L., Yang, S., Yaghi, O. M., & Wang, E. N.
(2018). Adsorption-based atmospheric water harvesting device for arid
climates. *Nature Communications*, *9*(1), 1-8.

Kim, H., Yang, S., Rao, S. R., Narayanan, S., Kapustin, E. A., Furukawa, H., Umans, A.
S., Omar M. Yaghi, O. M. & Wang, E. N. (2017). Water harvesting from air

with metal-organic frameworks powered by natural

sunlight. *Science*, *356*(6336), 430-434.

Kimball, J. S., Running, S. W., & Nemani, R. (1997). An improved method for

estimating surface humidity from daily minimum temperature. *Agricultural and*

Forest Meteorology, 85(1-2), 87-98.

Kipcak, A. S., Ismail, O., Doymaz, I., & Piskin, S. (2014). Modeling and investigation

of the swelling kinetics of acrylamide-sodium acrylate hydrogel. *Journal of*

Chemistry.

Klein, T., Yakir, D., Buchmann, N., & Grünzweig, J. M. (2014). Towards an advanced

assessment of the hydrological vulnerability of forests to climate change-

induced drought. *New Phytologist, 201*(3), 712-716.

Koech, R., & Langat, P. (2018). Improving irrigation water use efficiency: A review of

advances, challenges and opportunities in the Australian context. *Water, 10*(12),

1771.

Kołodyńska, D., Skiba, A., Górecka, B., & Hubicki, Z. (2016). Hydrogels from

fundaments to application. Emerging concepts in analysis and applications of

hydrogels, 69-100.

Kosmas, C., Marathianou, M., Gerontidis, S., Detsis, V., Tsara, M., & Poesen, J. (2001).

Parameters affecting water vapor adsorption by the soil under semi-arid climatic

conditions. *Agricultural Water Management, 48(*1), 61-78.

Koupai, J. A., Eslamian, S. S., & Kazemi, J. A. (2008). Enhancing the available water

content in unsaturated soil zone using hydrogel, to improve plant growth indices.

*Ecohydrology & Hydrobiology, 8(*1), 67-75.

Kousari, M. R., & Zarch, M. A. A. (2011). Minimum, maximum, and mean annual temperatures, relative humidity, and precipitation trends in arid and semi-arid regions of Iran. *Arabian Journal of Geosciences, 4(*5-6), 907-914.

Lavergne, A., Sandoval, D., Hare, V. J., Graven, H., & Prentice, I. C. (2020). Impacts of soil water stress on the acclimated stomatal limitation of photosynthesis: Insights from stable carbon isotope data. *Global Change Biology, 26*(12), 7158-7172.

Li, L., Zhang, Y.-J., Novak, A., Yang, Y., & Wang, J. (2021). Role of Biochar in Improving Sandy Soil Water Retention and Resilience to Drought. *Water, 13*(4), 407.

Li, R., Shi, Y., Alsaedi, M., Wu, M., Shi, L., & Wang, P. (2018). Hybrid hydrogel with high water vapor harvesting capacity for deployable solar-driven atmospheric water generator. *Environmental Science and Technology*, *52*(19), 11367-11377.

Liu, M., & Guo, T. (2001). Preparation and swelling properties of crosslinked sodium polyacrylate. *Journal of Applied Polymer Science, 82*(6), 1515-1520.

Long, F., & Richman, D. (1960). Concentration gradients for diffusion of vapors in glassy polymers and their relation to time dependent diffusion phenomena1, 2. Journal of the *American Chemical Society, 82*(3), 513-519.

Łuczak, K., Czerniawska-Kusza, I., Rosik-Dulewska, C., & Kusza, G. (2021). Effect of NaCl road salt on the ionic composition of soils and Aesculus hippocastanum L. foliage and leaf damage intensity. *Scientific Reports, 11*(1), 1-10.

Luo, M., & Lau, N.-C. (2019). Characteristics of summer heat stress in China during 1979–2014: climatology and long-term trends. *Climate Dynamics, 53*(9), 5375-5388.

Malek, E., McCurdy, G., & Giles, B. (1999). Dew contribution to the annual water balances in semi-arid desert valleys. *Journal of Arid Environments, 42*(2), 71-80.

Mancosu, N., Snyder, R. L., Kyriakakis, G., & Spano, D. (2015). Water scarcity and future challenges for food production. *Water, 7(*3), 975-992.

Mao, R., Tang, J., & Swanson, B. (2001). Water holding capacity and microstructure of gellan gels. *Carbohydrate polymers, 46*(4), 365-371.

Maolin, Z., Jun, L., Min, Y., & Hongfei, H. (2000). The swelling behavior of radiation prepared semi-interpenetrating polymer networks composed of polyNIPAAm and hydrophilic polymers. *Radiation Physics and Chemistry, 58*(4), 397-400.

Matsumoto, K., Sakikawa, N., & Miyata, T. (2018). Thermo-responsive gels that absorb moisture and ooze water. *Nature Communications*, *9*(1), 1-7.

McHugh, T. A., Morrissey, E. M., Reed, S. C., Hungate, B. A., & Schwartz, E. (2015). Water from air: an overlooked source of moisture in arid and semiarid regions. *Scientific Reports, 5(*1), 1-6.

Molloy, P. J., Smith, M. J., & Cowling, M. J. (2000). The effects of salinity and temperature on the behaviour of polyacrylamide gels. *Materials and Design, 21*(3), 169-174.

Montesano, F. F., Parente, A., Santamaria, P., Sannino, A., & Serio, F. (2015). Biodegradable superabsorbent hydrogel increaseswater retention properties of growing media and plant growth. *Agriculture and Agricultural Science Procedia, 4,* 451-458.

Moura, M. R. D., Rubira, A. F., & Muniz, E. C. (2008). Semi-IPN hydrogels based on alginate-Ca2+ network and PNIPAAm: hydrophilic, morphological and mechanical properties. *Polímeros, 18*(2), 132-137.

Mudiyanselage, T. K., & Neckers, D. C. (2008). Highly absorbing superabsorbent polymer. Journal of Polymer Science Part A: *Polymer Chemistry, 46*(4), 1357-1364.

Narjary, B., Aggarwal, P., Singh, A., Chakraborty, D., & Singh, R. (2012). Water availability in different soils in relation to hydrogel application. *Geoderma, 187,* 94-101.

Neethu, T., Dubey, P., & Kaswala, A. (2018). Prospects and applications of hydrogel technology in agriculture. *Int. J. Curr. Microbiol. App. Sci, 7*(5), 3155-3162.

Omidian, H., Hashemi, S., Sammes, P., & Meldrum, I. (1998). A model for the swelling of superabsorbent polymers. *Polymer, 39*(26), 6697-6704.

Omidian, H., Rocca, J. G., & Park, K. (2005). Advances in superporous hydrogels. *Journal of controlled release, 102*(1), 3-12

Ono, T., Sugimoto, T., Shinkai, S., & Sada, K. (2007). Lipophilic polyelectrolyte gels as super-absorbent polymers for nonpolar organic solvents. *Nature materials, 6*(6), 429-433.

Ostrowska-Czubenko, J., Pieróg, M., & Gierszewska-Drużyńska, M. (2011). State of water in noncrosslinked and crosslinked hydrogel chitosan membranes–DSC studies. *Progress on Chemistry and Application of Chitin and its Derivatives, 16*, 147-156.

Paarakh, M. P., Jose, P. A., Setty, C., & Christoper, G. (2018). Release kinetics–concepts and applications. *Int. J. Pharm. Res. Tech, 8*(1), 12-20.

Pathak, P., & Wani, S. (2011). New tools and best bet options for efficient management of soil and water resources in drylands of Asia. In: Techniques of water conservation and rainwater harvesting for drought management: *SAARC International Training Program*, 18-29 July 2011, Hyderabad, India.

Pattanaaik, S. K., Wangchu, L., Singh, B., Hazarika, B. N., Singh, S. M., & Pandey, A. K. (2015). Effect of hydrogel on water and nutrient management of Citrus reticulata. *Research on crops, 16*(1).

Paudel, D., Dhakal, S., Parajuli, S., Adhikari, L., Peng, Z., Qian, Y., Adhikari, L.,. Shahi, D., Avci, M.,. Makaju, S. O. & Kannan, B. (2020). Use of quantitative trait loci to develop stress tolerance in plants. In *Plant Life Under Changing Environment* (pp. 917-965). Academic Press.

Paulino, A. T., Belfiore, L. A., Kubota, L. T., Muniz, E. C., Almeida, V. C., & Tambourgi, E. B. (2011). Effect of magnetite on the adsorption behavior of Pb (II), Cd (II), and Cu (II) in chitosan-based hydrogels. *Desalination, 275*(1-3), 187-196.

Perry, R. A., & Slatyer, R. O. (Eds.). (1969). *Arid Lands of Australia*. Canberra: Australian National University Press.

Pooley, S. A., Rivas, B. L., Lillo, F. E., & Pizarro, G. D. C. (2010). Hydrogels from acrylic acid with N, N-dimethylacrylamide: synthesis, characterization, and water absorption properties. *Journal of the Chilean Chemical Society, 55*(1), 19-24.

Quintanilla de Stéfano, J. C., Abundis-Correa, V., Herrera-Flores, S. D., & Alvarez, A. J. (2020). pH-Sensitive Starch-Based Hydrogels: Synthesis and Effect of Molecular Components on Drug Release Behavior. *Polymers, 12*(9), 1974.

Ragab, R., & Hamdy, A. (2008, November). 1.1. Climate change and water resources management in arid and semi-arid regions. In *Sustainable Development in Drylands–Meeting the Challenge of Global Climate Change* (Vol. 7, p. 279).

Ragab, R., & Prudhomme, C. (2002). Sw—soil and Water: climate change and water resources management in arid and semi-arid regions: prospective and challenges for the 21st century. *Biosystems engineering, 81*(1), 3-34.

Siddique, K. H. M., & Bramley, H. (2014). Water deficits: development. *Encyclopedia of Natural Resources*: 1–4.

Salleh, K. M., Zakaria, S., Sajab, M. S., Gan, S., Chia, C. H., Jaafar, S. N. S., & Amran, U. A. (2018). Chemically crosslinked hydrogel and its driving force towards superabsorbent behaviour. *International Journal of Biological Macromolecules, 118,* 1422-1430.

Save, R., Perry, M., Marfa, O., & Serrano, L. (1995). The effect of a hydrophilic polymer on plant water status and survival of transplanted pine seedlings. *HortTechnology* (USA).

Scholes, R. J. (2020). The Future of Semi-Arid Regions: A Weak Fabric Unravels. *Climate, 8*(3), 43.

Seneviratne, S. I., Corti, T., Davin, E. L., Hirschi, M., Jaeger, E. B., Lehner, I., Orlowsky, B. & Teuling, A. J. (2010). Investigating soil moisture–climate interactions in a changing climate: A review. *Earth-Science Reviews, 99*(3-4), 125-161.

Serrano-Aroca, Á., & Deb, S. (2020). Acrylic-Based Hydrogels as Advanced Biomaterials. In *Acrylate Polymers for Advanced Applications*. IntechOpen.

Shahid, S. A., Qidwai, A. A., Anwar, F., Ullah, I., & Rashid, U. (2012). Effects of a novel poly (AA-co-AAm)/AlZnFe2O4/potassium humate superabsorbent hydrogel nanocomposite on water retention of sandy loam soil and wheat seedling growth. *Molecules, 17*(11), 12587-12602.

Shen, Y. & Pei, H. (2019). Water Conservation for Sustainable Agriculture. Encyclopedia of Water: *Science, Technology, and Society,* 1-11.

Siepmann, J., & Peppas, N. A. (2012). Modeling of drug release from delivery systems based on hydroxypropyl methylcellulose (HPMC). *Advanced Drug Delivery Reviews, 64,* 163-174.

Skoug, J. W., Mikelsons, M. V., Vigneron, C. N., & Stemm, N. L. (1993). Qualitative evaluation of the mechanism of release of matrix sustained release dosage forms by measurement of polymer release. *Journal of Controlled Release, 27*(3), 227-245.

Specht, A., & Harvey, J. (2000). Improving water delivery to the roots of recently transplanted seedling trees: The use of hydrogels to reduce leaf and hasten root establishment. *Journal of Forest Research, (1)*117 - 123.

Tanaka, T., & Fillmore, D. J. (1979). Kinetics of swelling of gels. *The Journal of Chemical Physics, 70*(3), 1214-1218.

Taylor, K., & Halfacre, R. (1986). The effect of hydrophilic polymer on media water retention and nutrient availability to Ligustrum lucidum. *HortScience, 21*(5), 1159-1161.

Thomas, R. J., El-Dessougi, H., & Tubeileh, A. (2006). Soil system management under arid and semi-arid conditions. In: Uphoff, N., Ball, A.S., Fernandes, E., Herren, H., Husson, O., Laing, M., Palm, Ch, Pretty, J., Sanchez, P., Sanginga, N., Thies, J. (Eds.), *Biological Approaches to Sustainable Soil Systems* (pp. 41- 55). CRC Press Publisher.

Tomar, R. S., Gupta, I., Singhal, R., & Nagpal, A. K. (2007). Synthesis of poly (acrylamide-co-acrylic acid)-based super-absorbent hydrogels by gamma

radiation: study of swelling behaviour and network parameters. *Designed monomers and polymers, 10*(1), 49-66.

Urbina, R., Lefavrais, S., Royon, L., Mongruel, A., González-Viñas, W., & Beysens, D. (2021). Gel-Induced Dew Condensation. *Journal of Hydrology*, *12*, 62-63.

van Lier, Q. d. J., Pinheiro, E. A. R., & Inforsato, L. (2019). Hydrostatic equilibrium between soil samples and pressure plates used in soil water retention determination: consequences of a questionable assumption. *Revista Brasileira de Ciência do Solo, 43*.

Verheye, W. H. (Ed.). (2009). Land Use, Land Cover and Soil Sciences-Volume V: Dry Lands and Desertification. EOLSS Publications.

Vermonden, T., & Klumperman, B. (2015). The past, present and future of hydrogels. *European Polymer Journal, 100*(72), 341-343.

Vundavalli, R., Vundavalli, S., Nakka, M., & Rao, D. S. (2015). Biodegradable nano-hydrogels in agricultural farming-alternative source for water resources. *Procedia Materials Science, 10*, 548-554.

Wang, J., Dang, Y., Meguerdichian, A. G., Dissanayake, S., Kankanam-Kapuge, T., Bamonte, S., Tobin, Z. M. . Achola, L. A. & Suib, S. L. (2019). Water harvesting from the atmosphere in arid areas with manganese dioxide. *Environmental Science & Technology Letters, 7*(1), 48-53.

Wang, J., Ren, S., & Guo, M. (2012). Preparation and humidity controlling behaviors of sepiolite/polyacrylic acid (sodium) composite. *Procedia Engineering*, *27*, 423-430.

Wang, M., Kong, L., & Zang, M. (2015). Effects of sample dimensions and shapes on measuring soil–water characteristic curves using pressure plate. *Journal of Rock Mechanics and Geotechnical Engineering, 7*(4), 463-468.

Watson, A. (1992). Desert soils. In Developments in Earth Surface Processes (Vol. 2, pp. 225-260): *Elsevier.*

Wei, Q., Xu, J., Liao, L., Yu, Y., Liu, W., Zhou, J., & Ding, Y. (2021). Indicators for evaluating trends of air humidification in arid regions under circumstance of climate change: Relative humidity (RH) vs. Actual water vapour pressure (ea). *Ecological Indicators*, *121*, 107043.

Woodhouse, J., & Johnson, M. (1991). Effect of superabsorbent polymers on survival and growth of crop seedlings. *Agricultural Water Management, 20*(1), 63-70.

Wu, Y., Li, S., & Chen, G. (2021). Impacts of mechanical and chemical factors on the water-holding capacity of polyacrylamide in sand: models and mechanisms. *Soil Research.*

Xie, J., Liu, X., Liang, J., & Luo, Y. (2009). Swelling properties of superabsorbent poly (acrylic acid-co-acrylamide) with different crosslinkers. *Journal of Applied Polymer Science, 112*(2), 602-608.

Xu, J., Li, T., Chao, J., Wu, S., Yan, T., Li, W., Li, W., Cao, B. & Wang, R. (2020). Efficient solar-driven water harvesting from arid air with metal–organic frameworks modified by hygroscopic salt. *Angewandte Chemie International Edition*, *59*(13), 5202-5210.

Yin, L., Fei, L., Cui, F., Tang, C., & Yin, C. (2007). Superporous hydrogels containing poly (acrylic acid-co-acrylamide)/O-carboxymethyl chitosan interpenetrating polymer networks. *Biomaterials, 28*(6), 1258-1266.

Zhang, H., Luan, Q., Huang, Q., Tang, H., Huang, F., Li, W., Wan, C., Liu, C., Xu, J., Zhou, Q. & Guo, P. (2017). A facile and efficient strategy for the fabrication of porous linseed gum/cellulose superabsorbent hydrogels for water conservation. *Carbohydrate polymers, 157,* 1830-1836.

Zhang, Q., Wang, S., Wang, S., Zhao, Y., & Wen, X. (2016). Influence factors and variation characteristics of water vapor absorption by soil in semi-arid region. *Science China Earth Sciences, 59*(11), 2240-2251.

Zhang, Q., Wang, S., Yang, F.-L., Yue, P., Yao, T., & Wang, W.-Y. (2015). Characteristics of dew formation and distribution, and its contribution to the surface water budget in a semi-arid region in China. *Boundary-Layer Meteorology, 154*(2), 317-331.

Zhao, D., Fang, Z., Tang, Y., & Tao, J. (2020). Graphene Oxide as an Effective Soil Water Retention Agent Can Confer Drought Stress Tolerance to Paeonia ostii without Toxicity. *Environmental Science & Technology, 54(*13), 8269-8279.

Zhao, F., Zhou, X., Liu, Y., Shi, Y., Dai, Y. & Yu, G. (2019). Super moisture-absorbent gels for all-weather atmospheric water harvesting. *Advanced materials, 31*(10), 1806446.

Zhou, W. J., Yao, K. J. & Kurth, M. J. (1997). Studies of crosslinked poly (AM-MSAS-AA) gels. II. Effects of polymerization conditions on the water absorbency. *Journal of Applied Polymer Science, 64*(5), 1009-1014.

Zhu, B., Ma, D., Wang, J., & Zhang, S. (2015). Structure and properties of semi-interpenetrating network hydrogel based on starch. *Carbohydrate Polymers,* 133, 448-455.

Zlatev, Z., & Lidon, F. C. (2012). An overview on drought induced changes in plant growth, water relationsand photosynthesis. *Emirates Journal of Food and Agriculture*, 57-72.

Zohuriaan-Mehr, M. J., & Kabiri, K. (2008). Superabsorbent polymer materials: a review. *Iranian Polymer Journal, 17,* 451-477.

Zohuriaan-Mehr, M., Omidian, H., Doroudiani, S., & Kabiri, K. (2010). Advances in non-hygienic applications of superabsorbent hydrogel materials. *Journal of Materials Science, 45(*21), 5711-5735.

Zonatto, F., et al. (2017). Adsorption and controlled release of potassium, phosphate and ammonia from modified Arabic gum-based hydrogel. *International Journal of Biological Macromolecules, 105*, 363-369.

<center>**APPENDIX**</center>

<center>**Appendix 1: Results on absorption swelling behaviour**</center>

A1.1 Modelling absorption graphs to the Korsmeyer Peppas model

Figure A1.1 represents graphs from CR hydrogel (best absorbing hydrogel) atmospheric absorbed water values at 20 ⁰C under different relative humidity percentages fitted to the Korsmeyer Peppas model, Equation 7, to determine the swelling parameters for describing the absorption behaviour at all relative humidity levels. The graphs were plotted with log M/Max (g/g) against log Time (in hours), and the swelling parameters are derived from the line equation. The R^2 values represents the closeness of the CR hydrogel absorbed water values to the Korsmeyer Peppas model.

A1.2 Modelling absorption graphs to the First Order kinetics model

Figure A1.2 represents graphs from CR hydrogel (best absorbing hydrogel) atmospheric absorbed water values at 20 ⁰C under different relative humidity percentages fitted to the First Order kinetics model, Equation 6, to determine the swelling parameters for describing the absorption behaviour at all relative humidity levels. The graphs were plotted with Y^1 (g/g) (predicted values) against C (g/g), and the swelling parameters are derived from the line equation. The R^2 values represents the closeness of the CR hydrogel absorbed water values to the First Order kinetics model.
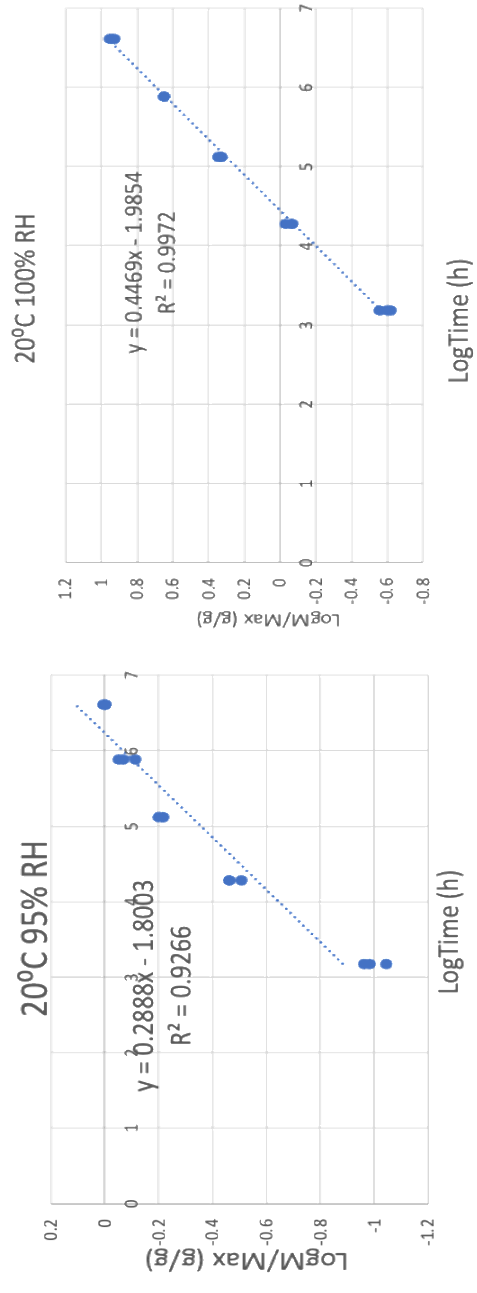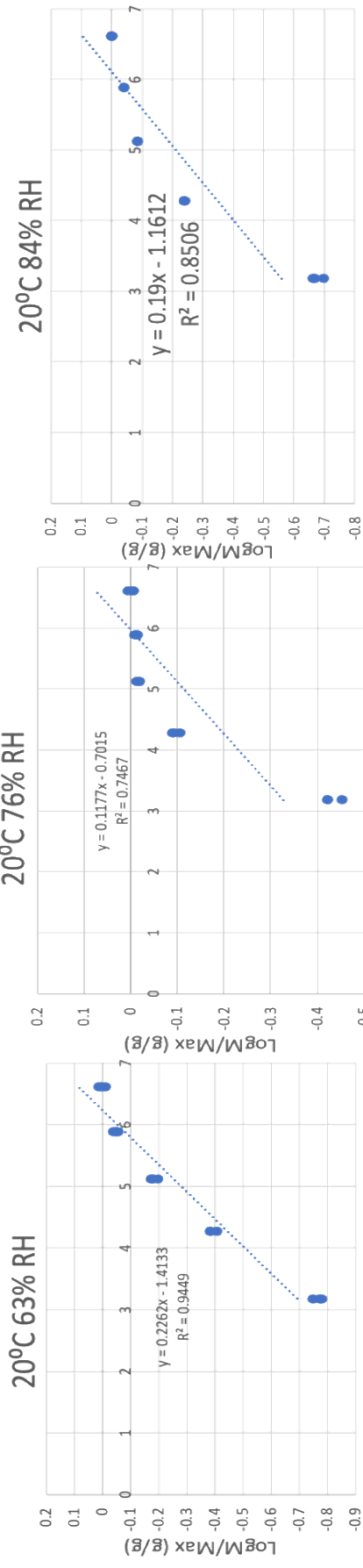
Figure A1.1 *Korsmeyer Peppas modelling of the mass of water gained by the CR hydrogel at 20 °C at different relative humidity (RH) levels (M/Mmax = ktⁿ).*
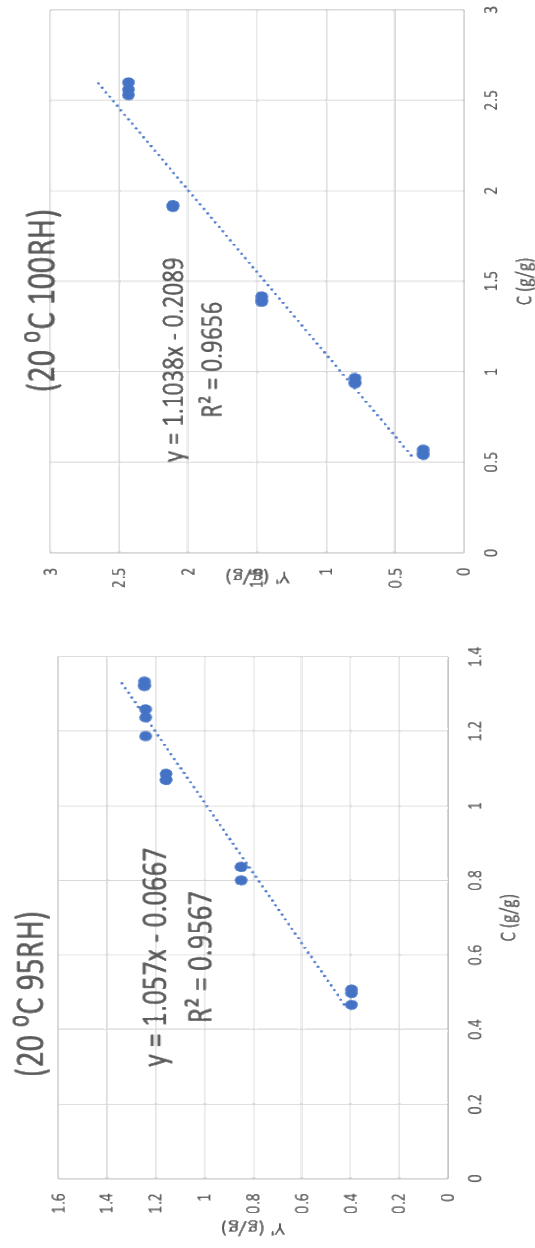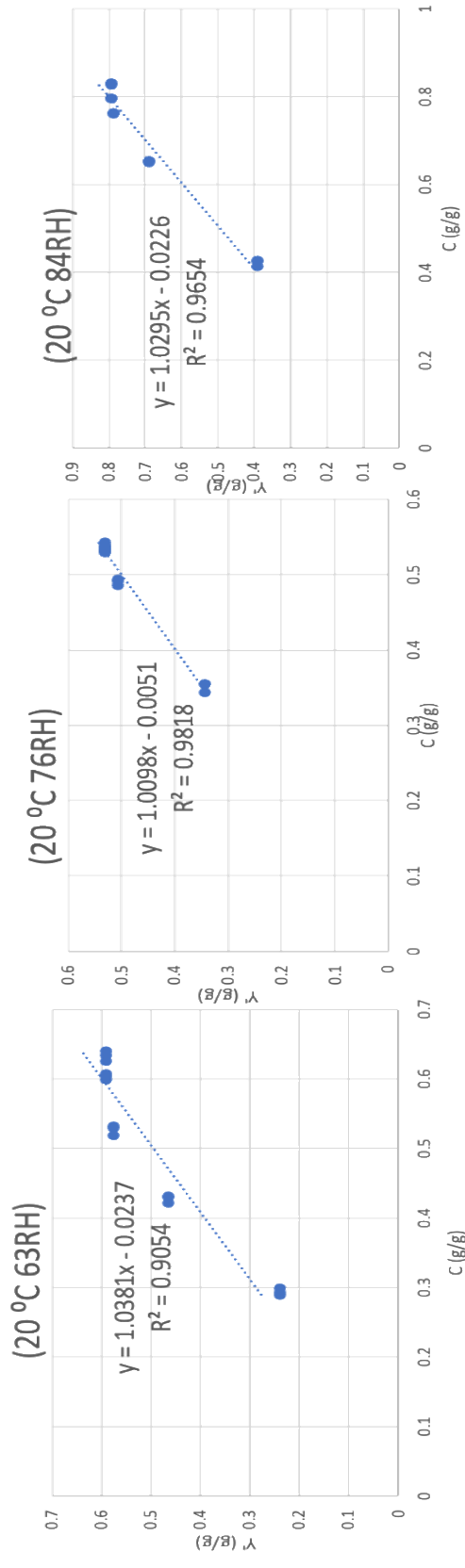
Figure A1.2 *First order kinetic modelling of the mass of water gained by the CR hydrogel at 20 °C at different relative humidity (RH) levels (Y' = Mmax(1-exp(kt)).*

Appendix 2: Results on mean absorption values

Representation of the mean absorption values data of different hydrogels at different time, temperature and relative humidity variations with their respective, sample size (N), standard deviation (sd), standard error (se) and confidence interval (ci).

Figure A2.1: *Mean mass of atmospheric water absorption experimental data among different hydrogels*

Gel	N	Mean_Absorption (g/g)	sd	se	ci
AR	225	0.642	0.541	0.036	0.071
BR	225	0.762	0.578	0.039	0.076
CR	225	0.824	0.561	0.037	0.074
DR	225	0.661	0.565	0.038	0.074
ER	225	0.594	0.520	0.035	0.068

Figure A2.2: *Mean mass of atmospheric water absorption experimental data among different hydrogels over temperature*

Gel	Temperature	N	Mean_Absorption (g/g)	sd	se	ci
AR	10	75	0.609	0.458	0.053	0.105
AR	20	75	0.644	0.522	0.060	0.120
AR	30	75	0.672	0.635	0.073	0.146
BR	10	75	0.691	0.499	0.058	0.115
BR	20	75	0.767	0.541	0.063	0.125
BR	30	75	0.827	0.677	0.078	0.156
CR	10	75	0.784	0.469	0.054	0.108
CR	20	75	0.828	0.518	0.060	0.119
CR	30	75	0.859	0.679	0.078	0.156
DR	10	75	0.626	0.474	0.055	0.109
DR	20	75	0.665	0.539	0.062	0.124
DR	30	75	0.693	0.670	0.077	0.154
ER	10	75	0.555	0.444	0.051	0.102
ER	20	75	0.600	0.500	0.058	0.115
ER	30	75	0.627	0.608	0.070	0.140

Figure A2.3: *Mean mass of atmospheric water absorption experimental data among*

different hydrogels over time

Gel	Time (hr)	N	Mean_Absorption (g/g)	sd	se	ci
AR	24	45	0.301	0.116	0.017	0.035
BR	24	45	0.271	0.153	0.023	0.046
CR	24	45	0.410	0.124	0.018	0.037
DR	24	45	0.301	0.118	0.018	0.035
ER	24	45	0.221	0.117	0.017	0.035
AR	72	45	0.506	0.243	0.036	0.073
BR	72	45	0.583	0.262	0.039	0.079
CR	72	45	0.663	0.235	0.035	0.071
DR	72	45	0.512	0.243	0.036	0.073
ER	72	45	0.448	0.226	0.034	0.068
AR	168	45	0.665	0.403	0.060	0.121
BR	168	45	0.820	0.392	0.058	0.118
CR	168	45	0.854	0.395	0.059	0.119
DR	168	45	0.686	0.413	0.062	0.124
ER	168	45	0.623	0.369	0.055	0.111
AR	360	45	0.799	0.591	0.088	0.178
BR	360	45	0.984	0.573	0.085	0.172
CR	360	45	1.009	0.583	0.087	0.175
DR	360	45	0.827	0.608	0.091	0.183
ER	360	45	0.759	0.535	0.080	0.161
AR	744	45	0.938	0.809	0.121	0.243
BR	744	45	1.150	0.798	0.119	0.240
CR	744	45	1.182	0.817	0.122	0.245
DR	744	45	0.980	0.852	0.127	0.256
ER	744	45	0.918	0.767	0.114	0.231

Figure A2.4: *Mean mass of atmospheric water absorption experimental data among*

different hydrogels over humidity

Gel	Relative Humidity (%)	N	Mean_Absorption (g/g)	sd	se	ci
AR	63	45	0.222	0.062	0.009	0.019
BR	63	45	0.381	0.181	0.027	0.054
CR	63	45	0.463	0.140	0.021	0.042
DR	63	45	0.231	0.063	0.009	0.019
ER	63	45	0.233	0.104	0.016	0.031
AR	76	45	0.332	0.053	0.008	0.016
BR	76	45	0.431	0.136	0.020	0.041
CR	76	45	0.485	0.081	0.012	0.024
DR	76	45	0.341	0.060	0.009	0.018
ER	76	45	0.289	0.072	0.011	0.022
AR	84	45	0.499	0.119	0.018	0.036
BR	84	45	0.624	0.206	0.031	0.062
CR	84	45	0.677	0.157	0.023	0.047
DR	84	45	0.513	0.133	0.020	0.040
ER	84	45	0.457	0.138	0.021	0.042
AR	95	45	0.807	0.284	0.042	0.085
BR	95	45	0.909	0.350	0.052	0.105
CR	95	45	0.957	0.307	0.046	0.092
DR	95	45	0.824	0.306	0.046	0.092
ER	95	45	0.725	0.288	0.043	0.086
AR	100	45	1.350	0.742	0.111	0.223
BR	100	45	1.464	0.823	0.123	0.247
CR	100	45	1.538	0.803	0.120	0.241
DR	100	45	1.398	0.780	0.116	0.234
ER	100	45	1.266	0.729	0.109	0.219

Figure A2.5: *Mean mass of atmospheric water absorption experimental data among*

CR hydrogels at different relative humidity over time

Relative Humidity (%)	Time (hr)	N	Mean_Absorption (g/g)	sd	se	ci
63	24	9	0.268	0.022	0.007	0.017
76	24	9	0.344	0.051	0.017	0.039
84	24	9	0.416	0.062	0.021	0.048
95	24	9	0.476	0.083	0.028	0.063
100	24	9	0.547	0.129	0.043	0.099
63	72	9	0.405	0.045	0.015	0.034
76	72	9	0.483	0.013	0.004	0.010
84	72	9	0.631	0.028	0.009	0.022
95	72	9	0.807	0.076	0.025	0.059
100	72	9	0.987	0.200	0.067	0.154
63	168	9	0.480	0.070	0.023	0.054
76	168	9	0.528	0.025	0.008	0.019
84	168	9	0.740	0.048	0.016	0.037
95	168	9	1.042	0.031	0.010	0.024
100	168	9	1.481	0.274	0.091	0.211
63	360	9	0.551	0.087	0.029	0.067
76	360	9	0.532	0.034	0.011	0.026
84	360	9	0.783	0.076	0.025	0.059
95	360	9	1.166	0.082	0.027	0.063
100	360	9	2.016	0.357	0.119	0.274
63	744	9	0.610	0.117	0.039	0.090
76	744	9	0.538	0.036	0.012	0.028
84	744	9	0.815	0.072	0.024	0.055
95	744	9	1.293	0.169	0.056	0.130
100	744	9	2.656	0.416	0.139	0.320

Figure A2.6: *Mean mass of atmospheric water absorption experimental data among*

CR hydrogels at different temperature over time

Time	Temperature	N	Mean_Absorption (g/g)	sd	se	ci
24	10	15	0.329	0.060	0.015	0.033
24	20	15	0.422	0.097	0.025	0.054
24	30	15	0.480	0.151	0.039	0.083
72	10	15	0.601	0.139	0.036	0.077
72	20	15	0.668	0.203	0.052	0.112
72	30	15	0.719	0.324	0.084	0.180
168	10	15	0.817	0.274	0.071	0.152
168	20	15	0.859	0.348	0.090	0.193
168	30	15	0.887	0.540	0.139	0.299
360	10	15	0.984	0.423	0.109	0.234
360	20	15	1.015	0.530	0.137	0.293
360	30	15	1.029	0.779	0.201	0.431
744	10	15	1.188	0.641	0.165	0.355
744	20	15	1.178	0.769	0.199	0.426
744	30	15	1.182	1.046	0.270	0.579